Aus der II. Medizinischen Klinik und Poliklinik

Klinikum rechts der Isar

Technische Universität München

Direktor: Prof. Dr. Roland M. Schmid

Mechanismen der lokalen Immunregulation in der Leber

Zusammenstellung wissenschaftlicher Veröffentlichungen zur Erlangung der Lehrbefähigung für das Fach Innere Medizin mit Schwerpunkt Gastroenterologie an der Medizinischen Fakultät der Technischen Universität München

vorgelegt von

Dr. med. Katrin Böttcher, PhD
(geb. Schölzel)

aus Heidenheim an der Brenz

2022

Mit Genehmigung der Medizinischen Fakultät

der Technischen Universität München

Fachmentorat:	Prof. Dr. Roland M. Schmid (Vorsitzender)
	Prof. Dr. Percy A. Knolle
	Prof. Dr. Norbert Hüser
Dekan:	Prof. Dr. Bernhard Hemmer
Tag des Kolloquiums:	12.10.2021

Inhaltsverzeichnis

1. Zusammenfassung

Chronische Lebererkrankungen und ihre Folgen gehören weltweit zu den häufigsten Todesursachen, gegen die bis heute effektive Therapien fehlen. Obwohl sowohl die Leberzirrhose als auch das hepatozelluläre Karzinom (HCC) auf dem Boden verschiedener Grunderkrankungen entstehen können, haben sie als pathogenetischen Mechanismus eine Störung der lokalen Immunregulation in der Leber gemein. Aufgrund ihrer speziellen Blutversorgung besteht in der Leber ein tolerogenes immunologisches Umfeld, das die Chronifizierung von Infektionen, sowie die Tumorgenese begünstigt. Dem gegenüber steht eine überschießende Inflammation, die z. B. im Rahmen einer hepatitischen Leberschädigung, sowie bei der Pathogenese der Leberfibrose und -zirrhose pathogenetische Relevanz hat. Auf diesem Verständnis aufbauend wurden bereits verschiedene Therapeutika entwickelt, die die immunologische Achse verschiedener Lebererkrankungen modulieren sollen. Jedoch ist z.B. das Ansprechen des HCC auf eine Immuncheckpoint blockierende Therapie weiterhin gering und zur Behandlung der Leberzirrhose gibt es bislang keine zugelassenen Medikamente.

Um molekulare Mechanismen, die an der Entstehung chronischer Lebererkrankungen beteiligt sind, zu entschlüsseln, wurden in den hier zusammengefassten Arbeiten unterschiedliche Aspekte der lokalen Immunregulation in der Leber untersucht.

So konnte gezeigt werden, dass der Austausch von MHC Klasse I (MHC I) Molekülen zwischen sinusoidalen Zellpopulationen mittels *cross-allocation* zu einer Verbesserung der antiviralen Immunantwort in der Leber beiträgt. Weiter konnte der Energiesensor Adenosinmonophosphat-aktivierte Proteinkinase (AMPK) als Regulator von Tumor-Stoma Interaktionen, die für die Entstehung und Progression des HCC wichtig sind, identifiziert werden. Zuletzt konnte außerdem gezeigt werden, dass mucosal-associated invariant T (MAIT) cells, semi-innate T Zellen, die v.a. in der Leber vorkommen, zur Entstehung der Leberfibrose in autoimmunen Lebererkrankungen beitragen können.

Insgesamt ermöglichen die hier vorgestellten Arbeiten also ein besseres Verständnis der lokalen Immunregulation in der Leber, und bilden somit die Basis zur Entwicklung neuer, immuntherapeutischer Ansätze zur Behandlung von chronischen Lebererkrankungen.

2. Einleitung

2.1 Chronische Lebererkrankungen und ihre Folgen

Die Leber ist ein Stoffwechselorgan, das durch verschiedene Einflüsse geschädigt werden kann. So kann es durch bestimmte Noxen, z.B. Medikamente oder die Infektion mit Hepatitis B oder C Virus, zu einer akuten, oft selbstlimitierenden Leberschädigung, oder infolge einer Langzeitschädigung zu einer chronischen Lebererkrankung kommen[1]. Diese entsteht in Europa am häufigsten durch Alkoholabusus, chronische Infektion mit Hepatitis B oder C, der nicht alkoholischen Fettlebererkrankung (NAFLD) oder seltener auf dem Boden autoimmuner (primär sklerosierende Cholangitis, primär biliäre Cholangitis, Autoimmunhepatitis) oder hereditärer (Hämochromatose, M. Wilson, α1-Antitrypsinmangel) Lebererkrankungen[2,3]. Als Folge der chronischen Leberschädigung kommt es im Laufe der Zeit, unabhängig von der Ätiologie, zur Entwicklung einer Leberzirrhose. Aktuell stellt die Lebertransplantation, die aufgrund der limitierten Organverfügbarkeit nur für wenige Patienten infrage kommt, die einzige kausale Therapiemöglichkeit der Leberzirrhose dar[1]. Dementsprechend steigt die Zahl der Todesfälle als Folge einer Leberzirrhose, sowie die Inzidenz des hepatozellulären Karzinoms (HCC) weltweit weiter an[3]. Dies verdeutlicht, dass ein besseres Verständnis der Pathogenese chronischer Lebererkrankungen und der Leberzirrhose, sowie die Entwicklung neuer therapeutischer Ansätze unerlässlich ist. Unabhängig von der Ätiologie der Leberzirrhose wird angenommen, dass die Inflammation für deren Pathogenese eine große Rolle spielt. So kann es unter anderem durch Zytokine wie TGF-β, IL-17A und IL-1β zur Aktivierung hepatischer Sternzellen (HSC), nicht-parenchymaler Leberzellen, die sich im Dissé Raum befinden, kommen. Sind HSC aktiviert, sezernieren sie große Mengen extrazellulärer Matrix Proteine, z.B. Kollagen I und pro-inflammatorischer Zytokine, die einen circulos vitiosus begünstigen, der zur Entstehung einer Leberfibrose und später -zirrhose führt[4]. Diese stellt einen wichtigen Risikofaktor für die Entstehung eines HCC dar und geht mit Komplikationen wie Varizenblutungen, Ascites, hepatischer Encephalopathie und dem hepatorenalen Syndrom einher[5,6]. Es ist daher von großer Bedeutung die immunologischen Prozesse, die zur Pathogenese chronischer Lebererkrankungen beitragen, zu entschlüsseln und dadurch die Entwicklung neuer therapeutischer Ansätze zu ermöglichen.

2.2 Das lokale Immunsystem in der Leber – zwischen Immuntoleranz und Inflammation

Neben ihren vielfältigen Funktionen für den Stoffwechsel erfüllt die Leber auch eine wichtige immunologische Funktion. Aufgrund ihrer besonderen, dualen Blutversorgung wird die Leber

zu ca. 70% durch venöses Blut aus dem Gastrointestinaltrakt versorgt. Dieses ist reich an nahrungsmittelassoziierten Antigenen und enthält zudem Bakterien, bakterielle Produkte und sog. *pathogen-associated molecular patterns* (PAMPs)[7]. Als Folge dieser ständigen Antigenexposition besteht in der Leber ein tolerogenes immunologisches Milieu. So sind z. B. die antigenpräsentierenden Zellen (APCs) in der Leber tolerant gegenüber PAMPs um die Entstehung einer Inflammation im physiologischen Kontext zu verhindern. Außerdem werden von Hepatozyten, sinusoidalen Leberendothelzellen (LSEC) und Kupfferzellen anti-inflammatorische Zytokine wie IL-10 und TGF-β ausgeschüttet um die T Zell Aktivierung durch APCs zu verhindern[8,9]. In ähnlicher Weise können LSEC und hepatische Sternzellen die T Zell Aktivierung durch dendritische Zellen (DCs) verhindern[10,11]. LSEC kleiden als spezialisierte Endothelzellen die Lebersinusoide aus und besitzen als nicht-professionelle APCs die Fähigkeit zur Antigenpräsentation. Sie sind in der Lage lösliche Antigene aufzunehmen und diese entweder über MHC II Moleküle an CD4+ T Zellen zu präsentieren, oder über MHC I Moleküle an CD8+ T Zellen zu kreuzpräsentieren[12,13]. Die Kreuzpräsentation von Antigen durch LSEC an naive CD8+ T Zellen führt kurzfristig zu deren Expansion, sowie zur Expression von Effektozytokinen. Darauffolgend entwicken diese CD8+ T Zellen jedoch einen ruhenden Phänotyp, der durch das Fehlen von Effektorfunktion gekennzeichnet ist[14,15]. Präsentieren LSEC Antigen an zytotoxische T Lymphozyten (CTLs), werden diese inaktiviert und sterben durch Apoptose[16]. Insgesamt führt also die Antigenpräsentation durch LSEC zur Ausbildung von Immuntoleranz in der Leber. HSC können zwar Antigen präsentieren, jedoch nehmen sie wenig Antigen auf und im Gegensatz zu LSEC und professionellen APCs fehlt HSCs die Fähigkeit zur Antigenkreuzpräsentation[10]. Sie induzieren außerdem die Expansion von regulatorischen T Zellen (Treg) und myeloiden Suppressorzellen[17], weshalb HSC bislang ebenfalls tolerogene Eigenschaften zugeschrieben wurden.

Es ist bekannt, dass das Immunsystem eine wichtige Rolle für die Elimination von infizierten oder entarteten Zellen spielt. Das spezielle, toleranzinduzierende immunologische Milieu in der Leber begünstigt also nicht nur die Entstehung von chronischen Infektionen, wie z.B. der chronischen Virushepatitis, sondern verhindert auch die immunologische Elimination von Krebszellen. Gleichzeitig kann eine überschießende Immunantwort auch zur Leberschädigung, z. B. im Rahmen eines akuten Leberversagens führen, und eine chronische Leberinflammation die Entstehung von Leberfibrose und -zirrhose und schließlich HCC begünstigen. Insgesamt ist also ein besseres Verständnis der lokalen Immunregulation in der Leber essentiell für die Entwicklung neuer therapeutischer Konzepte zur Behandlung chronischer Lebererkrankungen und des HCCs.

In der Leber existiert außerdem eine spezielle Zusammensetzung von Immunzellen. So herrschen dort, anders als im peripheren Blut, CD8+ T Zellen vor. Zudem sind in der Leber innate Zellpopulationen, wie NK Zellen besonders angereichert[18]. Die semi-innaten Mucosal-

associated invariant T (MAIT) cells repräsentieren einen Großteil der Lymphozyten in der Leber (bis zu 50% der CD3+ Lymphozyten)[19-21]. Sie exprimieren einen speziellen T Zell Rezeptor TCR), der durch eine invariante α Kette (Vα7.2) gekennzeichnet ist und MAIT cells zur Antigenerkennung auf dem monomorphen MHC Klasse I-related Molekül MR1 befähigt[22]. MAIT cells erkennen eine neue Klasse von Antigenen, d.h. Vitamin B Metabolite wie 5-(2-oxopropylidenamino)-6-d-ribitylaminouracil (5-OP-RU) und 6-formylpterin (6-FP)[23]. Interessanterweise können MAIT cells aufgrund ihrer semi-innaten Eigenschaften nicht nur über den T Zell Rezeptor aktiviert werden, sondern auch über Zytokinrezeptoren wie IL-12 und IL-18 Rezeptor[24]. Unabhängig vom Aktivierungsweg können MAIT cells, ähnlich wie innate Immunzellen, schnell Zytokine (IFNγ, TNFα, IL-17) und zytolytische Moleküle (Perforin, Granzym B (GrzB) ausschütten[19,21,24]. Diese Eigenschaft befähigt MAIT cells zur Elimination bakteriell infizierter Zellen, sowie zur Koordination der sterilen Inflammation[25,26]. Insgesamt werden MAIT cells also als wichtige Mediatoren der hepatischen Inflammation angesehen.

2.3 Therapeutische Konzepte und aktuelle Herausforderungen bei der Therapie chronischer Lebererkrankungen

Die oben beschriebenen Mechanismen der Toleranzentwicklung und das spezielle immunologische Milieu in der Leber führen zur Etablierung chronischer Infektionen in der Leber und begünstigen die Krebsentstehung. In den letzten Jahren wurden deshalb verschiedene immuntherapeutische Konzepte zur Behandlung chronischer Lebererkrankungen entwickelt. So existieren verschiedene Ansätze zur Behandlung der chronischen HBV Infektion, wie z. B. die therapeutische Vakzinierung oder das *T- cell engineering* von HBV-spezifischen CD8+ T Zellen[27]. Für die Behandlung des HCC ist kürzlich eine neue *Checkpointinhibitor*-basierte, gegen programmed death 1 ligand 1 (PD-L1) gerichtete Immuntherapie als Erstlinientherapie des fortgeschrittenen HCC zugelassen worden. Jedoch sprechen auf diese Therapie nur ca. 30% der HCC Patienten an und das progressionfreie Überleben beträgt auch unter Immuntherapie nur wenige (durchschnittlich 6,8) Monate[28]. Folglich ist die Entwicklung neuer, verbesserter Immuntherapeutika zur Behandlung des HCC essentiell. Da bekannt ist, dass neben veränderten immunologischen Voraussetzungen in der Leber der Metabolismus für die Krebsentstehung eine wichtige Rolle spielt[29], ist auch eine Manipulation und das bessere Verständnis metabolischer Aspekte der Karzinogenese in den Fokus der Forschung gerückt. So konnte zum Beispiel gezeigt werden, dass die HCC Inzidenz in Patienten, die Metformin einnehmen, niedriger ist[30]. Zudem hemmt Metformin die Angiogenese in einem HCC in vitro Kokulturmodell mit HSC[31]. Für die

Behandlung der Leberzirrhose, sowie für die Behandlung der NAFLD, die bereits heute ca. 25% der erwachsenen Weltbevölkerung betrifft, gibt es aktuell keine zugelassenen Therapeutika, sodass die Lebertransplantation die einzige kausale Therapieoption für die Fortgeschrittene Leberzirrhose darstellt. Insgesamt besteht also ein dringender Bedarf für die Entwicklung neuer therapeutischer Konzepte für die Behandlung von chronischen Lebererkrankungen.

3. Ergebnisse und Diskussion eigener Arbeiten

3.1 Der Austausch von MHC I Molekülen zwischen sinusoidalen Zellpopulationen trägt zur Verbesserung der Immunüberwachung in der Leber bei

Es ist bereits bekannt, dass die nicht-parenchymalen LSEC sehr effizient Antigen kreuzpräsentieren können. Sie besitzen eine sogenannte *scavenger* Aktivität und können in kurzer Zeit große Mengen zirkulierendes Antigen aufnehmen und dieses effektiv an CD8 T Zellen kreuzpräsentieren[13,32]. HSC sind nicht-parenchymale Leberzellen, die maßgeblich an der Entstehung der Leberzirrhose beteiligt sind[33,34]. Die Bedeutung von HSC für die lokale Immunregulation in der Leber wurde bisher kontrovers diskutiert [35,36] und es blieb unklar, ob HSC in vivo zur Kreuzpräsentation von Antigen an CD8+ T Zellen fähig sind, und ob eine solche Kreuzpräsentation durch HSC zur Aktivierung oder Toleranz von CD8 T Zellen führt. In dieser Arbeit wurde deshalb die Fähigkeit von HSC zur Kreuzpräsentation in vivo und somit deren Beteiligung an der Immunüberwachung in der Leber untersucht.
Um die Kreuzpräsentationfähigkeit von HSCs in vivo zu untersuchen wurde GFAP-K^b Mäusen 1mg OVA intravenös injiziert und anschließend OT-I T Zellen transferiert, die das OVA Peptid SIINFEKL im Kontext von H-$2K^b$, dem murinen MHC-I Molekül, erkennen. OT-I Zellen proliferieren in GFAP-K^b Mäusen in nahezu gleichem Umfang wie in Wildtyp Mäusen (Abb. 1A) und exprimieren die Oberflächenmarker CD25, CD44 und CD69 (Abb. 1B), welches auf eine Aktivierung dieser Zellen hindeutet. Überraschenderweise konnte in der Leber von GFAP-K^b Mäusen H-$2K^b$ Oberflächenexpression nicht nur auf HSC, sondern auch auf LSEC, gemessen werden (Abb. 1C). Trotz der Anwesenheit von funktional intaktem H2-K^b auf LSEC in GFAP-K^b Mäusen konnte mittels RT-PCR keine mRNA Expression für H-$2K^b$ in LSEC festgestellt werden (Abb. 1D). Dies führte zu der Annahme, dass ein Transfer von H-$2K^b$ Molekülen zwischen HSC und LSEC in der Leber der GFAP-K^b Maus stattfinden könnte.

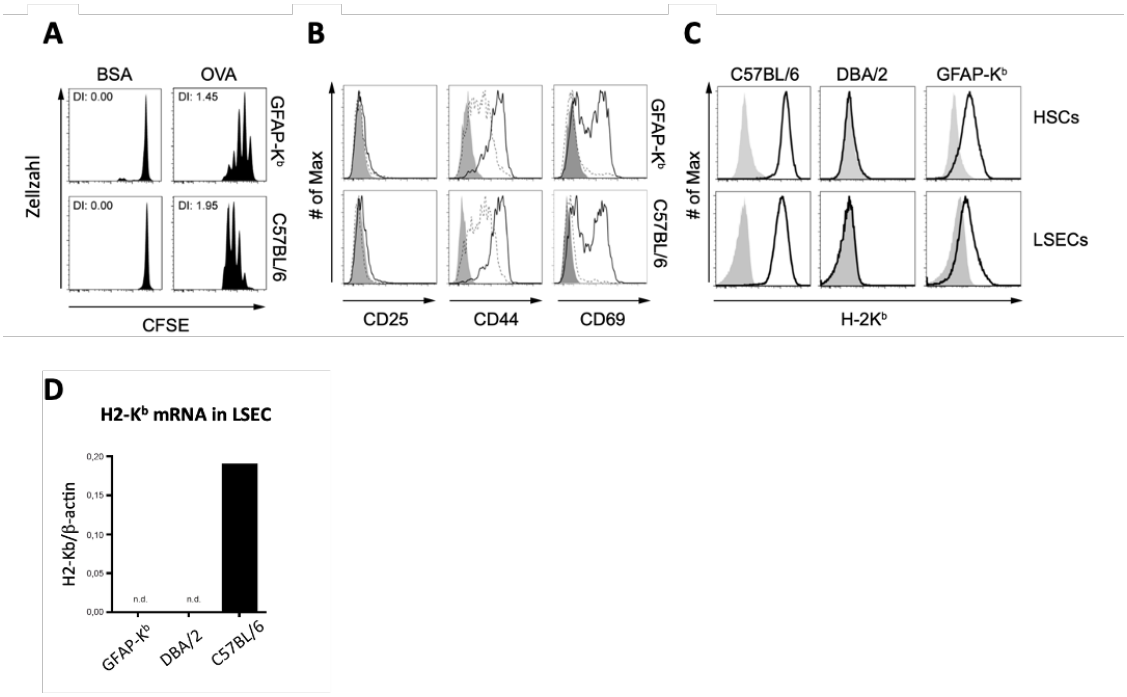

Abbildung 1: Der Transfer von MHC-I Molekülen auf LSEC ermöglicht die Stimulation von CD8+ T Zellen in Mäusen mit HSC-spezifischer MHC-I Expression

(A) Proliferation und (B) Oberflächenexpression von Aktivierungsmarkern an Tag 2 nach adoptivem Transfer von CFSE-markierten, naiven, OVA-spezifischen CD45.1+ OT-I T Zellen (1,5 x 10^6/Maus) in CD45.2+ C57BL/6 oder GFAP-K^b transgene Mäuse, die mit OVA oder BSA (1mg/Maus) behandelt wurden. (C) Ex vivo H2-K^b Expression in HSCs und LSECs aus C57BL/6, DBA/2 oder GFAP-K^b Mäusen. (D) H2-K^b mRNA Expression in LSEC aus GFAP-K^b Mäusen. n.d. = nicht detektiert

Basierend auf einem in vitro Kokulturmodell konnte gezeigt werden, dass ein Transfer von H-2K^b Molekülen zwischen HSC und LSEC stattfindet, welcher als *cross-allocation* bezeichnet wurde (Abb. 2A-C). Um zu untersuchen, ob die durch *cross-allocation* erworbenen H-2K^b Moleküle zur Antigenkreuzpräsentation verwendet werden können, wurden LSEC aus GFAP-K^b Mäusen isoliert, mit OVA beladen und mit OVA-spezifischen T Zellen kultiviert. Hierbei zeigte sich, dass diese LSEC H-2K^b aufnehmen und die erworbenen H-2K^b Moleküle sogar zur Antigenkreuzpräsentation verwenden können (Abb. 2 D-E).

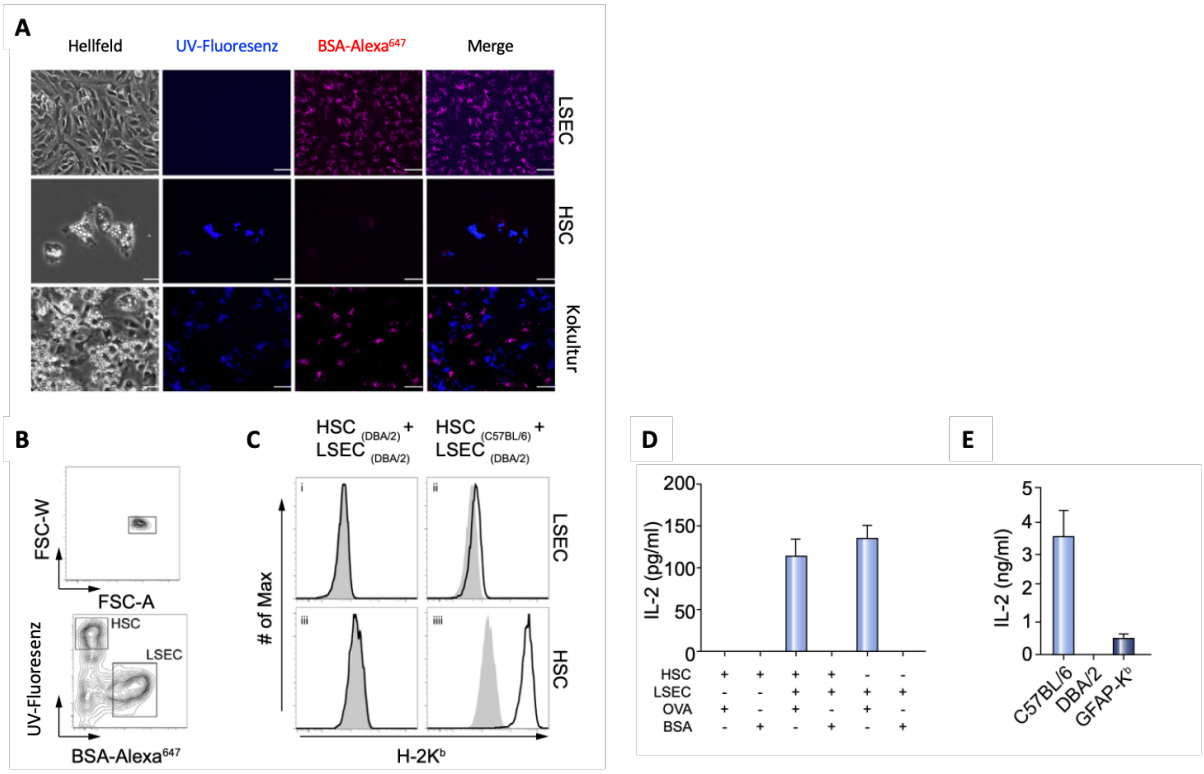

Abbildung 2: Transfer von H2-K^b Molekülen von HSCs auf LSECs in Kokultur in vitro.
(A) Kultur von durchfusszytometrisch sortierten LSECs oder HSCs oder Kokultur. HSCs sind UV-fluoreszent, LSECs sind durch Aufnahme von BSA-Alexa 647 markiert. Maßstabsskala 25um. (B) Durchflusszytometrie Gating Strategie für die Analyse sortierter HSCs und LSECs nach Kokultur in (A). (C) H2-K^b Oberflächenexpression in LSECs oder HSCs, Isotypkontrolle in grau. (D) Ex vivo Kreuzpräsentationskapazität von durchfusszytometrisch sortierten HSCs, die 1h nach i.v. Gabe von peptidfreiem OVA oder BSA aus Mäusen isoliert wurden: IL-2 Expression von B3Z Zellen nach Kokultur mit HSCs. (E) Kreuzpräsentation von LSECs aus C57BL/6, DBA/2 oder GFAP-K^b Mäusen, nach in vitro Inkubation mit peptidfreiem OVA: IL-2 Expression von B3Z Zellen.

Weiter konnte gezeigt werden, dass der Transfer von H-2K^b Molekülen zwischen HSC und LSEC mit einem Austausch von Teilen der Zellmembran einher geht (Abb. 3A). Ein solcher Austausch von Membranbestandteilen fand sowohl von HSC zu LSEC als auch von LSEC zu HSC statt (Abb. 3B-C). Weiterhin konnte in GFAP-K^b Mäusen ausschließlich in der Leber ein Transfer von H-2K^b Molekülen von HSC zu Kupffer Zellen und dendritischen Zellen festgestellt werden (Abb. 3D).

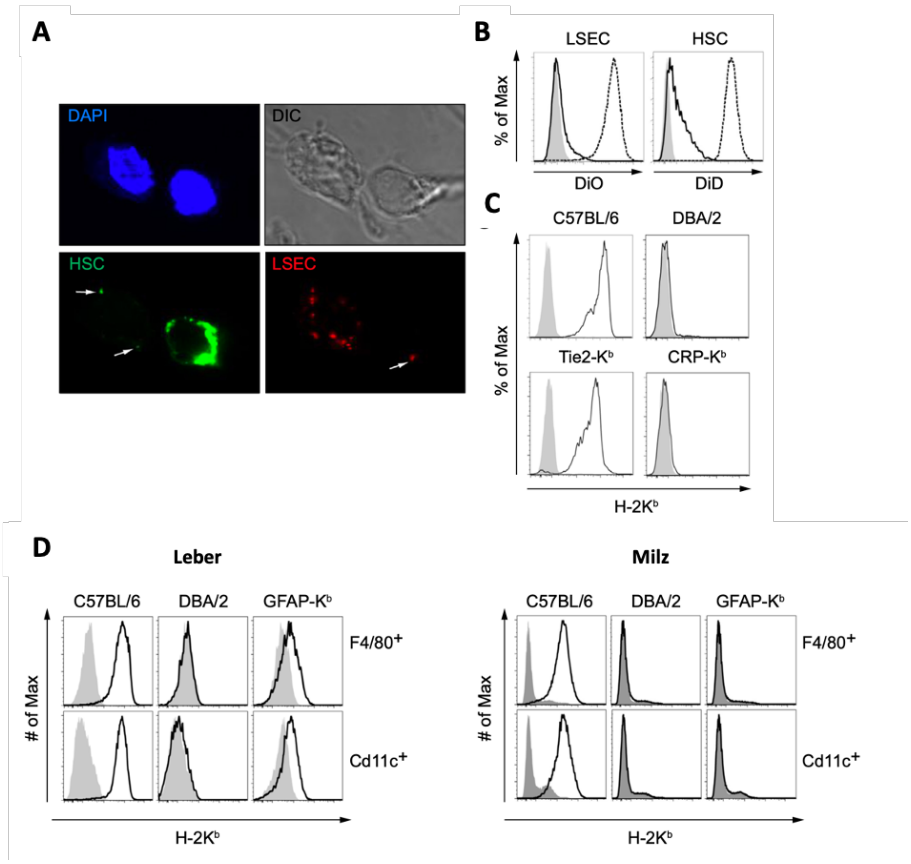

Abbildung 3: Bidirektionale *cross-allocation* in sinusoidalen Leberzellen

(A) Visualisierung des Membranaustausches zwischen LSECs und HSCs durch Konfokalmikroskopie. Kokultur der HSC Zelllinie LX-2 markiert mit DiO (grün) und der LSEC Zelllinie SKHEP markiert mit DiD (rot) für 12 Stunden. (B) Durchflusszytometrische Analyse der DiO Fluoreszenz in LSEC und der DiD Fluoreszenz in HSCs nach Kokultur (durchgängige Linien), Hintergrund-Kontrollen in grau, positive Kontrollen in gestrichelten Linien. (C) H2-K^b Oberflächenexpression in HSC aus C57BL/6, DBA/2, Tie-K^b oder CRP-K^b Mäusen. (D) H2-K^b Oberflächenexpression ex vivo auf F4/80+ Kupffer Zellen und CD11c DCs aus Leber oder Milz von C57BL/6, DBA/2 oder GFAP-K^b Mäusen.

Um die Relevanz des Phänomens *cross-allocation* im Kontext einer viralen Hepatitis zu untersuchen, wurden GFAP-K^b Mäuse mit einem Adenovirus infiziert, welcher OVA exprimiert (AdOVA) und vorzugsweise Hepatozyten infiziert. OVA wird in diesem Modell an OVA-spezifische CTLs kreuzpräsentiert, welche dann virusinfizierte Hepatozyten eliminieren. Außerdem kommt es zur Infiltration weiterer Leukozyten in die Leber. In der GFAP-K^b Maus konnte in histologischen Schnitten der Leber ein ähnliches Ausmaß an Leukozyteninfiltration festgestellt werden, wie in Wildtyp Mäusen (Abb. 4A). Außerdem war die Leberschädigung gemessen anhand des Serum ALT Levels genauso stark wie in Wildtyp Mäusen (Abb. 4B), was auf eine vollständige Immunaktivierung in diesem Hepatitismodell hinweist. Um auszuschließen, dass in diesem Modell außer Hepatozyten auch andere Zellen das Antigen OVA exprimieren und zur Immunaktivierung beitragen, wurden GFAP-K^b Mäuse nun mit

einem Adenovirus infiziert, der OVA unter dem heptozytenspezifischen TTR-Promoter exprimiert. Auch in diesem Experiment entwickelten GFAP-K^b Mäusen eine Leberschädigung, die vergleichbar zu der in Wildtyp Mäusen war (Abb. 4C), was darauf hinweist, dass LSEC OVA über durch *cross-allocation* erworbene H-$2K^b$ Moleküle an OVA-spezifische zytotoxische T Zellen kreuzpräsentieren.

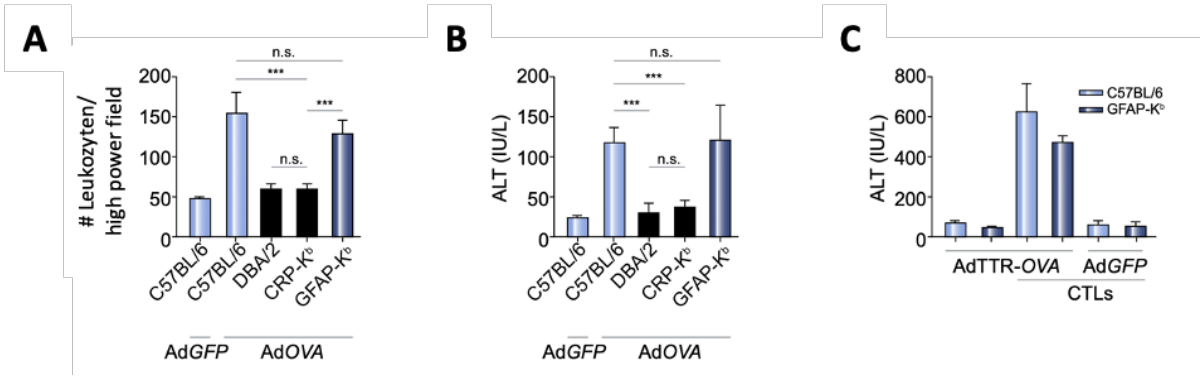

Abbildung 4: Bedeutung der *cross-allocation* von HSC H2-K^b Molekülen für die Immunüberwachung in der Leber

Infektion von C57BL/6, DBA/2 oder transgenen Mäusen mit H2-K^b Expression unter zelltypspezifischen Promotern mit AdOVA (2 x 10^8 pfu/Maus) and Transfer von in vitro-aktivierten OVA-spezifischen OT-1 CTLs (1x10^7/Maus) nach 48h. (A) Quantifizierung von Leukozyten pro high power field aus histologischen Schnitten der Mausleber. (C) Serum ALT Levels 48h nach CTL Transfer. (D) Infektion von C57BL/6 oder GFAP-K^b Mäusen mit einem Adenovirus, der OVA unter dem TTR-Promoter exprimiert (AdTTR-OVA, 2 x 10^9 pfu/Maus) und Transfer von in vitro-aktivierten, OVA-spezifischen CTLs (1 x 10^7/Maus). Serum ALT Levels 48h nach CTL Transfer. ***p<0.001, n.s. = nicht signifikant

Somit unterstützt *cross-allocation* von MHC I Molekülen die antivirale Immunantwort in der Leber und könnte deshalb einen wichtigen Mechanismus für die Verbesserung der lokalen Immunüberwachung in der Leber darstellen. Besondere Relevanz kommt der *cross-allocation* von MHC I Molekülen möglicherweise bei Entwicklung neuer therapeutischer Strategien gegen die Umgehung sog. *immune escape* Mechanismen von Erregern oder Tumoren zu, die durch Herabregulation der MHC I Expression auf der Zelloberfläche die Induktion einer Immunantwort verhindern.

3.2 AICAR and Compound C modulieren die HCC-induzierte Aktivierung primärer hepatischer Sternzellen negativ

Das HCC gehört zu den häufigsten Krebsarten weltweit und verursacht einen großen Anteil der krebsbedingten Todesfälle[37]. In über 80% der Fälle entwickelt sich das HCC auf dem

Boden einer Leberzirrhose, bei der aktivierte HSC große Mengen Kollagen produzieren, das sich dann als Gewebesepten ablagert[38]. Dieses Stroma, insbesondere aktivierte HSC, sind für die Entstehung des HCC von zentraler Bedeutung[39-41]. Zudem konnte gezeigte werden, dass das Enzym Adenosinmonohosphat-aktivierte Proteinkinase (AMPK), das als Energiesensor der Zelle fungiert und somit u.a. für die Aktivierung von Zellen wichtig ist, zu verschiedenen Schritten der Tumorgenese und -progression des HCC beiträgt[42-44]. In dieser Studie wurde die Wechselwirkung zwischen HCC Zelllinien und HSC untersucht. Insbesondere wurde der Effekt von HCC Zellen auf die Aktivierung, Proliferation und AMPK Aktivität in HSC analysiert.

Hierzu wurden primäre, humane HSC mit konditioniertem Medium verschiedener HCC Zelllinien kultiviert und deren Aktivierungsstatus, Proliferation und AMPK Aktivität gemessen. Sowohl HepG2, als auch PLC/PRF/5 Zellen induzierten die Expression verschiedener Gene, die auf eine Aktivierung von HSC hindeuten (Abb. 5A). Interessanterweise stimulierte jedoch nur das konditionierte Medium von HepG2 Zellen die HSC Proliferation (Abb. 5B). Die Aktivierung von AMPK ist durch Phosphorylierung der katalytischen α-Untereinheit an Thr172 (AMPK-Thr172) gekennzeichnet und reguliert neben dem zellulären Metabolismus deren Proliferation im negativen Sinne (siehe Schema in Abb. 5D). Passend zur Induktion der Proliferation durch HepG2 konditioniertes Medium beobachteten wir ausschließlich nach Kultur mit konditioniertem Medium von PLC/PRF/5, jedoch nicht von HepG2 Zellen, eine Aktivierung von AMPK durch deren Phosphorylierung in HSC (Abb. 5C).

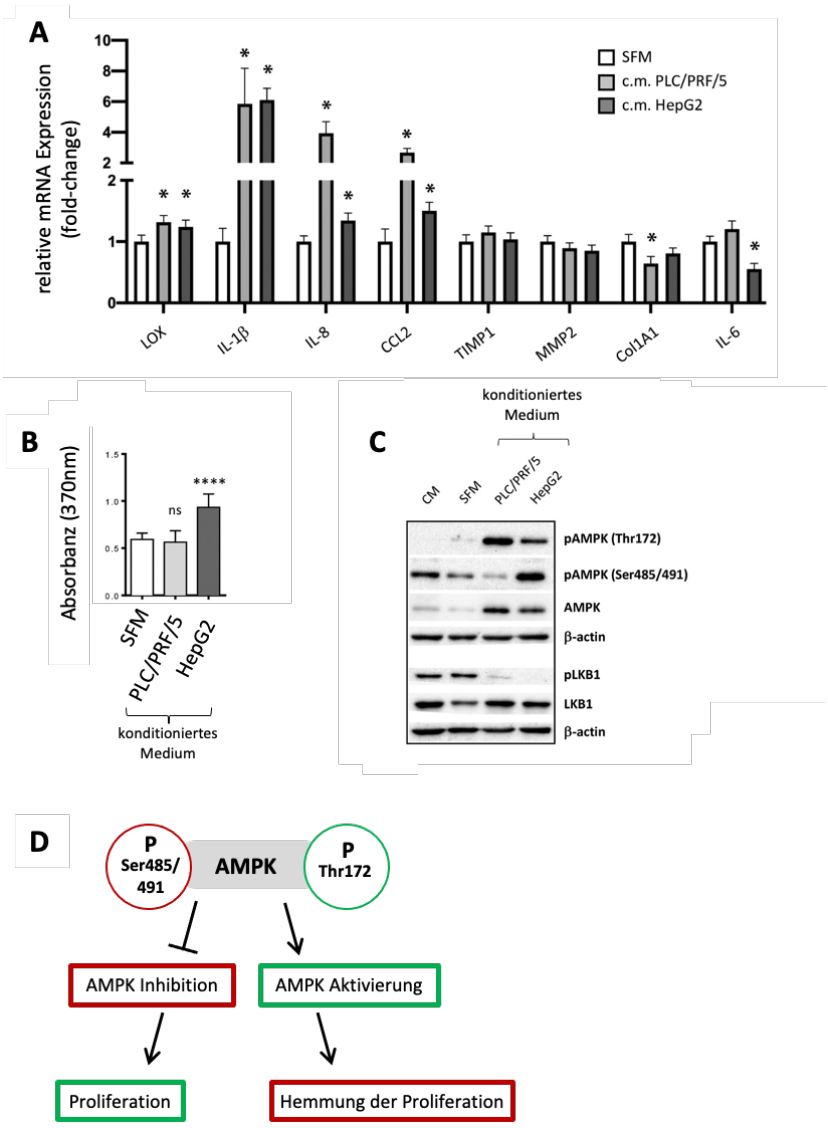

Abbildung 5: Konditioniertes Medium von HCC Zellen aktiviert HSC und beeinflusst den AMPK Signalweg in HSC

Genexpression (A) und Proliferation (B) und AMPK Aktivierung (C) in HSC, die für 24h mit konditioniertem Medium von PLC/PRF/5 oder HepG2 Zellen kultiviert wurden. (D) Schema über AMPK Phosphorylierungsstellen und AMPK Aktivierung. (A) Mittelwert +/- 95% Konfidenzintervall, *p=0,05, (B) Mittelwert +/- Standardabweichung ****p<0,0001, ns = nicht signifikant

Weiter wurde der Effekt von AMPK-modulierenden Substanzen auf die HSC Aktivierung und Proliferation durch HCC Zellen untersucht. Wie in Abbildung 6 dargestellt, konnten sowohl 5-Aminoimidazol-4-Carboxamid-1-b-d-Ribofuranosid (AICAR) als auch Compound C die HCC-induzierte Aktivierung (Abb. 6A) und Proliferation (Abb. 6B) von HSC rückgängig machen. Während AICAR eine Aktivierung durch p-AMPK-Thr172 in HSC induzierte, konnte keine AMKP Aktivierung durch Compound C beobachtet werden (Abb. 6C), was darauf hinweist,

dass die beiden Substanzen ihre Effekte auf Tumor-Stroma-Interaktionen im HCC auf unterschiedliche Weise vermitteln.

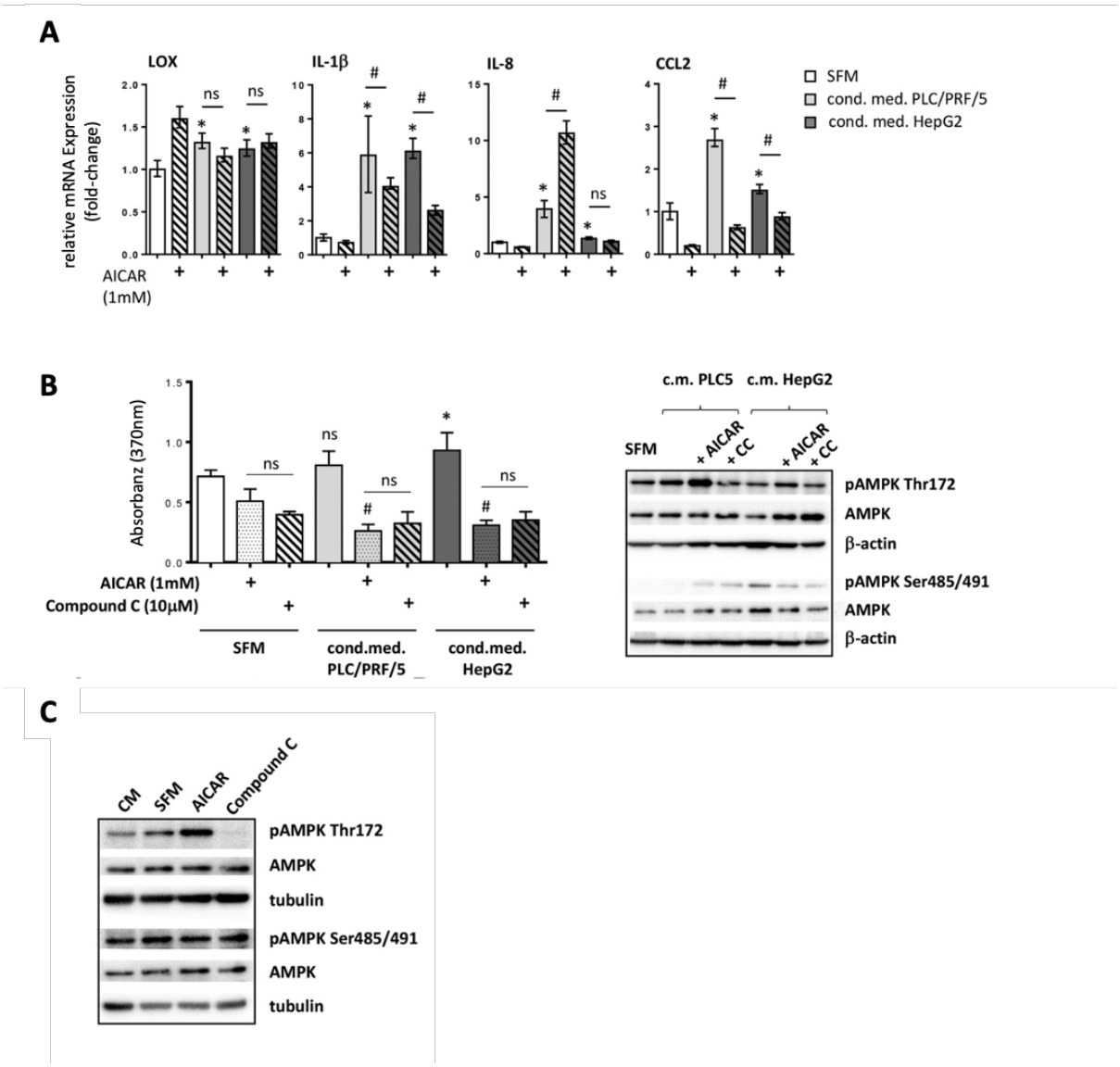

Abbildung 6: AICAR und Compound C machen die HCC-induzierte HSC Aktivierung rückgängig

Genexpression (A), Proliferation und Proteinexpression (B) in HSC, die für 24h mit HCC konditioniertem Medium und AICAR (1mM) oder Compound C (10μm) behandelt wurden. (C) Proteinexpression in HSC nach Behandlung mit AICAR (1mM) oder Compound C (10 μm) für 24h. (A) Mittelwert +/- 95% Konfidenzintervall, (B) Mittelwert +/- Standardabweichung, *p<0,05 vs. SFM, # p< 0,05 vs. nicht mit AICAR behandelte Kontrolle, ns = nicht signifikant

Mithilfe von AMPK knockout Mausembryofibroblasten (MEFs) konnte gezeigt werden, dass sowohl AICAR als auch Compound C den Zellzyklus unabhängig von AMPK hemmen (Abb. 7A-B). Weiter führte die Behandlung mit AICAR in HSC zu einer AMPK-abhängigen

Hemmung des mTORC1 Signalweges (Abb. 7C-D), der dem AMPK Signalweg nachgeschaltet und als wichtiger Regulator der Zellproliferation bekannt ist.

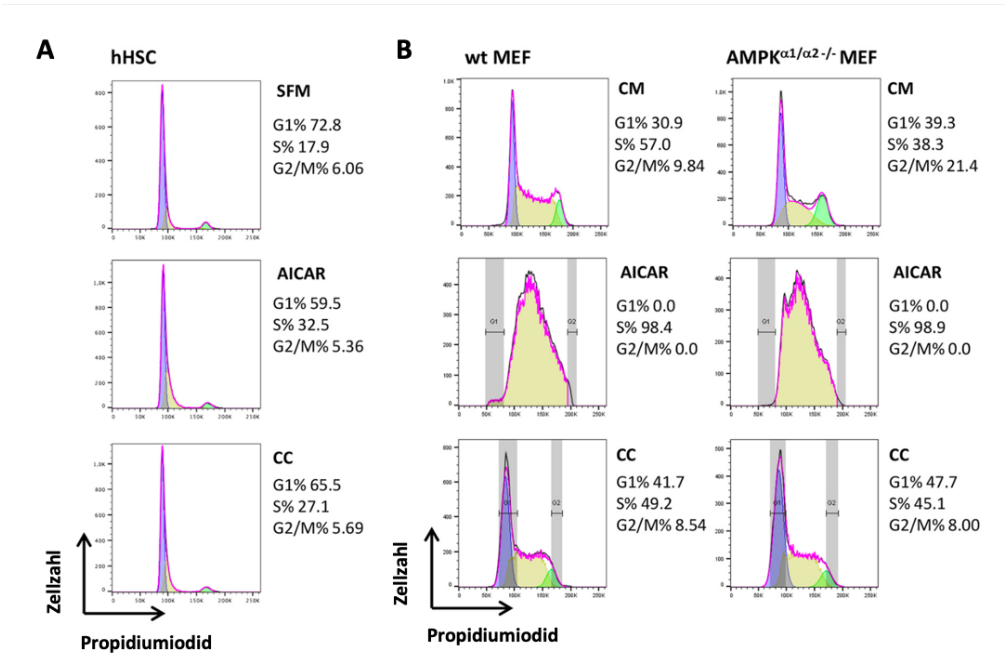

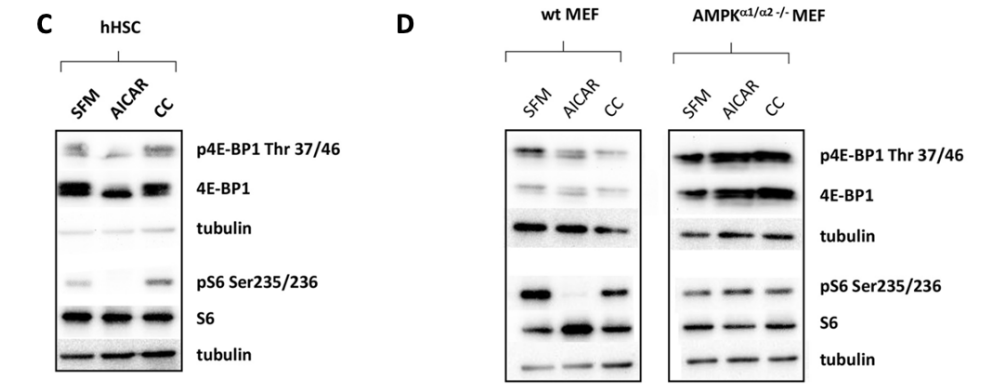

Abbildung 7: AICAR und Compound C hemmen die HSC Proliferation über verschiedene Mechanismen
(A) Zellzyklusanalyse in HSC, die für 24h mit 1mM AICAR oder 10μm Compound C behandelt wurden. (B) Zellzyklusanalyse in Wildtyp (wt) und AMPK$^{\alpha1/\alpha2-/-}$ MEFs, die für 24h mit 0,5mM AICAR oder 10μm Compound C behandelt wurden. (C) Proteinexpression in HSC, die für 24h mit 1mM AICAR oder 10 μm Compound C behandelt wurden. (D) Proteinexpression in wt und AMPK$^{\alpha1/\alpha2-/-}$ MEFs, die für 24h mit 0,25mM AICAR oder 10 μm Compound C behandelt wurden. AMPK$^{\alpha1/\alpha2-/-}$ = AMPK Untereinheit α1α2-defizient; CC = Compound C; CM = Komplettes Medium; hHSC, humane HSC; SFM = Serum-freies Medium

Somit konnte gezeigt werden, dass AICAR und Compound C ihre Effekte auf die Zellproliferation auf unterschiedliche, teils AMPK abhängige Weise vermitteln. Insgesamt

weisen diese Daten darauf hin, dass AMPK an Tumor-Stroma Interaktionen in HCC beteiligt ist und ein potentielles Zielmolekül für die Entwicklung neuer therapeutische Ansätze zur HCC Therapie darstellt.

3.3 MAIT cells sind in Patienten mit autoimmunen Lebererkrankungen aktiviert und fördern die pro-fibrogene Aktivierung hepatischer Sternzellen

Autoimmune Lebererkrankungen (AIL) wie Autoimmunhepatitis, primär sklerosierende Cholangitis und primär biliäre Cholangitis gehen mit der Entwicklung einer Leberfibrose und -zirrhose einher[45,46]. Bis heute sind die therapeutischen Optionen zu deren Behandlung jedoch limitiert. MAIT cells sind sog. *innate-like* T Zellen, die durch einen semi-invarianten TCR gekennzeichnet sind. Dieser befähigt sie zur Erkennung von Antigenen, die aus dem Vitamin-B Stoffwechsel stammen[23]. Abgesehen von der TCR-abhängigen Stimulation können MAIT cells auch durch Zytokine, v.a. IL-12 und IL-18 aktiviert werden[24]. MAIT cells kommen v.a. in der Leber vor, wo sie bis zu 30% der intrahepatischen T Zellen ausmachen und werden als wichtige Mediatoren der hepatischen Inflammation angesehen[47]. In dieser Studie wurde untersucht, welche Rolle MAIT cells für die Entwicklung der Leberfibrose in AIL spielen, und ob diese phänotypisch und funktionell verändert sind.
Es konnte gezeigt werden, dass MAIT cells im Blut von AIL Patienten signifikant vermindert sind (Abb. 8A), und dass die MAIT cell Zahl negativ mit dem Fibrosestadium der Patienten korreliert (Abb. 8B).

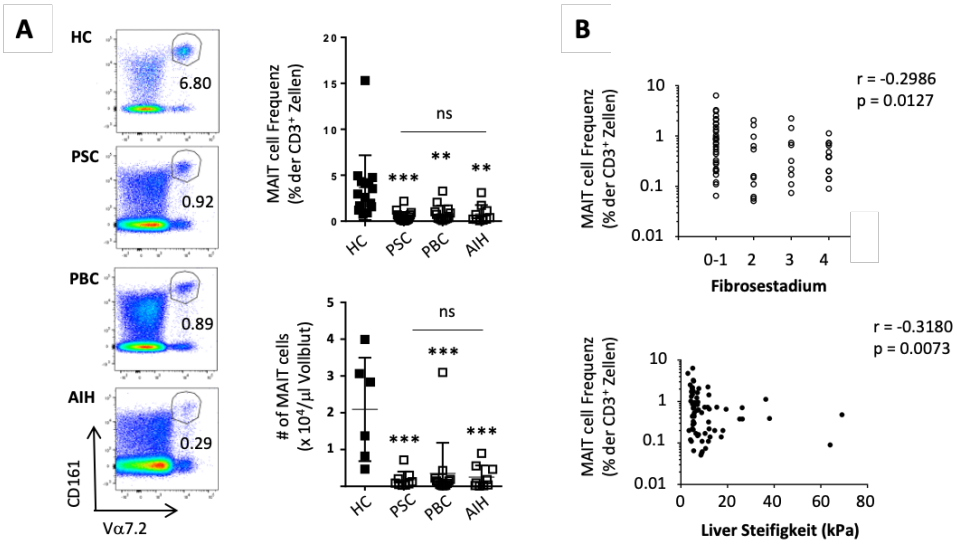

Abbildung 8: Die MAIT cell Frequenz ist in Patienten mit AIL signifikant vermindert

(A) MAIT cell Frequenz und absolute Zellzahl im peripheren Blut von AIL Patienten (B) Spearman Korrelation zwischen MAIT cell Frequenz und Fibrosestadium bzw. Lebersteifigkeit (n=70). ** $p<0.01$, ***$p<0.001$, ns = nicht signifikant. HC = Gesunde Kontrolle, PSC = primär sklerosierende Cholangitis, PBC = primär biliäre Cholangitis, AIH = Autoimmunhepatitis.

Die verbleibenden MAIT cells wiesen einen aktivierten Phänotyp auf, exprimierten aber auch vermehrt Marker, die auf sog. *exhaustion* hinweisen (Abb. 9A-B). Zudem produzierten AIL MAIT cells nach in vitro Re-stimulation signifikant weniger IFNγ (Abb. 9C) und GrzB (Abb. 9D) als MAIT cells von gesunden Kontrollen, während die Expression von TNFα und dem profibrogenen Zytokin IL-17A unverändert waren (Abb. 9E).

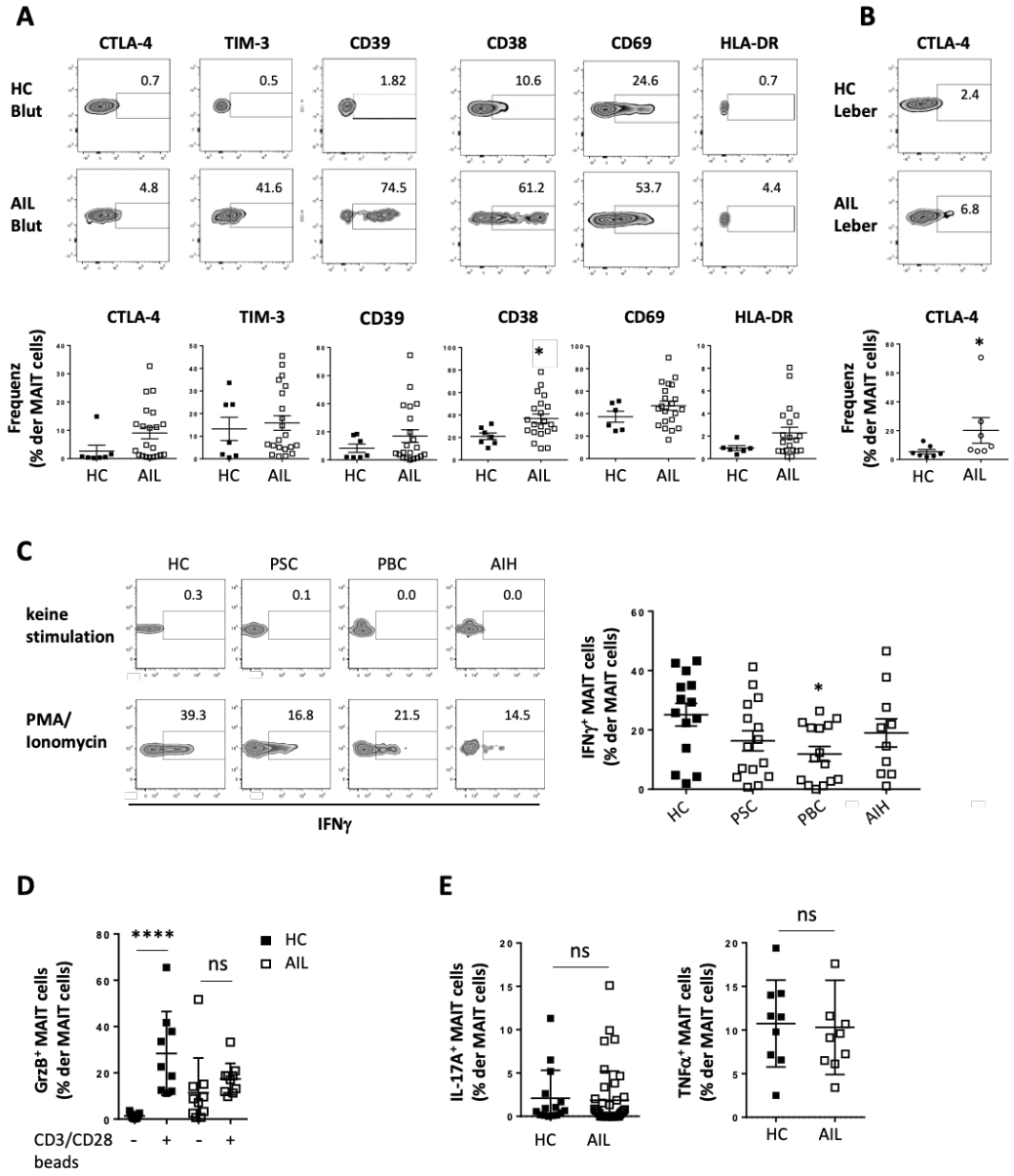

Abbildung 9: AIL MAIT cells weisen Merkmale der *exhaustion* auf und können IL-17A exprimieren

Oberflächenexpression von Aktivierungs- und *exhaustion*markern in MAIT cells aus peripherem But (A) und Leber (B) von AIL Patienten und gesunden Kontrollen. Intrazelluläre Expression von (C) IFNγ, (D) GrzB, (E) IL-17A und TNFα in MAIT cells aus AIL Patienten und gesunden Kontrollen nach in vitro Stimulation mit PMA/Ionomycin (C, E) oder anti-CD3/CD28 beads (D) für 16h. *p<0.05, ****p<0.0001, ns = nicht signifikant. HC = Gesunde Kontrolle, PSC = primär sklerosierende Cholangitis, PBC = primär biliäre Cholangitis, AIH = Autoimmunhepatitis.

Das Phänomen der *exhaustion*, gekennzeichnet durch einen Rückgang der IFNγ Expression (Abb. 10A-B) und eine höhere Expression inhibitorischer Rezeptoren (Abb. 10C), konnte in vitro durch Langzeit-Exposition von MAIT cells gegenüber den Zytokinen IL-12 und IL-18 rekapituliert werden.

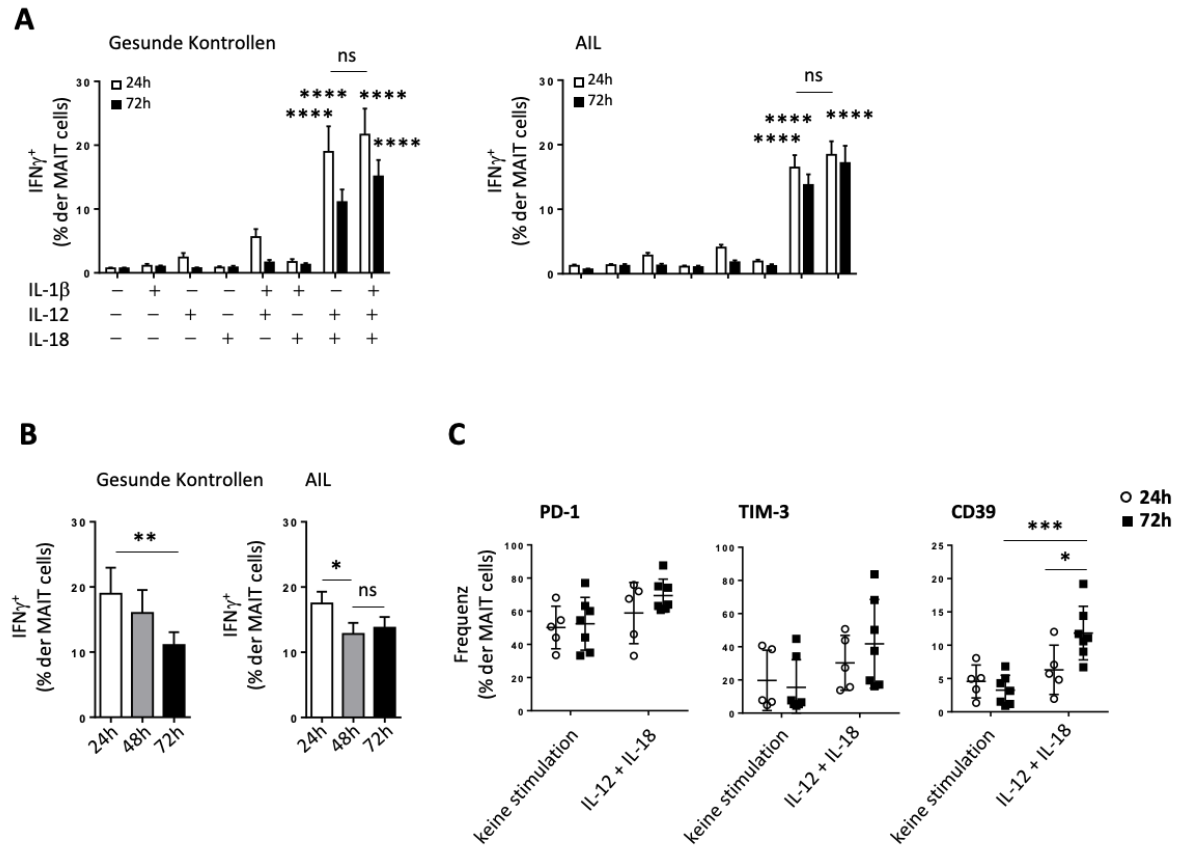

Abbildung 10: MAIT cell Exhaustion wird durch Langzeitbehandlung mit Zytokinen verursacht

Intrazelluläre IFNγ Expression in MAIT cells von AIL Patienten und gesunden Kontrollen nach Stimulation mit IL-1β, IL-12 und IL-18 für 24 -72h. (B) Intrazelluläre IFNγ Expression und (C) Oberflächenexpression von Exhaustionmarkern in MAIT cells nach Stimulation mit IL-12 + IL-18 für 24-72h. *p<0.05, **p>0.01, ***p>0.001, ****p<0.0001, ns = nicht signifikant.

Eine Langzeitstimulation mit IL-12 führte aber sowohl in MAIT cells von gesunden Kontrollen, als auch von AIL Patienten auch zur Expression von IL-17A von MAIT cells (Abb. 11A-B).

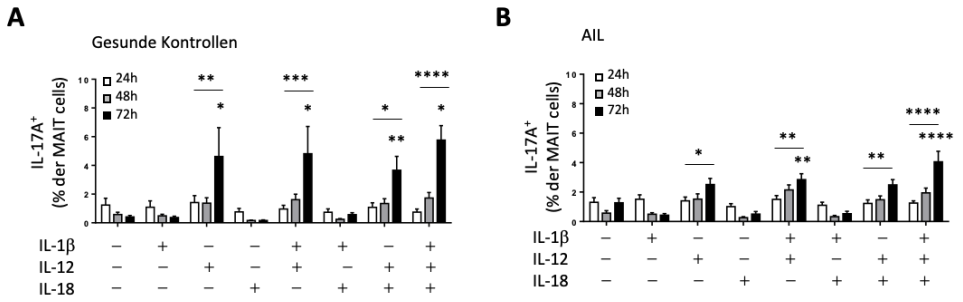

Abbildung 11: Langzeitstimulation mit IL-12 führt zur Expression von IL-17A von MAIT cells

Intrazelluläre Expression von IL-17A in (A) Gesunden Kontrollen und (B) AIL Patienten nach Stimulation mit IL-1β, IL-12 und IL-18 für 24-72h. *p<0.05, **p>0.01, ***p>0.001, ****p<0.0001, ns = nicht signifikant.

Deshalb wurde als nächstes untersucht, ob MAIT cells die Aktivierung von HSC vermitteln können. Eine solche HSC Aktivierung ist für die Entstehung der Leberfibrose von zentraler Bedeutung, da aktivierte HSC große Mengen extrazellulärer Matrixproteine produzieren, die dann die fibrotischen Septen bilden. Hierzu wurden MAIT cells von gesunden Kontrollen oder AIL Patienten mit primären HSC kokultiviert. Es konnte gezeigt werden, dass HSC nach Kokultur mit MAIT cells signifikant mehr proliferieren (Abb. 12A) und pro-fibrotische Gene wie z.B. Col1A1 (Kollagen 1), LOX (Lysyloxidase) und TIMP-1 (tissue-inhibitor of metalloproteinase), sowie IL-1, IL-6 und CCL2 signifikant hochregulierten (Abb. 12B). Diese Effekte sind typisch für eine HSC Aktivierung und konnten durch Kokultur mit gesunden und AIL MAIT cells erreicht werden. Weiter konnte gezeigt werden, dass die Aktivierung von HSC durch MAIT cells sowohl von IL-17 (Abb. 12C), als auch von direktem Zellkontakt (Abb. 12D) abhängig ist.

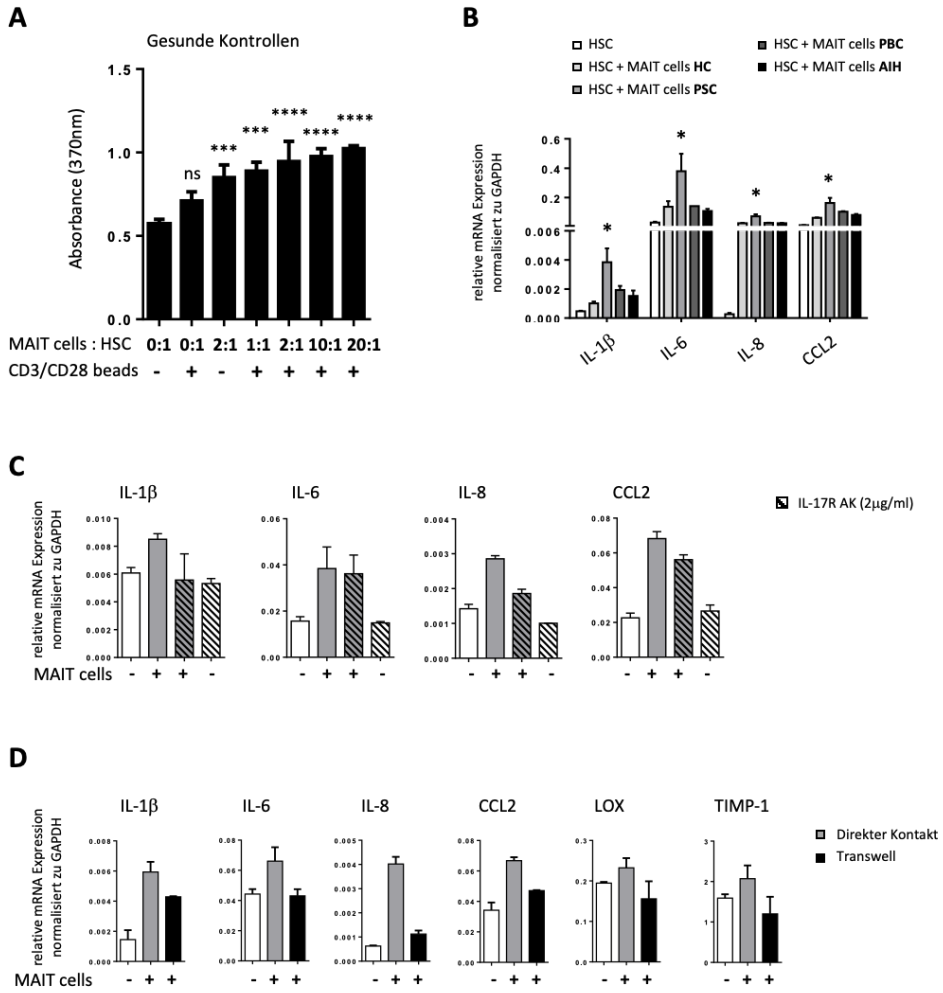

Abbildung 12: MAIT cells vermitelln die Aktivierung von HSC abhängig von IL-17 und Zell-Zell-Kontakt.
(A) Bromodeoxyuridin Aufnahme und (B) Genexpression in HSC nach 48h Kokultur mit MAIT cells von AIL Patienten oder gesunden Kontrollen. Genexpression von HSC nach 48h Kokultur mit MAIT cells aus gesunden Kontrollen mit IL-17-Rezeptor Antikörper (C) oder in einem Transwell System (D). *p<0.05, ***p>0.001, ****p<0.0001, ns = nicht signifikant. HC = Gesunde Kontrolle, PSC = primär sklerosierende Cholangitis, PBC = primär biliäre Cholangitis, AIH = Autoimmunhepatitis.

Zusammenfassend zeigen diese Daten, dass MAIT cells in Patienten mit AIL einen speziellen, IL-17 exprimierenden Phänotyp aufweisen und dass IL-17 produzierende MAIT cells zur Fibroseentstehung in AIL beitragen können.
Insgesamt tragen die hier zusammengefassten Arbeiten zum besseren Verständnis der lokalen Immunregulation in der Leber bei und bilden so möglicherweise die Grundlage für die Entwicklung neuer therapeutischer Ansätze zur Behandlung chronischer Lebererkrankungen.

4. Abkürzungsverzeichnis

NAFDL	Nicht-alkoholische Fettlebererkrankung
AdOVA	Ovalbumin exprimierendes Adenovirus
AICAR	5-aminoimidazole-4-carboxamide-1-b-d-ribofuranosid
AIL	Autoimmune Lebererkrankungen
ALT	Alaninaminotransferase
AMPK	Adenosine monohosphate-activated kinase
APCs	Antigenpräsentierenden Zellen
CD	Cluster of differentiation
CTLs	Zytotoxische T Lymphozyten
DCs	Zendritische Zellen
GFAP	Glial fibrillary acidic protein
GrzB	Granzym B
H2-Kb	Murines MHC Klasse I Molekül
HCC	Hepatozelluläres Karzinom
HSC	Hepatische Sternzellen
IFNγ	Interferon gamma
IL	Interleukin
LSEC	Sinusoidalen Leberendothelzellen
MAIT cell	Mucosal-associated invariant T cell
MEFs	Mausembryofibroblasten
MHC-I	Major histocompatibility complex I
mRNA	Messenger Ribonukleinsäure
mTORC1	Mammalian target of rapamycin complex 1
OVA	Ovalbumin
PAMP	Pathogen-associated molecular patterns
PD-L1	Programmed death 1 ligand 1
RT-PCR	Real-time Polymerasekettenreaktion
TCR	T-Zell Rezeptor
TGFβ	Tumour growth factor beta
TNFα	Tumornekrosefaktor alpha
Treg	Regulatorische T Zellen

5. Literaturverzeichnis

1 Friedman, S. L. & Pinzani, M. Hepatic fibrosis 2022: Unmet needs and a blueprint for the future. *Hepatology* **75**, 473-488, doi:10.1002/hep.32285 (2022).

2 Bataller, R. & Brenner, D. A. Liver fibrosis. *Journal of Clinical Investigation* **115**, 209-218, doi:10.1172/JCI200524282 (2005).

3 Younossi, Z. M. *et al.* Epidemiology of chronic liver diseases in the USA in the past three decades. *Gut* **69**, 564-568, doi:10.1136/gutjnl-2019-318813 (2020).

4 Seki, E. & Schwabe, R. F. Hepatic Inflammation and Fibrosis: Functional Links and Key Pathways. *Hepatology*, doi:10.1002/hep.27332 (2014).

5 Bataller, R., Paik, Y. H., Lindquist, J. N., Lemasters, J. J. & Brenner, D. A. Hepatitis C virus core and nonstructural proteins induce fibrogenic effects in hepatic stellate cells. *Gastroenterology* **126**, 529-540 (2004).

6 Thorgeirsson, S. S. & Grisham, J. W. Molecular pathogenesis of human hepatocellular carcinoma. *Nat Genet* **31**, 339-346 (2002).

7 Knolle, P. A. & Gerken, G. Local control of the immune response in the liver. *Immunological Reviews* **174**, 21-34, doi:10.1034/j.1600-0528.2002.017408.x (2000).

8 Thomson, A. W. & Knolle, P. A. Antigen-presenting cell function in the tolerogenic liver environment. *Nature Publishing Group* **10**, 753-766, doi:10.1038/nri2858 (2010).

9 Tiegs, G. & Lohse, A. W. Immune tolerance: What is unique about the liver. *Journal of Autoimmunity* **34**, 1-6, doi:10.1016/j.jaut.2009.08.008 (2010).

10 Schildberg, F. A., Kurts, C. & Knolle, P. A. Prominent regulatory but weak antigen-presenting cell function of hepatic stellate cells. *Hepatology* **54**, 1108, doi:10.1002/hep.24565 (2011).

11 Schildberg, F. A. *et al.* Murine hepatic stellate cells veto CD8 T cell activation by a CD54-dependent mechanism. *Hepatology* **54**, 262-272, doi:10.1002/hep.24352 (2011).

12 Limmer, A. *et al.* Efficient presentation of exogenous antigen by liver endothelial cells to CD8+ T cells results in antigen-specific T-cell tolerance. *Nat Med* **6**, 1348-1354, doi:10.1038/82161 (2000).

13 Schurich, A. *et al.* Distinct kinetics and dynamics of cross-presentation in liver sinusoidal endothelial cells compared to dendritic cells. *Hepatology* **50**, 909-919, doi:10.1002/hep.23075 (2009).

14 Diehl, L. *et al.* Tolerogenic maturation of liver sinusoidal endothelial cells promotes B7-homolog 1-dependent CD8+ T cell tolerance. *Hepatology* **47**, 296-305, doi:10.1002/hep.21965 (2007).

15 Schurich, A. *et al.* Dynamic Regulation of CD8 T Cell Tolerance Induction by Liver Sinusoidal Endothelial Cells. *The Journal of Immunology* **184**, 4107-4114, doi:10.4049/jimmunol.0902580 (2010).

16 Karrar, A., Broome, U., Uzunel, M., Qureshi, A. R. & Sumitran-Holgersson, S. Human liver sinusoidal endothelial cells induce apoptosis in activated T cells: a role in tolerance induction. *Gut* **56**, 243-252, doi:10.1136/gut.2006.093906 (2007).

17 Hochst, B. *et al.* Activated human hepatic stellate cells induce myeloid derived suppressor cells from peripheral blood monocytes in a CD44-dependent fashion. *J Hepatol* **59**, 528-535, doi:10.1016/j.jhep.2013.04.033 (2013).

18 Protzer, U., Maini, M. K. & Knolle, P. A. Living in the liver: hepatic infections. *Nature reviews. Immunology* **12**, 201-213, doi:10.1038/nri3169 (2012).

19 Dusseaux, M. *et al.* Human MAIT cells are xenobiotic-resistant, tissue-targeted, CD161hi IL-17-secreting T cells. *Blood* **117**, 1250-1259, doi:10.1182/blood-2010-08-303339 (2011).

20 Tang, X. Z. *et al.* IL-7 licenses activation of human liver intrasinusoidal mucosal-associated invariant T cells. *Journal of immunology* **190**, 3142-3152, doi:10.4049/jimmunol.1203218 (2013).

21 Böttcher, K. *et al.* MAIT cells are chronically activated in patients with autoimmune liver disease and promote pro-fibrogenic hepatic stellate cell activation. *Hepatology*, doi:10.1002/hep.29782 (2018).

22 Porcelli, S., Yockey, C. E., Brenner, M. B. & Balk, S. P. Analysis of T cell antigen receptor (TCR) expression by human peripheral blood CD4-8- alpha/beta T cells demonstrates preferential use of several V beta genes and an invariant TCR alpha chain. *The Journal of experimental medicine* **178**, 1-16, doi:10.1084/jem.178.1.1 (1993).

23 Kjer-Nielsen, L. *et al.* MR1 presents microbial vitamin B metabolites to MAIT cells. *Nature* **491**, 717-723, doi:10.1038/nature11605 (2013).

24 Ussher, J. E. *et al.* CD161 ++CD8 +T cells, including the MAIT cell subset, are specifically activated by IL-12+IL-18 in a TCR-independent manner. *European Journal of Immunology* **44**, 195-203, doi:10.1002/eji.201343509 (2013).

25 Kurioka, A. *et al.* MAIT cells are licensed through granzyme exchange to kill bacterially sensitized targets. *Mucosal immunology*, doi:10.1038/mi.2014.81 (2014).

26 Kurioka, A., Walker, L. J., Klenerman, P. & Willberg, C. B. MAIT cells: new guardians of the liver. *Clin Transl Immunology* **5**, e98, doi:10.1038/cti.2016.51 (2016).

27 Boni, C. *et al.* HBV Immune-Therapy: From Molecular Mechanisms to Clinical Applications. *International journal of molecular sciences* **20**, doi:10.3390/ijms20112754 (2019).

28 Finn, R. S. *et al.* Atezolizumab plus Bevacizumab in Unresectable Hepatocellular Carcinoma. *New England Journal of Medicine* **382**, 1894-1905, doi:10.1056/NEJMoa1915745 (2020).

29 Hanahan, D. & Weinberg, R. A. Hallmarks of cancer: the next generation. *Cell* **144**, 646-674, doi:10.1016/j.cell.2011.02.013 (2011).

30 Chen, H.-P. *et al.* Metformin decreases hepatocellular carcinoma risk in a dose-dependent manner: population-based and in vitro studies. *Gut* **62**, 606-615, doi:10.1136/gutjnl-2011-301708 (2013).

31 Qu, Z. *et al.* Exosomes derived from HCC cells induce sorafenib resistance in hepatocellular carcinoma both in vivo and in vitro. *J Exp Clin Cancer Res* **35**, 159, doi:10.1186/s13046-016-0430-z (2016).

32 Knolle, P. A. & Limmer, A. Control of immune responses by savenger liver endothelial cells. *Swiss Med Wkly* **133**, 501-506, doi:2003/37/smw-10261 (2003).

33 Friedman, S. L. Hepatic Stellate Cells: Protean, Multifunctional, and Enigmatic Cells of the Liver. *Physiological Reviews* **88**, 125-172, doi:10.1152/physrev.00013.2007 (2008).

34 Pinzani, M. Pathophysiology of Liver Fibrosis. *Dig Dis* **33**, 492-497, doi:10.1159/000374096 (2015).

35 Ichikawa, S., Mucida, D., Tyznik, A. J., Kronenberg, M. & Cheroutre, H. Hepatic stellate cells function as regulatory bystanders. *Journal of immunology (Baltimore, Md. : 1950)* **186**, 5549-5555, doi:10.4049/jimmunol.1003917 (2011).

36 Winau, F. *et al.* Ito cells are liver-resident antigen-presenting cells for activating T cell responses. *Immunity* **26**, 117-129, doi:10.1016/j.immuni.2006.11.011 (2007).

37 Ferlay, J. *et al.* Cancer incidence and mortality worldwide: Sources, methods and major patterns in GLOBOCAN 2012. *International Journal of Cancer* **136**, E359-E386, doi:10.1002/ijc.29210 (2015).

38 Llovet, J. M. *et al.* Hepatocellular carcinoma. *Nature Reviews Disease Primers* **7**, 6, doi:10.1038/s41572-020-00240-3 (2021).

39 Amann, T. *et al.* Activated hepatic stellate cells promote tumorigenicity of hepatocellular carcinoma. *Cancer Science* **100**, 646-653, doi:10.1111/j.1349-7006.2009.01087.x (2009).

40 Carloni, V., Luong, T. V. & Rombouts, K. Hepatic stellate cells and ECM in HCC: more complicated than ever. *Liver International*, n/a-n/a, doi:10.1111/liv.12465 (2014).

41 Coulouarn, C. *et al.* Hepatocyte-stellate cell cross-talk in the liver engenders a permissive inflammatory microenvironment that drives progression in hepatocellular carcinoma. *Cancer research* **72**, 2533-2542, doi:10.1158/0008-5472.CAN-11-3317 (2012).

42 Chen, H. P. *et al.* Metformin decreases hepatocellular carcinoma risk in a dose-dependent manner: population-based and in vitro studies. *Gut* **62**, 606-615, doi:10.1136/gutjnl-2011-301708 (2013).

43 Cheng, J. *et al.* AMP-Activated Protein Kinase Suppresses the In Vitro and In Vivo Proliferation of Hepatocellular Carcinoma. *PLoS One* **9**, e93256, doi:10.1371/journal.pone.0093256 (2014).

44 Qu, H. & Yang, X. Metformin inhibits angiogenesis induced by interaction of hepatocellular carcinoma with hepatic stellate cells. *Cell Biochem Biophys* **71**, 931-936, doi:10.1007/s12013-014-0287-8 (2015).

45 Arndtz, K. & Hirschfield, G. M. The Pathogenesis of Autoimmune Liver Disease. *Dig Dis* **34**, 327-333, doi:10.1159/000444471 (2016).

46 Liaskou, E., Hirschfield, G. M. & Gershwin, M. E. Mechanisms of tissue injury in autoimmune liver diseases. *Seminars in immunopathology* **36**, 553-568, doi:10.1007/s00281-014-0439-3 (2014).

47 Lett, M. J. *et al.* Stimulatory MAIT cell antigens reach the circulation and are efficiently metabolised and presented by human liver cells. *Gut*, doi:10.1136/gutjnl-2021-324478 (2022).

6. Verzeichnis eigener Schriften

6.1 Originalarbeiten

1. Deschler S, Kager J, Erber J, Fricke L, Koyumdzhieva P, Georgieva A, Lahmer T, Wiessner JR, Voit F, Schneider J, Horstmann J, Iakoubov R, Treiber M, Winter C, Ruland J, Busch DH, Knolle PA, Protzer U, Spinner CD, Schmid RM, Quante M and **Böttcher K**. Mucosal-associated invariant T (MAIT) cells are highly activated and functionally impaired in COVID-19 patients. Viruses 2021. 13(2): 241

2. **Böttcher K**, Longato L, Marrone G, Mazza G, Ghemtio L, Hall A, Luong TV, Caruso S, Viollet B, Zucman-Rossi J, Pinzani M and Rombouts K. AICAR and Compound C negatively modulate HCC-induced primary human hepatic stellate cell activation in vitro. American Journal of Physiology Gastrointestinal and Liver Physiology 2021. doi.org/10.1152/ajpgi.00262.2020

3. Mazza G, Telese A, Al-Akkad W, Frenguelli L, Levi A, Maralli M, Longato L, Thanapirom K, Vilia MG, Lombardi B, Crowley C, Crawford M, Karsdal MA, Leeming DJ, Marrone G, **Bottcher K**, et al. Cirrhotic Human Liver Extracellular Matrix 3D Scaffolds Promote Smad-Dependent TGF-β1 Epithelial Mesenchymal Transition. Cells 2019 .10.3390/cells9010083.

4. **Böttcher K**, Rombouts K, Saffioti F, Roccarina D, Rosselli M, Hall A, Luong T, et al. MAIT cells are chronically activated in patients with autoimmune liver disease and promote pro-fibrogenic hepatic stellate cell activation. Hepatology 2018. 68(1):172-186

5. Alberts R, de Vries EMG, Goode EC, Jiang X, Sampaziotis F, Rombouts K, **Böttcher K**, et al. Genetic association analysis identifies variants associated with disease progression in primary sclerosing cholangitis. Gut 2018;67:1517-1524.

6. Marrone G, De Chiara F, **Böttcher K**, Levi A, Dhar D, Longato L, Mazza G, et al. The adenosine monophosphate-activated protein kinase-vacuolar adenosine triphosphatase-pH axis: A key regulator of the profibrogenic phenotype of human hepatic stellate cells. Hepatology 2018; 68(3):1140-1153

7. Singh HD, Otano I, Rombouts K, Singh KP, Peppa D, Gill US, **Böttcher K**, et al. TRAIL regulatory receptors constrain human hepatic stellate cell apoptosis. Sci Rep 2017;7:5514.

8. **Schölzel K**, Schildberg FA, Welz M, Börner C, Geiger S, Kurts C, Heikenwälder M, et al. Transfer of MHC-class-I molecules among liver sinusoidal cells facilitates hepatic immune surveillance. J Hepatol 2014;61:600-608.

6.2 Reviews und Case Reports

1. Huber W, Lorenz G, Heilmaier M, **Böttcher K**, Sahm P, Middelhoff M, Ritzer B, Schulz D, Bekka E, Hesse F, Poszler A, Geisler F, Spinner CD, Schmid RM and Lahmer T. Extracorporeal multiorgan support including CO2-removal with the ADVanced Organ Support (ADVOS) system for COVID-19: A case report. The International Journal of Artificial Organs 2020. DOI: 10.1177/0391398820961781

2. **Böttcher K**, Pinzani M. Pathophysiology of liver fibrosis and the methodological barriers to the development of anti-fibrogenic agents. Adv Drug Deliv Rev 2017;121:3-8.

Eingeworbene Drittmittel

Else Kröner Fresenius Stiftung: Rotationsstelle Ärztin 24 Monate, Sachmittel	230.000€
Deutsche Forschungsgemeinschaft (DFG): Rotationsstelle Ärztin 12 Monate, Dokotrandenstelle 36 Monate, Sachmittel	354.400€
Fakultät für Medizin der TUM, **Bayerisches Staatministerium für Wissenschaft und Kunst**: Doktorandenstelle für 10 Monate, Sachmittel	70.000€
Kommission für Klinische Forschung (KKF) der Medizinischen Fakultät der TUM: Rotationsstelle Ärztin für 12 Monate, Sachmittel	74.000€
European Association for the Study of the Liver (EASL) Physician Scientist Stipendium: Postdoktorandenstelle für 12 Monate	40.000€

8. Danksagung

Wissenschaftliches Arbeiten ist immer auch ein *team effort* und lebt vom Diskurs, von fachlicher Auseinandersetzung und Kollaboration. Auf meinem bisherigen wissenschaftlichen Weg haben mich viele Vorbilder geprägt und Kollegen begleitet, denen mein Dank gebührt.

Prof. Percy Knolle hat mit der Möglichkeit meine medizinische Doktorarbeit in seiner Arbeitsgruppe an der Universität Bonn anzufertigen den Grundstein für mein wissenschaftliches Interesse, insbesondere für die Leberimmunologie, gelegt. Seine kollegiale, positive und unterstützende Art prägen bis heute mein wissenschaftliches Arbeiten. Dafür, sowie für seine langjährige Unterstützung als Mentor, möchte ich mich von Herzen bedanken.
PD Dr. Dirk Wohlleber und meinen Mitdoktoranden in Bonn danke ich für das Heranführen an die praktische Laborarbeit während meines Promotionsstudiums.

Mein Dank gebührt auch Prof. Massimo Pinzani, MD, PhD, FRCP, der mich nicht nur während meines PhDs in seiner Arbeitsgruppe am University College London immer unterstütze. Hier durfte ich vieles über die Fibroseentstehung in der Leber lernen, und konnte auf unabhängige Weise mein wissenschaftliches Denken und Arbeiten vertiefen, während er mir auch das klinische Arbeiten in der renommierten Abteilung für Hepatologie des Royal Free Hospital ermöglichte.

Herrn Prof. Roland Schmid möchte ich für seine umfassende Unterstützung meines wissenschaftlichen und klinischen Arbeitens am Klinikum rechts der Isar großen Dank aussprechen. Er ermöglicht mir durch seine Unterstützung nun den nächsten Schritt als *clinician scientist* zu gehen: meine Arbeitsgruppe zu etablieren und gleichzeitig meinen klinischen Schwerpunkt in der Hepatologie zu setzen.

Herrn Prof. Norbert Hüser und seinem Team danke ich von Herzen für die außerordentlich kollegiale und konstruktive Zusammenarbeit.

Meinen FreundInnen und KollegInnen, die mich an allen Stationen meines Arbeitens begleitet haben und begleiten, gilt mein außerordentlicher Dank – ich durfte und darf stets in einem Umfeld der Unterstützung, des Austausches und des kollegialen Zusammenhaltes arbeiten. Diesem Umstand verdanke ich meine Freude am klinischen und wissenschaftlichen Arbeiten, meine Motivation und viele, teils enge und langjährige Freundschaften.

Mein größter Dank gilt meiner Familie, deren Unterstützung ich mir immer sicher sein kann – meinen Eltern Sonja und Werner Schölzel, meinem Bruder Jochen Schölzel und meinem Mann Dr. Jan Böttcher, dem ich für den wissenschaftlichen Austausch und seinen Rückhalt auf allen Ebenen unendlich dankbar bin.

9. Publikationen im Original

9.1 Transfer of MHC-class-I molecules among liver sinusoidal cells facilitates hepatic immune surveillance

Research Article

EASL EUROPEAN ASSOCIATION FOR THE STUDY OF THE LIVER | JOURNAL OF HEPATOLOGY

Transfer of MHC-class-I molecules among liver sinusoidal cells facilitates hepatic immune surveillance

Katrin Schölzel[1,†], Frank A. Schildberg[1,†], Meike Welz[1], Carolin Börner[1], Sergej Geiger[1], Christian Kurts[1], Mathias Heikenwälder[2], Percy A. Knolle[1,3,*], Dirk Wohlleber[1,*]

[1]*Institutes of Molecular Medicine and Experimental Immunology, Universität Bonn, Germany;* [2]*Institute of Virology, Technische Universität München, & Helmholtz Zentrum München, Germany;* [3]*Institute of Molecular Immunology, Technische Universität München, Germany*

See Editorial, pages 464–465

Background & Aims: In the liver, antigen-presenting cell populations such as Kupffer cells, liver dendritic cells, and liver sinusoidal endothelial cells (LSECs) participate through cross-presentation to CD8 T cells (CTLs) in hepatic immune-regulation and immune-surveillance. The participation of hepatic stellate cells (HSCs) in immune regulation is controversial. Here we studied HSC's contribution to antiviral CTL immunity.

Methods: Flow cytometric analysis of MHC-I molecules at the cell surface of liver cells from mice with cell-type restricted MHC-I expression. Mice with HSC-restricted MHC-I expression were infected with a hepatotropic virus and analyzed for development of viral hepatitis after CTL transfer.

Results: HSCs transferred MHC-I molecules to LSECs and these molecules were employed for LSEC cross-presentation to CTLs. Such transfer of MHC-I molecules was sufficient to support *in vivo* LSEC cross-presentation of soluble antigens to CTLs. Importantly, this transfer of MHC-I molecules contributed to anti-viral CTL immunity leading to development of immune-mediated hepatitis.

Conclusions: Our findings demonstrate transfer of MHC-I molecules among sinusoidal liver cell populations as a potent mechanism to increase anti-viral CTL effector function. The transfer of MHC-I molecules from HSCs supplies LSECs with additional MHC-I molecules for their own cell-intrinsic cross-presentation. Such cross-allocation of MHC-I molecules in liver cell populations is distinct from cross-dressing that occurs among immune cell populations in lymphoid tissues where peptide-loaded MHC-I molecules are transferred. Our findings thus reveal a novel mechanism that increases local cross-presentation and CTL effector function in the liver, which may be instrumental for immune-surveillance during viral infection of antigen-presenting liver cells.

Keywords: LSEC; HSC; Cross-presentation; MHC-I.
Received 31 October 2013; received in revised form 16 April 2014; accepted 18 April 2014; available online 4 May 2014
☆ DOI of original article: http://dx.doi.org/10.1016/j.jhep.2014.06.003.
* Corresponding authors. Address: Institute of Molecular Immunology, Technische Universität München, Schneckenburgerstr. 8, 81667 München, Germany (P.A. Knolle). Address: Institutes of Molecular Medicine and Experimental Immunology, University Hospital Bonn, Sigmund-Freud-Str. 25, 53105 Bonn, Germany (D. Wohlleber).
E-mail addresses: percy.knolle@tum.de (P.A. Knolle), dirk.wohlleber@uni-bonn.de (D. Wohlleber).
† These authors contributed equally to this work.
Abbreviations: LSEC, liver sinusoidal endothelial cell; HSC, hepatic stellate cell.

Introduction

The regulation of immune responses in the liver is achieved by organ-resident antigen-presenting cells, bone marrow-derived immune cells residing in the liver and passenger immune cells that transit through the liver within blood and are arrested by local inflammation [1–4]. Also the hepatic microenvironment rich in immune regulatory factors locally influences the immune functions of cell populations in the liver [2]. Almost all liver cell populations are reported to engage in antigen-presentation [4] but only some of these are capable of cross-presenting exogenous antigens to CD8 T cells (CTLs) on MHC class I molecules (MHC-I) [5]. In particular, the role of hepatic stellate cells (HSCs) in local antigen (cross)-presentation in the liver has been controversially discussed [6–8]. Since HSCs are located in direct vicinity to the most prominent scavenger cell populations of the body, Kupffer cells and liver sinusoidal endothelial cells (LSECs), that are both endowed with potent capacity for antigen presentation [9,10], it remained an open question whether HSCs functioned as cross-presenting cell population in direct competition with other APC populations *in vivo*.

The cross-presentation competence among bone marrow-derived immune cells is restricted to certain cell populations [11]. However, several mechanisms were discovered that allow immune cells with poor cross-presenting capacity to present exogenous antigens on MHC-I to CTLs. Among these mechanisms are transfer of peptide-loaded MHC-I, a process referred to as cross-dressing [12,13], peptide-transfer between cells via gap-junctions [14] or antigen-transfer between migratory and lymph

node-resident dendritic cells [15] all of which facilitate presentation of exogenous antigens on MHC-I. The transfer of MHC-I and transfer of membrane constituents, called trogocytosis, has been reported to occur among immune cell populations [16,17]. Little is known whether such transfer of MHC-I occurs also among non-bone marrow-derived cells with immune functions such as liver-resident cells. Here we report that transfer of MHC-I occurs from HSCs to LSECs, i.e., among non-immune cells, which led us to propose the term cross-allocation for this process that facilitates antigen-presentation in the liver sinusoid. Such cross-allocation of MHC-I among liver sinusoidal cells improved antiviral CTL immunity, which reveals a so far unrecognized principle of immune surveillance by sharing of MHC-I among liver sinusoidal cell populations.

Materials and methods

Mice and materials

Animal experiments were performed in accordance with German legislation governing animal studies and the *Principles of Laboratory Animal Care* guidelines. C57Bl/6, DBA/2, GFAP-K^b, Tie2-K^b, CRP-K^b, H-$2K^{bSIINFEKL}$-restricted T cell receptor (TCR)-transgenic animals (OT-I) were bred and maintained under specific pathogen-free conditions according to the guidelines of the Federation of Laboratory Animal Science Association. Recombinant adenovirus expressing Ovalbumin, GFP and Luciferase driven by a CMV promoter (AdOVA), adenovirus expressing GFP and Luciferase driven by CMV promoters (AdGFP) were generated, grown, and purified as described [18]. We generated a recombinant adenovirus expressing Ovalbumin, GFP, and Luciferase driven by the hepatocytes-specific *TTR* promoter (Ad-TTR-OVA). The TTR-promoter was excised from plasmid-DNA encoding for the TTR-promoter (gift from U. Protzer) by using following restriction enzymes: *Afl*II and *Hind*III and chosen because its high specificity for hepatocyte restricted expression [19].

Isolation of primary liver cell populations

Primary murine HSCs were isolated by a two-step pronase-collagenase perfusion from murine livers followed by a Nycodenz (Axis-Shield, Norway) two-layer discontinuous density gradient centrifugation, as described previously [20]. HSCs were cultured on coated 24-well plates (Costar Corning, US) in DMEM containing 10% FCS and 1% penicillin/streptomycin. Where indicated, after this initial separation step HSCs were then FAC-sorted with a FACSAria III based on their high auto-fluorescence and lack of scavenger cell activity (BD Bioscience, Heidelberg, Germany). HSC specific vitamin A fluorescence was detected by a 375 mm UV laser with a 450/40 bandpass filter.

For co-culture experiments, HSCs and LSECs were co-cultured at a ratio of 1:5 on collagen coated 24-well plates in DMEM (4500 mg/ml glucose) (Gibco) with 10% FCS, glutamine, and antibiotics. Cells were detached from plates with Accutase (PAA, Austria). To recognizing OVA-derived SIINFEKL peptide on H-$2K^b$ molecules, were co-cultured at a 1:1 ratio with HSCs or LSECs for 18 h.

Histology

Livers were perfused for 2 min with 4% paraformaldehyde (PFA) and then fixed overnight in 10% neutral buffered formalin. 3 μm sections of formalin fixed, paraffin embedded tissues were prepared and used for H&E and immunohistochemical staining.

Flow cytometry

Antibodies and reagents for flow cytometry were purchased from BD Bioscience (Heidelberg, Germany) or eBioscience (San Diego, CA). To quantify the absolute number of H-$2K^b$ surface molecules per cell PE-conjugated anti-H-$2K^b$ antibodies and QuantiBRITE PE beads (BD Biosciences) were used. Measurements were performed on FACS Canto II or LSR II (BD Biosciences, Germany).

Statistical analysis

Results are shown as means ± standard deviation (SD) of at least triplicates. Analysis of data was performed using Prism software with Student's *t* test.

Results

MHC-I molecule transfer from HSCs to LSECs enables proliferation of naïve OT-1 T-cells in transgenic mice with HSC-restricted MHC-I gene expression

HSCs are situated in the space of Dissé between LSECs and hepatocytes. We addressed the contribution of HSCs to hepatic immune surveillance in the physiological context of the liver as an organ where scavenger cell populations such as LSECs and Kupffer cells are the predominant antigen-presenting cell populations for blood-borne molecules. Therefore we used a transgenic mouse line with HSC-specific expression of the MHC-I H-$2K^b$ gene under control of the GFAP promoter (GFAP-K^b). In GFAP-K^b mice, H-$2K^b$ expression is observed in astrocytes within the central nervous system [21], enterocytes [19], and within the liver on GFAP-expressing quiescent HSC (Supplementary Fig. 1A). We did not detect H-$2K^b$ expression on bone marrow-derived immune cells such as monocytes, macrophages, dendritic cells, B cells or T cells in spleen, lung, or kidney (Supplementary Fig. 1B and C), demonstrating that this transgenic mouse model can be used to study the antigen presenting cell function of HSCs within the liver *in vivo*. The low signals for H-$2K^b$ in immune cells from lung and kidney are due to the high auto-fluorescence that makes detection of expression levels in these cell populations difficult.

After intravenous injection of soluble OVA into GFAP-K^b mice adoptively transferred OVA-specific H-$2K^b$-restricted CFSE-labeled naïve CD8 T-cells (OT-1) showed proliferation, although at a lower levels compared to proliferation after transfer into wild type C57BL/6 mice with ubiquitous H-$2K^b$-expression (Fig. 1A). Such naïve T cell stimulation *in vivo* was H-$2K^b$-specific because in mice lacking H-$2K^b$ (DBA/2) circulating soluble OVA did not result in OT-1 T cell proliferation (not shown). Upon transfer into GFAP-K^b mice challenged with soluble OVA naive OT-1 cells were activated showing a similar phenotype as OT-1 cells transferred into mice with ubiquitous H-$2K^b$ expression, i.e., upregulation of activation markers such as CD25, CD44, and CD69 (Fig. 1B).

The discrepant results reported previously [22] between the low efficiency of HSC antigen uptake and cross-presentation *ex vivo* and the prominent CD8 T cell stimulation in GFAP-K^b mice *in vivo* are difficult to explain and are unlikely to result from improved HSC immune functions *in vivo* but rather indicate exchange of MHC-I molecules among sinusoidal cell populations, a mechanism previously reported to occur between bone marrow-derived immune cells [12,13]. This led us to investigate whether in GFAP-K^b mice LSECs had H-$2K^b$ molecules on their cell surface. Direct *ex vivo* flow cytometric analysis of HSCs from GFAP-K^b mice confirmed surface expression of H-$2K^b$ molecules albeit at lower levels than in H-$2K^b$ wildtype mice (Fig. 1C). As expected, no H-$2K^b$ molecules were found on HSCs isolated from control H-$2K^d$ mice (DBA/2) (Fig. 1C) that constitute the genetic background of GFAP-K^b mice. However, we detected strong surface expression of H-$2K^b$ molecules *ex vivo* on LSECs that were isolated from GFAP-K^b mice (Fig. 1C). Incubation with

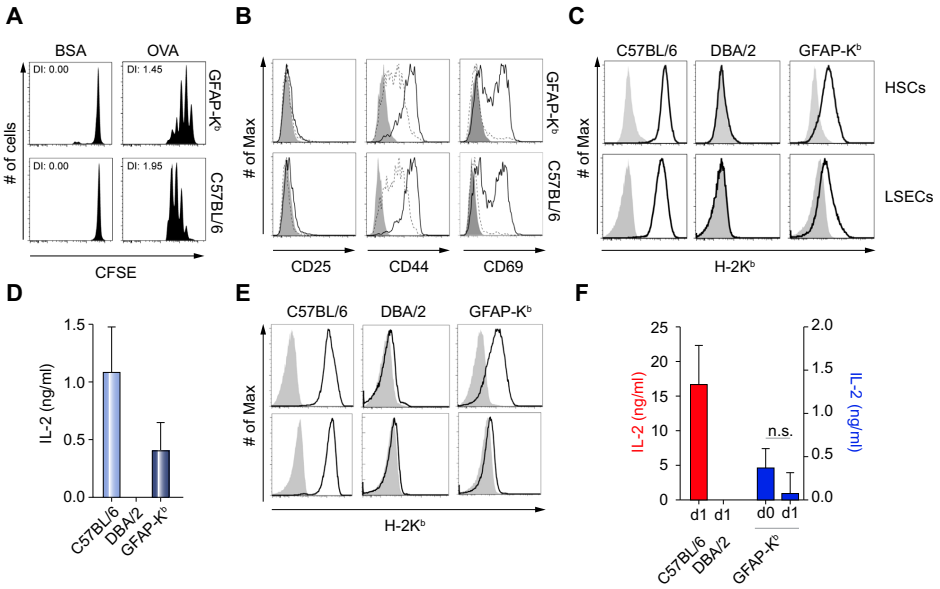

Fig. 1. Transfer of MHC-I molecules to LSECs enables CD8 T cell stimulation in mice with HSC-specific MHC-I expression. (A) Proliferation at d2 after adoptive transfer of CFSE-labeled naïve OVA-specific CD45.1$^+$ OT-I T cells (1.5×10^6/mouse) in CD45.2$^+$ C57BL/6 or GFAP-K^b transgenic mice challenged with OVA or BSA (1 mg/mouse). DI = division index. (B) Activation markers on CD45.1$^+$ OT-I T cells from (A). Isotype control shaded grey, marker expression after BSA dotted lines; after OVA solid lines. (C) *Ex vivo* H-2K^b surface expression in HSCs and LSECs isolated from C57BL/6, DBA/2, or GFAP-K^b mice. Isotype control shaded grey. (D) LSECs from C57BL/6, DBA/2 or GFAP-K^b transgenic mice were pulsed *in vitro* with SIINFEKL (0.5 μM), IL-2 release from B3Z determined by ELISA. (E) H-2K^b surface expression on LSECs directly *ex vivo* (d0) or d1 after isolation; isotype control shaded grey. (F) LSECs from GFAP-K^b transgenic mice were pulsed with SIINFEKL (0.5 μM) directly *ex vivo* (d0) or d1 after isolation and presentation to B3Z was determined by IL-2 ELISA. LSECs from C57BL/6 or DBA/2 served as controls. Shown is always one representative experiment out of three. n.s., not significant (p >0.05).

SIINFEKL-peptide revealed that those H-2K^b molecules found on the surface of LSECs from GFAP-K^b mice were functional in antigen presentation to SIINFEKL-specific CTLs (Fig. 1D).

Since transcriptome analysis had not revealed GFAP expression in LSECs [23], we next investigated whether H-2K^b was expressed at the transcriptional level in LSEC isolated from GFAP-K^b mice. Quantitative RT-PCR analysis demonstrated a lack of H-2K^b mRNA in FAC-sorted LSEC from GFAP-K^b mice (Supplementary Fig. 1D) excluding leaky expression of H-2K^b within LSECs in GFAP-K^b mice as an explanation for the presence of H-2K^b molecules at the cell surface. This raised the question whether H-2K^b molecules may have been transferred by exchange of membrane constituents between LSECs and HSCs *in vivo*. In line with this assumption, LSECs isolated from GFAP-K^b mice showed a decline of cell surface H-2K^b molecules after 1 d of *in vitro* culture (Fig. 1E), which is consistent with lack of H-2K^b gene expression and the half-life of H-2K^b molecules at the cell surface. Flow cytometric quantification of absolute numbers of H-2K^b surface molecules per cell showed a decline of H-2K^b molecules by more than 90% within 24 h of *in vitro* culture (Supplementary Fig. 1E). In LSEC isolated from H-2K^b mice there was only a small yet statistically significant reduction of surface expression of H-2K^b molecules by 15% after 24 h of *in vitro* culture (Supplementary Fig. 1E). Parallel to these lower H-2K^b levels LSECs from GFAP-K^b transgenic mice were less capable of MHC-I restricted antigen-presentation (Fig. 1F). These results suggest that H-2K^b molecules were transferred from HSCs to LSECs *in vivo* and that such molecules remained functional for a short period of time in LSECs for antigen presentation to CTLs.

In vitro model for H-2K^b molecule transfer from HSC to LSEC

We established an *in vitro* co-culture system of freshly isolated LSECs and HSCs to study H-2K^b molecule transfer. However, we found that HSC preparations obtained with standard gradient centrifugation isolation methods were contaminated with LSECs that were clearly identified by their scavenger activity (Supplementary Fig. 2A). This led us to deploy an additional FAC-sorting step, where parameters such as size, granularity, and UV-fluorescence in combination with absence of scavenger activity allowed us to separate HSCs from contaminating LSECs (Supplementary Fig. 2B). This combinatorial isolation procedure yielded highly pure HSC and LSEC populations that were then employed for co-culture experiments. Also *in vitro*, we identified LSECs by scavenger function and HSCs by UV-fluorescence (Fig. 2A). After 2 d co-culture of H-2K^b HSCs (from C57BL/6 mice) with H-2K^d LSECs (from DBA/2 mice) we determined LSEC H-2K^b surface levels. A significant proportion of LSECs showed H-2K^b molecules on their

surface when incubated with H-2K^b expressing HSCs but not when incubated with H-2K^d expressing HSCs (Fig. 2B and C, and Supplementary Fig. 2C), consistent with physical proximity to HSCs of only some LSEC (see Fig. 2A). Flow cytometric quantification revealed approximately 550 H-2K^b molecules/cell present on the cell surface of LSECs after co-culture with HSCs (Fig. 2D). Analysis of FAC-sorted LSEC for GFAP mRNA by real-time PCR confirmed that LSECs were not contaminated with HSCs (Supplementary Fig. 2D).

To investigate the functional relevance of H-2K^b molecules allocated from HSCs to LSECs, we FAC-sorted liver cell co-cultures into scavenger BSA-Alexa^{647pos}-LSECs with no UV-fluorescence and BSA-Alexa^{647neg}-HSCs with high UV-fluorescence. Those FAC-sorted LSECs were capable of employing the transferred H-2K^b molecules for antigen presentation to CTLs (Fig. 2E), demonstrating that MHC-I molecules initially generated in HSCs and transferred to LSECs are employed for antigen presentation to CTLs.

Because of the contamination of standard HSC preparations with LSECs we wondered whether the reported cross-presentation capacity of HSCs may have been caused by contaminating LSECs. To address this question we injected mice with soluble OVA and isolated highly pure HSCs and LSECs by FAC-sorting 60 min later. Highly pure HSCs, HSCs contaminated with LSECs, and highly pure LSECs were co-cultured with OVA-specific CTLs. Under these conditions, highly pure HSCs devoid of any contaminating LSECs did not activate OVA-specific CTLs (Fig. 2F). In the presence of contaminating LSECs in HSC preparations, however, cross-presentation to CTLs was observed (Fig. 2F). This indicates that HSCs are not capable of direct *ex vivo* cross-presentation of soluble circulating antigens.

We next addressed the question whether those H-2K^b molecules derived from HSCs would enable LSECs for cross-presentation of soluble antigen to naïve CD8 T cells. Thus, we isolated LSECs from GFAP-K^b mice, pulsed them with OVA protein and co-cultured these LSECs with naive OT-1 cells. Clearly, LSECs from GFAP-K^b mice used the transferred H-2K^b molecules for cross-presentation and therefore stimulated IL-2 production of naïve OT-1 T-cells (Fig. 2G). This also demonstrated that the low numbers of transferred H-2K^b molecules sufficed for stimulation of naïve CD8 T cells by cross-presenting LSECs.

Mutual exchange of H-2K^b molecules between LSECs and HSCs

To visualize the transfer of molecules between cells involving exchange of membrane components, we co-cultured LSEC and HSC lines labeled with different membrane dyes. Confocal microscopy revealed that parts of plasma membranes were exchanged when cells were in direct physical contact (Fig. 3A and B). We also observed that the directionality of membrane

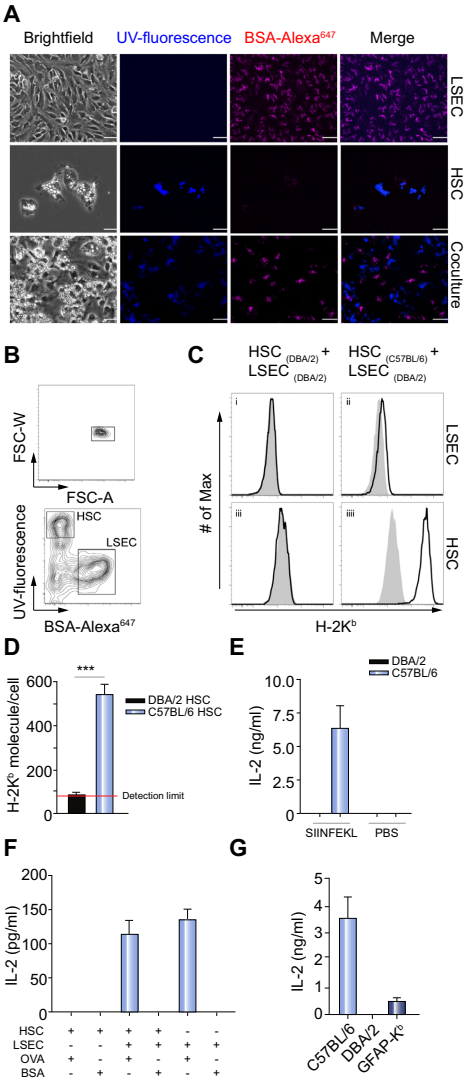

Fig. 2. Transfer of H-2K^b from HSCs to LSECs in coculture *in vitro*. (A) Cultures of FAC-sorted LSECs or HSCs or co-cultures of both. HSCs are discriminated by UV-fluorescence and LSECs by uptake of Alexa^{647}-labelled BSA. Scale bar 25 μm. (B) Flow cytometric gating strategy for re-analysis of initially FAC-sorted HSCs and LSECs from co-cultures in (A). HSCs were excluded by UV-fluorescence and LSECs identified by scavenger activity (uptake of Alexa^{647}-labelled BSA). (C) H-2K^b surface expression levels on LSECs or HSCs identified as outlined in (B); isotype control shaded grey. (D) Absolute numbers of cell surface H-2K^b molecules in DBA/2 LSECs detected by flow cytometry after *in vitro* coculture with either DBA/2 HSCs or C57BL/6 HSCs. (E) H-2K^b–restricted SIINFEKL presentation of DBA/2 LSECs FAC-sorted from co-cultures with C57BL/6 HSCs or DBA/2 HSCs. Gating strategy for FACsorting as in (B). IL-2 release from B3Z was determined by ELISA. (F) *Ex vivo* cross-presentation capacity of FAC-sorted HSCs (gating strategy as in Supplementary Fig. 2B) isolated from mice 1 h after i.v. injection of peptide-free OVA or BSA, was determined directly *ex vivo* by co-incubation with B3Z and determination of IL-2 by ELISA. (G) Cross-presentation of LSECs from C57BL/6, DBA/2 or GFAP-K^b mice pulsed with peptide-free OVA *in vitro*, IL-2 release from B3Z by ELISA. Shown is always one representative experiment out of three, except

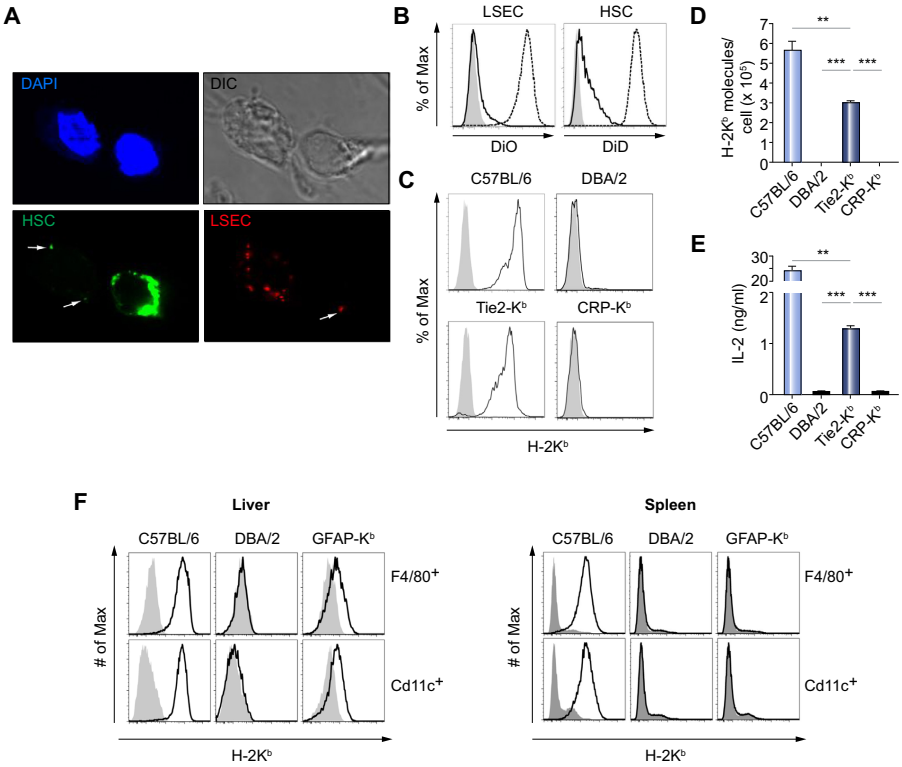

Fig. 3. Bi-directional H-2K^b cross-allocation in sinusoidal liver cells. (A and B) Visualization of HSC/LSEC-membrane exchange using confocal microscopy. The HSC cell-line LX2 labeled with DiO (green) and the LSEC cell line SKHEP labeled with DiD (red) were co-incubated for 12 h, cells were fixed and nuclei labeled with DAPI. (B) Flow cytometric analysis of DiO fluorescence in LSECs or DiD fluorescence in HSCs (solid lines); controls in shaded grey, spikes of DiO-labeled HSCs and DiD-labeled LSEC dotted lines. (C) Surface expression of H-2K^b on HSCs from C57BL/6 or DBA/2, tie2-K^b or CRP-K^b mice (gating strategy Supplementary Fig. 2b). (D) Absolute numbers of H-2K^b molecules per HSCs from (c). (E) HSCs from C57BL/6 (H-2K^b), DBA/2 (H-2K^d), Tie2-K^b or CRP-K^b mice were pulsed with SIINFEKL (0.5 μM) and IL-2 release from B3Z was measured by ELISA. (F) H-2K^b surface expression *ex vivo* on F4/80$^+$ Kupffer cells and CD11c$^+$ DCs isolated from livers or spleens of C57BL/6, DBA/2 or GFAP-K^b transgenic mice. Shown is always one representative experiment out of three, except 3d (one out of two). $^{**}p$ <0.01; $^{***}p$ <0.001.

transfer was not restricted from HSCs to LSECs but also occurred in the other direction from LSECs to HSCs (Fig. 3A and B).

This transfer of membrane constituents raised the question whether such bi-directional transfer occurred also *in vivo* and whether it was restricted to certain liver cell populations. To this end we determined H-2K^b surface levels on HSCs isolated from tie2-K^b-transgenic mice expressing H-2K^b selectively in LSECs or from CRP-K^b transgenic mice expressing H-2K^b exclusively in hepatocytes. We only detected H-2K^b on the cell surface of HSCs in mice where H-2K^b was expressed by LSECs but not hepatocytes (Fig. 3C and D). Similar to the transfer of H-2K^b molecules from HSCs to LSECs, also H-2K^b molecules transferred from LSECs engaged in antigen presentation because peptide pulsing of those HSCs isolated from H-2^b or tie2-K^b-transgenic mice resulted in T cell activation (Fig. 3E), but they did not acquire cross-presentation competence (not shown). This is consistent with the observed lack of *ex vivo* cross-presentation function by HSCs.

If H-2K^b molecules were exchanged between HSCs and LSECs we wondered whether such transfer occurred also to bone-marrow derived immune cells that localized in the liver. Indeed, we found that in GFAP-K^b transgenic mice also Kupffer cells and liver dendritic cells stained positive for H-2K^b molecules (Fig. 3F), whereas macrophages or dendritic cells in the spleen did not show any staining for H-2K^b (Fig. 3F). Together these results support the notion that the transfer of MHC-I molecules occurs among liver-resident as well as myeloid sinusoidal cell populations.

HSC-derived H-2K^b molecules facilitate hepatic CD8 T cell immune surveillance

To evaluate the role of HSC-derived H-2K^b molecules for immune surveillance against viral infection of the liver we employed a CTL-dependent hepatitis model where mice are infected with a

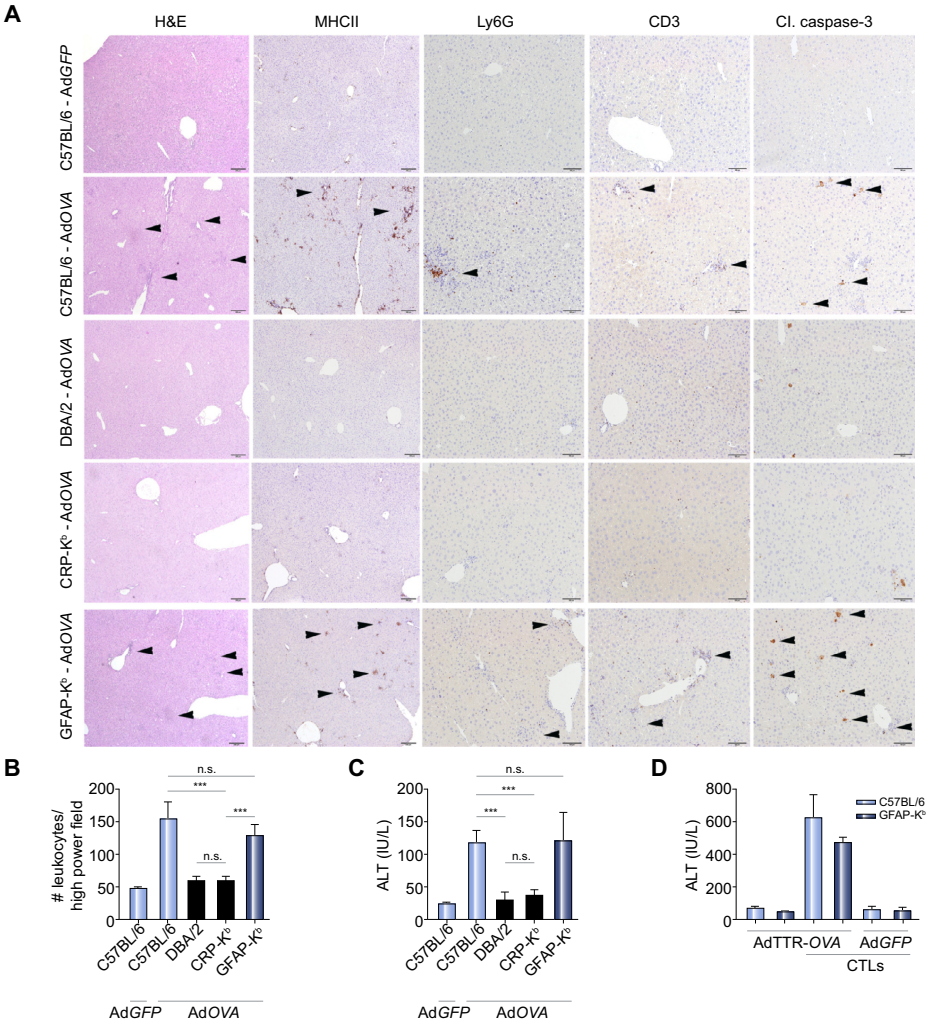

Fig. 4. Relevance of HSC cross-allocation of H-2K^b molecules for hepatic immune surveillance. Infection of C57BL/6, DBA/2 or transgenic mice with H-2K^b expression under cell-type-specific promoters with AdOVA (2×10^8 pfu/mouse) and 48 h later received *in vitro*-activated OVA-specific OT-1 effector CTLs (10^7/mouse). (A) H&E staining and immunohistochemistry of liver sections at 48 h after CTL transfer; scale bar 100 μm. (B) Quantification of infiltrating leukocytes per high power field of H&E staining in (A). (C) sALT levels were determined 48 h after CTL transfer. (D) Infection of C57BL/6 or GFAP-K^b mice with adenovirus expressing OVA under the *TTR*-promoter (AdTTR-OVA, 2×10^9 pfu/mouse). 48 h after infection mice received *in vitro*-activated OVA-specific OT-1 effector CTLs (10^7/mouse). sALT levels were determined 48 h after CTL transfer. Shown is always one representative experiment out of three. n.s., not significant ($p > 0.05$); ***$p < 0.001$.

replication-deficient recombinant adenovirus coding for OVA (AdOVA) preferentially infecting hepatocytes [24,25]. Cross-presentation of OVA released from infected hepatocytes triggers activation and TNF-release from OVA-specific CTLs that in turn kills virus-infected hepatocytes even in the absence of direct MHC-restricted target cell recognition [24]. There was reduced CD3$^+$-lymphocyte, and MHC-II$^+$- and Ly6G$^+$-leukocyte infiltration into livers of AdOVA-infected CRP-K^b transgenic mice after

transfer of OVA-specific CTLs (Fig. 4A and B) where OVA is only presented by hepatocytes to CTLs. This is consistent with an important role of cross-presentation of OVA derived from AdOVA-infected hepatocytes, as we have previously reported [24]. In GFAP-K^b mice, however, we observed a similar infiltration by leukocytes as compared to mice with ubiquitous H-2K^b expression (Fig. 4A and B). Additionally, we found apoptotic hepatocytes, shown by the presence of activated cleaved effector caspase 3, in GFAP-K^b mice and C57BL/6 mice (Fig. 4A). This suggested that H-2K^b molecules generated by HSCs were functional in local immune activation by facilitating cross-presentation of hepatocyte derived OVA to OVA-specific CTLs. Consistent with this notion we found that HSC-derived H-2K^b molecules also allowed CTL-dependent development of viral hepatitis that was comparable to hepatitis induced in wild type mice with ubiquitous H-2K^b expression (Fig. 4C). Since we cannot exclude that adenoviral infection of liver cells other than hepatocytes may have contributed to development of hepatitis, we generated a recombinant adenovirus, where expression of OVA is driven by the hepatocyte-specific TTR promoter (AdTTR-OVA). Infection with AdTTR-OVA virus and adoptive transfer of OVA-specific CTLs in GFAP-K^b transgenic mice led to development of hepatitis measured by a rise of sALT (Fig. 4D). Thus, hepatocyte-restricted expression and release of OVA led to cross-presentation that triggered CTL-activation and caused hepatitis. Since we have excluded cross-presentation by HSCs, CTL-mediated hepatitis in AdTTR-OVA infected GFAP-K^b transgenic mice was most likely initiated by cross-presenting LSECs that were furnished with MHC-I molecules through cross-allocation of MHC-I molecules from HSCs.

Discussion

Liver-resident cell populations have a key role as antigen presenting cells that govern local regulation of immune responses [2,4] but the relevance of hepatic stellate cells (HSCs) as hepatic antigen-presenting cells is controversially discussed [6–8]. Here we characterize the *in vivo* role of HSCs in hepatic immune surveillance by CTLs. Cross-presentation has been suggested to be a feature of HSCs although occurring at lower efficiency compared to other antigen presenting cell populations. In transgenic mice with HSC-specific MHC-I expression (GFAP-K^b mice) we found a potent antigen-specific stimulation of adoptively transferred naïve CD8 T cells in response to circulating soluble antigen. To obtain direct evidence for HSC cross-presentation under these conditions we isolated HSCs and tested their capacity for cross-presentation directly *ex vivo*. We discovered that the conventional gradient-centrifugation isolation protocol yielded HSC preparations with contaminating LSECs that may easily escape detection because LSECs are very thin and cannot be easily discriminated from HSCs. Their extraordinary scavenger function, however, allows the unequivocal identification of contaminating LSECs and therefore also isolation of pure HSC preparations by FAC-sorting. Such highly pure FAC-sorted HSCs that were devoid of all contaminating scavenger LSECs did not show *ex vivo* cross-presentation at all. Together with other reports that failed to detect MHC-II-restricted antigen-presentation by HSCs to CD4 T cells [7] our results suggest that in direct competition with other liver cell populations *in vivo* HSCs do not directly contribute to local antigen-presentation in the liver.

This raised the question how H-2K^b expression by HSCs may then have facilitated cross-presentation in GFAP-K^b transgenic mice *in vivo*. We made the unexpected discovery that LSECs isolated from GFAP-K^b transgenic mice had H-2K^b molecules on their cell surface that gradually vanished upon *in vitro* culture. Together with the lack of H-2K^b gene expression in LSECs from GFAP-K^b transgenic mice these results suggest the existence of a molecule transfer between HSCs and LSECs.

Intercellular protein transfer is increasingly recognized as a mean of cell-cell communication [12,26,27] and for acquisition of particular functional properties in immune cell populations [28–30]. Cross-dressing, i.e., transfer of peptide-loaded MHC-I molecules from one cell to another, as a distinct form of such intercellular molecule transfer is critical for memory T cell activation and immune surveillance [13]. The underlying molecular mechanisms have not been fully elucidated so far, but it is known to involve exchange of parts of surface plasma membranes rather than transfer of individual molecules [31]. Similarly, exchange of plasma membrane fragments between HSCs and LSECs was observed during *in vitro* co-culture. Although we cannot formally exclude molecule transfer by exosomes this possibility appears unlikely, because only a small percentage of LSECs that were co-cultured with H-2K^b expressing HSCs displayed H-2K^b molecules on their cell surface rather arguing for a direct cell-cell transfer that requires close physical contact. Also, exosomes were rather identified as source of peptides for subsequent loading on the recipient cell MHC-I molecules than as a source of MHC-I molecules itself [13].

Here, we report for the first time the transfer of immunologically relevant surface molecules, i.e., MHC-I, among non-immune cells namely sinusoidal cell populations in the liver. Notably, such cross-allocation of H-2K^b molecules also occurred from HSCs to liver-resident immune cells like Kupffer cells and dendritic cells that are localized within hepatic sinusoids, but not to macrophages or dendritic cells in other organs. However, no detectable cross-allocation of H-2K^b molecules from hepatocytes to HSCs or LSECs was observed [24], which may be related to the low density of H-2K^b molecules on hepatocytes that have a 10 to 20 fold higher volume than LSEC and thus a larger cumulative cell surface area. It is unclear whether such cross-allocation of H-2K^b molecules occurs also in other organs or whether it is unique to the liver. The combination of absence of a basement membrane in liver sinusoids facilitating close physical contact between sinusoidal liver cells, the small sinusoidal diameter causing blood cells to exert strong shear forces on sinusoidal cells and the close physical proximity of the delicate cell extensions of LSECs, HSCs, and Kupffer cells may together create a unique liver microenvironment that fosters the exchange of membrane constituents and transfer of H-2K^b molecules among liver sinusoidal cell populations.

Our findings raised the question whether cross-allocated H-2K^b molecules helped to augment antigen-presenting cell function in the recipient cell population. Indeed, cross-allocated H-2K^b molecules from HSCs sufficed to enable cross-presentation in LSECs that do not express H-2K^b themselves. It is possible that cross-allocated H-2K^b molecules may be preferentially used for cross-presentation and not for presentation of endogenous peptides, because cross-presentation i.e., peptide loading of exogenous antigens on H-2K^b molecules occurs preferentially in recycling endosomal compartments [32,33]. Thus, cross-allocation of H-2K^b molecules may contribute to the unusual efficiency

of LSEC cross-presentation capacity that cannot be saturated even at very high antigen concentrations [34]. The continuous exchange of MHC-I molecules may serve to avoid immune escape by infectious agents that down-regulate MHC-I expression in infected cells. Since LSEC are target cells for infection with cytomegalovirus or HIV infection, that are known to interfere with MHC-I expression [35], it is possible that MHC-I cross-allocation may help to sustain LSEC cross-presentation during viral infection. It is further possible that cross-allocation provides MHC-I molecules for LSEC cross-presentation when inhibitory mediators such as IL-10 limit MHC-I gene expression. Thus, our data indicate that cross-allocation functions as a backup system to restore cross-presentation capacity in case LSECs are compromised in MHC-I synthesis. Under normal physiological conditions, however, it is not clear to which extent such transfer accounts for the overall LSEC cross-presentation capacity. This transfer may assure continuous immune surveillance in the context of the liver's immune regulatory microenvironment [2,4]. Since anti-viral CTL immunity depends to 50 percent on LSEC cross-presentation of hepatocyte-derived viral antigens that triggers a non-canonical CTL effector function [24], the efficiency of LSEC cross-presentation to CTLs is a critical factor in local immune control of viral infection in the liver.

Cross-dressing, the acquisition of peptide-loaded MHC-I molecules from neighboring immune cells, confers cross-presentation function to immune cells that do not have cross-presentation capacity themselves [13,36]. Although we have not formally addressed cross-dressing, the observation that HSCs isolated from OVA-challenged mice failed to stimulate OT-1 T cells *ex vivo* argues against cross-dressing of HSCs with peptide-loaded H-2K^b molecules from LSEC. Notwithstanding, cross-dressing may occur but the number of transferred peptide-loaded H-2K^b molecules may be too low to achieve CTL activation. Cross-dressing and cross-allocation apparently serve different functions. Cross-dressing enhances the complexity of immune activation by conferring cross-presentation capacity among different APC populations in lymphoid tissues to enhance the development of immunity. In contrast, cross-allocation enhances the already existing cross-presentation capacity in non-immune cells like LSEC and thereby increases the execution of CTL effector functions in the peripheral organs such as the liver.

Taken together, our findings unravel a so far unknown process for distribution of MHC-I molecules among liver sinusoidal cell populations. Such cross-allocation by HSCs provides additional MHC-I molecules for cross-presentation by scavenger LSEC. Cross-allocation of MHC-I molecules in liver sinusoidal cells supports anti-viral CTL immunity in the liver and may therefore represent an important mechanism in hepatic immune surveillance.

Financial support

This work was supported by a BONFOR grant of the University of Bonn medical faculty to KS, SFBTR57 to PK and CK, SFB 704 to PK.

Conflict of interest

The authors who have taken part in this study declared that they do not have anything to disclose regarding funding or conflict of interest with respect to this manuscript.

Supplementary data

Supplementary data associated with this article can be found, in the online version, at http://dx.doi.org/10.1016/j.jhep.2014.04.028.

References

[1] Crispe IN. The liver as a lymphoid organ. Annu Rev Immunol 2009;27:147–163.
[2] Protzer U, Maini MK, Knolle PA. Living in the liver: hepatic infections. Nat Rev Immunol 2012;12:201–213.
[3] Hickey MJ, Kubes P. Intravascular immunity: the host-pathogen encounter in blood vessels. Nat Rev Immunol 2009;9:364–375.
[4] Thomson AW, Knolle PA. Antigen-presenting cell function in the tolerogenic liver environment. Nat Rev Immunol 2010;10:753–766.
[5] Ebrahimkhani MR, Mohar I, Crispe IN. Cross-presentation of antigen by diverse subsets of murine liver cells. Hepatology 2011;54:1379–1387.
[6] Winau F, Hegasy G, Weiskirchen R, Weber S, Cassan C, Sieling PA, et al. Ito cells are liver-resident antigen-presenting cells for activating T cell responses. Immunity 2007;26:117–129.
[7] Ichikawa S, Mucida D, Tyznik AJ, Kronenberg M, Cheroutre H. Hepatic stellate cells function as regulatory bystanders. J Immunol 2011;186:5549–5555.
[8] Schildberg FA, Kurts C, Knolle P. Prominent regulatory but weak antigen-presenting cell function of hepatic stellate cells. Hepatology 2011;54:1108.
[9] Klein I, Cornejo JC, Polakos NK, John B, Wuensch SA, Topham DJ, et al. Kupffer cell heterogeneity: functional properties of bone marrow derived and sessile hepatic macrophages. Blood 2007;110:4077–4085.
[10] Schurich A, Bottcher JP, Burgdorf S, Penzler P, Hegenbarth S, Kern M, et al. Distinct kinetics and dynamics of cross-presentation in liver sinusoidal endothelial cells compared to dendritic cells. Hepatology 2009;50:909–919.
[11] den Haan JM, Lehar SM, Bevan MJ. CD8(+) but not CD8(−) dendritic cells cross-prime cytotoxic T cells in vivo. J Exp Med 2000;192:1685–1696.
[12] Yewdell JW, Haeryfar SM. Understanding presentation of viral antigens to CD8+ T cells in vivo: the key to rational vaccine design. Annu Rev Immunol 2005;23:651–682.
[13] Wakim LM, Bevan MJ. Cross-dressed dendritic cells drive memory CD8+ T-cell activation after viral infection. Nature 2011;471:629–632.
[14] Mendoza-Naranjo A, Saez PJ, Johansson CC, Ramirez M, Mandakovic D, Pereda C, et al. Functional gap junctions facilitate melanoma antigen transfer and cross-presentation between human dendritic cells. J Immunol 2007;178:6949–6957.
[15] Allan RS, Waithman J, Bedoui S, Jones CM, Villadangos JA, Zhan Y, et al. Migratory dendritic cells transfer antigen to a lymph node-resident dendritic cell population for efficient CTL priming. Immunity 2006;25:153–162.
[16] Huang JF, Yang Y, Sepulveda H, Shi W, Hwang I, Peterson PA, et al. TCR-Mediated internalization of peptide-MHC complexes acquired by T cells. Science 1999;286:952–954.
[17] Smyth LA, Harker N, Turnbull W, El-Doueik H, Klavinskis L, Kioussis D, et al. The relative efficiency of acquisition of MHC: peptide complexes and cross-presentation depends on dendritic cell type. J Immunol 2008;181:3212–3220.
[18] Stabenow D, Frings M, Truck C, Gartner K, Forster I, Kurts C, et al. Bioluminescence imaging allows measuring CD8 T cell function in the liver. Hepatology 2010;51:1430–1437.
[19] Costa RH, Grayson DR. Site-directed mutagenesis of hepatocyte nuclear factor (HNF) binding sites in the mouse transthyretin (TTR) promoter reveal synergistic interactions with its enhancer region. Nucleic Acids Res 1991;19:4139–4145.
[20] Siegmund SV, Uchinami H, Osawa Y, Brenner DA, Schwabe RF. Anandamide induces necrosis in primary hepatic stellate cells. Hepatology 2005;41:1085–1095.
[21] Schonrich G, Kalinke U, Momburg F, Malissen M, Schmitt-Verhulst AM, Malissen B, et al. Down-regulation of T cell receptors on self-reactive T cells as a novel mechanism for extrathymic tolerance induction. Cell 1991;65:293–304.
[22] Schildberg FA, Wojtalla A, Siegmund SV, Endl E, Diehl L, Abdullah Z, et al. Murine hepatic stellate cells veto CD8 T cell activation by a CD54-dependent mechanism. Hepatology 2011;54:262–272.

[23] Kern M, Popov A, Scholz K, Schumak B, Djandji D, Limmer A, et al. Virally infected mouse liver endothelial cells trigger CD8+ T-cell immunity. Gastroenterology 2010;138:336–346.
[24] Wohlleber D, Kashkar H, Gartner K, Frings MK, Odenthal M, Hegenbarth S, et al. TNF-induced target cell killing by CTL activated through cross-presentation. Cell Rep 2012;2:478–487.
[25] Waddington SN, McVey JH, Bhella D, Parker AL, Barker K, Atoda H, et al. Adenovirus serotype 5 hexon mediates liver gene transfer. Cell 2008;132:397–409.
[26] Joly E, Hudrisier D. What is trogocytosis and what is its purpose? Nat Immunol 2003;4:815.
[27] Davis DM. Intercellular transfer of cell-surface proteins is common and can affect many stages of an immune response. Nat Rev Immunol 2007;7:238–243.
[28] Nakamura K, Nakayama M, Kawano M, Amagai R, Ishii T, Harigae H, et al. Fratricide of natural killer cells dressed with tumor-derived NKG2D ligand. Proc Natl Acad Sci U S A 2013;110:9421–9426.
[29] Rossi EA, Goldenberg DM, Michel R, Rossi DL, Wallace DJ, Chang CH. Trogocytosis of multiple B-cell surface markers by CD22-targeting with epratuzumab. Blood 2013;122:3020–3029.
[30] Osborne DG, Wetzel SA. Trogocytosis results in sustained intracellular signaling in CD4(+) T cells. J Immunol 2012;189:4728–4739.
[31] Dopfer EP, Minguet S, Schamel WW. A new vampire saga: the molecular mechanism of T cell trogocytosis. Immunity 2011;35:151–153.
[32] Burgdorf S, Kautz A, Bohnert V, Knolle PA, Kurts C. Distinct pathways of antigen uptake and intracellular routing in CD4 and CD8 T cell activation. Science 2007;316:612–616.
[33] Burgdorf S, Scholz C, Kautz A, Tampe R, Kurts C. Spatial and mechanistic separation of cross-presentation and endogenous antigen presentation. Nat Immunol 2008;9:558–566.
[34] Schurich A, Berg M, Stabenow D, Bottcher J, Kern M, Schild HJ, et al. Dynamic regulation of CD8 T cell tolerance induction by liver sinusoidal endothelial cells. J Immunol 2010;184:4107–4114.
[35] Petersen JL, Morris CR, Solheim JC. Virus evasion of MHC class I molecule presentation. J Immunol 2003;171:4473–4478.
[36] Li L, Kim S, Herndon JM, Goedegebuure P, Belt BA, Satpathy AT, et al. Cross-dressed CD8alpha+/CD103+ dendritic cells prime CD8+ T cells following vaccination. Proc Natl Acad Sci U S A 2012;109:12716–12721.

AMERICAN JOURNAL OF PHYSIOLOGY
GASTROINTESTINAL AND LIVER PHYSIOLOGY

Am J Physiol Gastrointest Liver Physiol 320: G543–G556, 2021.
First published January 6, 2021; doi:10.1152/ajpgi.00262.2020

RESEARCH ARTICLE

Translational Human Pathophysiology

AICAR and compound C negatively modulate HCC-induced primary human hepatic stellate cell activation in vitro

Katrin Böttcher,[1,2] Lisa Longato,[1] Giusi Marrone,[1] Giuseppe Mazza,[1] Leo Ghemtio,[3] Andrew Hall,[2,4] Tu Vinh Luong,[4] Stefano Caruso,[5] Benoit Viollet,[6] Jessica Zucman-Rossi,[5,7] Massimo Pinzani,[1,2] and Krista Rombouts[1]

[1]*Regenerative Medicine and Fibrosis Group, Institute for Liver and Digestive Health, University College London, Royal Free Campus, London, United Kingdom;* [2]*Sheila Sherlock Liver Centre, Royal Free Hospital, London, United Kingdom;* [3]*Drug Research Program, Division of Pharmaceutical Biosciences, Faculty of Pharmacy, University of Helsinki, Helsinki, Finland;* [4]*Department of Cellular Pathology, Royal Free Hospital, London, United Kingdom;* [5]*Centre de Recherche des Cordeliers, INSERM, Functional Genomics of Solid Tumors Laboratory, Sorbonne Université, Université de Paris, Paris, France;* [6]*Université de Paris, Institut Cochin, CNRS, INSERM, Paris, France; and* [7]*Hôpital Européen Georges Pompidou, Assistance Publique-Hôpitaux de Paris, Paris, France*

Abstract

Tumor stroma and microenvironment have been shown to affect hepatocellular carcinoma (HCC) growth, with activated hepatic stellate cells (HSC) as a major contributor in this process. Recent evidence suggests that the energy sensor adenosine monophosphate-activated kinase (AMPK) may mediate a series of essential processes during carcinogenesis and HCC progression. Here, we investigated the effect of different HCC cell lines with known *TP53* or *CTNBB1* mutations on primary human HSC activation, proliferation, and AMPK activation. We show that conditioned media obtained from multiple HCC cell lines differently modulate human hepatic stellate cell (hHSC) proliferation and hHSC AMPK activity in a paracrine manner. Pharmacological treatment of hHSC with AICAR and Compound C inhibited the HCC-induced proliferation/activation of hHSC through AMPK-dependent and AMPK-independent mechanisms, which was further confirmed using mouse embryonic fibroblasts (MEFs) deficient of both catalytic AMPKα isoforms (*AMPK*$^{\alpha 1^{f/}\alpha 2^{-/-}}$) and wild type (wt) MEF. Both compounds induced S-phase cell-cycle arrest and, in addition, AICAR inhibited the mTORC1 pathway by inhibiting phosphorylation of 4E-BP1 and S6 in hHSC and wt MEF. Data mining of the Cancer Genome Atlas (TCGA) and the Liver Cancer (LICA-FR) showed that AMPKα1 (*PRKAA1*) and AMPKα2 (*PRKAA2*) expression differed depending on the mutation (*TP53* or *CTNNB1*), tumor grading, and G1-G6 classification, reflecting the heterogeneity in human HCC. Overall, we provide evidence that AMPK modulating pharmacological agents negatively modulate HCC-induced hHSC activation and may therefore provide a novel approach to target the mutual, tumor-promoting interactions between hHSC and HCC.

NEW & NOTEWORTHY HCC is marked by genetic heterogeneity and activated hepatic stellate cells (HSC) are considered key players during HCC development. The paracrine effect of different HCC cell lines on the activation of primary hHSC was accompanied by differential AMPK activation depending on the HCC line used. Pharmacological treatment inhibited the HCC-induced hHSC activation through AMPK-dependent and AMPK-independent mechanisms. This heterogenic effect on HCC-induced AMPK activation was confirmed by data mining TCGA and LICA-FR databases.

adenosine monophosphate-activated kinase; hepatic stellate cells; hepatocellular carcinoma; LICA-FR; liver fibrosis; TCGA; tumor-stromal interactions

INTRODUCTION

Hepatocellular carcinoma (HCC) is the most common primary liver tumor and one of the leading causes of cancer deaths (1). More than 80% of HCC develop on the background of liver cirrhosis following long-standing liver injury most commonly caused by chronic infection with hepatitis B or C viruses, excess alcohol consumption, or nonalcoholic steatohepatitis (2). In these clinical conditions, chronic liver damage is characterized by the activation of hepatic stellate cells (HSC),

Correspondence: K. Rombouts (k.rombouts@ucl.ac.uk).
Submitted 8 July 2020 / Revised 14 December 2020 / Accepted 29 December 2020

which represents the main cellular effectors of hepatic fibrosis and consequent progression to liver cirrhosis (3). Activation of HSC is characterized by the transition from a quiescent pericyte to a myofibroblast-like cell with increased proliferation, migration, contraction and expression of profibrogenic factors, proinflammatory cytokines, and extracellular matrix (ECM) components, resulting in the formation of a scar tissue (4, 5). There is growing evidence that the tumor microenvironment, in particular the bidirectional cross talk between HCC and HSC, is a crucial factor for HCC onset and progression (6) as activated HSC enhance HCC cell proliferation, migration, and tumor growth (7) by fostering the proinflammatory and proangiogenic microenvironment of the tumor (8).

The energy-sensing enzyme adenosine monophosphate-activated kinase (AMPK) is a highly sensitive safeguard that responds to changes in ATP production and promotes catabolic pathways while inhibiting anabolic pathways when activated (9). Importantly, AMPK has been implicated in tumor development and progression as AMPK regulates the cell cycle by stabilizing p53 and p27 (10, 11). Thus, AMPK inhibits cell growth, metabolism, and proliferation through inhibition of the mTOR pathway (12). Further evidence for AMPK as a tumor suppressor is originating from clinical and experimental data, showing that pharmacological AMPK modulators inhibit cancer development and progression (13, 14). Indeed, the incidence of HCC is lower in diabetic patients treated with metformin which induces AMPK activity (15). Metformin has also been shown to inhibit angiogenesis in an HCC–HSC cell line in vitro coculture model, supporting an inhibitory role for AMPK in tumor–stromal interactions (16). In addition, AICAR, another well-established AMPK activator, suppresses HCC cell proliferation and inhibits tumor growth in murine HCC models in vivo (17). Of note, pharmacological activation of AMPK has been shown to reverse HSC activation in vitro and AICAR and metformin inhibits PDGF-induced HSC proliferation (18, 19).

Nevertheless, there is limited evidence for a role of AMPK in the tumor-stromal interaction between HCC cells and primary human HSC, as well as for the possible working mechanisms of AMPK in such cross talk. Accordingly, the present study was designed to provide further evidence on the involvement of this pathway in the cross talk between HCC and its stroma. As HCC is known to be a highly heterogeneous cancer (20, 21), several HCC cell lines with different types of mutations were investigated in this study.

The results of the study show that activation of AMPK is involved in HCC tumor–stromal interaction and suggests AMPK as a potential target for novel treatments for the overall stromal derangement typical of chronic liver disease and the associated development of HCC.

MATERIALS AND METHODS

Patients and Tumors

The expression levels of AMPKα1 (*PRKAA1*) and AMPKα2 (*PRKAA2*) were assessed by RNA-seq in two independent data sets, including 160 HCC samples from LICA-FR cohort previously described, and 339 HCC samples from the TCGA (The Cancer Genome Atlas) cohort. Patients with co-occurring *TP53* and *CTNNB1* mutations were excluded from the analysis. At least two liver pathologists used multiple slides of the same tumor to establish the Edmondson–Steiner grades in both cohorts, as previously described (22). Furthermore, the expression of AMPKα1 (*PRKAA1*) and AMPKα2 (*PRKAA2*) was investigated in relation to the G1–G6 classification (23). Detailed clinical characteristics for both data sets are provided in Supplemental Table S1 (all Supplemental material for this article is available online at https://doi.org/10.5522/04/12562631.v2).

Immunohistochemistry

Immunostaining of AMPKα1 subunit was performed as previously described on formalin-fixed paraffin-embedded human liver sections from histologically normal tissue retrieved from sites remote to colorectal liver metastasis, cirrhotic liver without HCC and HCC in the context of a cirrhotic liver obtained from the Royal Free Hospital histopathology archives (ethics 07/Q0501/50) (24). Liver sections were deparaffinized and hydrated through xylenes and ethanol. Antigen retrieval was achieved by microwaving the section at 640 W for 20 min in 1 L of pH 9.0 Tris EDTA buffer. The slides were soaked in TBS with 0.04% Tween-20 (Sigma) for 5 min and blocked for endogenous peroxidase and nonspecific binding of secondary antibodies using reagents from the Novolink kit (Leica), 5 min each. AMPKα1 antibody (Abcam ab32047) was incubated for 1 hr at room temperature. The primary antibody was then detected using Novolink kit reagents, post primary 30 min, polymer 30 min and DAB 5 min. The slides were then counterstained with Mayer's hematoxylin. All sections were dehydrated, cleared in xylene, mounted with DPX (Leica biosystems), and observed using a Zeiss Axioskop 40. Images were captured with an Axiocam IcC5 using Zeiss Axiovision (version 4.8.2).

Human HSC Isolation

Human HSC (hHSC) were isolated from wedge sections of human liver tissue, obtained from patients undergoing liver surgery at the Royal Free Hospital after giving informed consent (NC2015.020 (B-ERC-RF)), as described before (25, 26). Briefly, 10 g of total human liver tissue was digested with 0.01% Collagenase type IV (Sigma-Aldrich), 0.05% Pronase (Calbiochem), and 0.001% DNase I (Sigma-Aldrich). The homogenate was filtered through a 100 μm cell strainer (BD Falcon), and the flowthrough was centrifuged at 50 *g* for 2 min at 4°C to remove hepatocytes. After the supernatant was washed, gradient centrifugation was performed at 1,400 *g* for 17 min using a 11.5% Optiprep gradient (Sigma-Aldrich). Finally, the interface was collected and washed. The obtained hHSC were cultured in Iscove's modified Dulbecco's medium supplemented with 20% fetal bovine serum (FBS), 2 mM/L glutamine, nonessential amino acids 1×, 1.0 mM/L sodium pyruvate, antibiotic–antimycotic 1× (all Gibco), referred to as complete HSC medium hereinafter. Experiments were performed on cells between passage 3 and 8 employing at least three different cell preparations/donors for all experiments.

Cell Lines

HepG2 and PLC/PRF/5 were purchased from American Type Culture Collection (ATCC) and cultured in minimum essential medium α supplemented with 10% FBS, nonessential amino

acids 1×, 1.0 mM/L sodium pyruvate, and antibiotic–antimycotic 1×. HCC cells lines SNU398, Mahlavu, Huh-6, and Huh-7 cells were kindly provided by Prof Jessica Zucman-Rossi, and identification of the cell lines was confirmed by sequencing (27). Cells were cultured in Dulbecco's modified Eagle's medium, supplemented with 10% FBS and penicillin/streptomycin. All cell cultures are frequently analyzed for mycoplasma using an in-house qPCR assay as previously described (28).

Mouse Embryonic Fibroblasts

Simian virus 40 large T antigen-immortalized mouse embryonic fibroblasts (MEFs) were kindly provided by Dr. Benoit Viollet. AMPK$\alpha1/\alpha2^{-/-}$ and wt MEFs were obtained from 10.5-day postcoitum embryos, the genotype was confirmed by PCR and immunoblot analysis. MEFs from the second or third culture passage were immortalized by introducing the SV 40 large T antigen using the pSV-Ori-vector (29). MEFs were cultured in Dulbecco's modified Eagle's medium supplemented with 10% FBS, 1 mM sodium pyruvate, and antibiotic–antimycotic 1× (all Gibco).

Preparation of Conditioned Medium

To obtain conditioned medium 3×10^6 HepG2 or PLC/PRF/5 cells, or 0.6×10^6 hHSC were cultured in a cell culture dish (100 × 22 mm) in complete HCC or hHSC medium. After 24 h, cells were washed twice with HBSS and incubated in serum-free medium for 48 h. Conditioned medium was collected and centrifuged at 247 *g*, 7 min, and 21°C. The supernatant was used immediately, or stored at −20°C, until used for experiments.

Treatment of Cells

Treatment of hHSC with conditioned medium of HepG2 or PLC/PRF/5 cells.

Human HSC were plated on a cell culture dish (0.3×10^6/6 well or 0.006×10^6/96 well) in complete HSC medium. After 24 h, cells were washed with HBSS (Gibco) and serum starved for 24 h. Subsequently cells were treated with conditioned medium of HepG2 or PLC/PRF/5 cells for 24 h.

Treatment of HepG2 and PLC/PRF/5 cells with conditioned medium of hHSC.

HepG2 or PLC/PRF/5 cells were plated on a cell culture dish (0.006×10^6/96 well) in complete HCC medium. After 24 h, cells were washed with HBSS (Gibco) and serum starved for 24 h, and cells were treated with conditioned medium of different primary hHSC preparations subsequently.

Treatment of cells with pharmacological compounds.

Human HSC were treated with different concentrations of AICAR (0.25–4 mM) reconstituted in water, or Compound C (2.5–40 μM) reconstituted to 10 mM in DMSO. Cells were plated in complete medium and serum starved for 24 h before treatment.

BrdU Incorporation Assay

Cell proliferation was quantified by BrdU Cell Proliferation ELISA kit (Roche) and as described before (25, 30). Human HSC (10^3) were plated in complete medium in a 96-well plate in quadruplicates. Cells were washed and serum starved for 24 h before treatment. BrdU labeling solution was added in parallel with treatment, BrdU ELISA was developed according to the manufacturer's protocol after 24 h treatment and absorbance was detected with Fluostar Omega Plate Reader (BMG labtech).

MTS Assay

To determine metabolic activity of cells, CellTiter 96 Aqueous One Solution Cell Proliferation Assay kit (Promega) was used according to the manufacturer's protocol and as previously described (24). Briefly, hHSC (10^3) were plated in complete medium in a 96-well plate in quadruplicates and were cultured and treated as described above. Following 24 h treatment, MTS was added for 2 h, and absorbance was measured with Fluostar Omega Plate Reader (BMG labtech).

Cell Cycle Analysis

For cell cycle analysis, 0.3×10^6 HSC were plated on a 6-well plate in complete medium. After 24 h, cells were washed and cultured in serum-free medium for 24 h followed by treatment. Cells were trypsinized after 24 h of treatment, washed, and fixed with ice-cold 70% ethanol, for 30 min at 4°C. Cells were washed twice before incubation with propidium iodide (50 μg/mL, Promega) for 10 min at room temperature. Propidium iodide accumulation was analyzed with BD LSR Fortessa (5 L SORP) using BD FACSDiva software (version 6.2) and analyzed with FlowJo version 10.0.

Cell Death Enzyme-Linked Immunosorbent Assay (ELISA)

To analyze apoptosis and necrosis in hHSC, Cell Death Detection ELISAPlus (Roche) was used according to the manufacturer's protocol. Cells were treated in triplicates. After 24 h treatment, supernatants were removed and cells were lysed. Nucleosomes were quantified in cell lysates (apoptosis) and supernatants (necrosis) photometrically. Absorbance at 420 nm was measured with Fluostar Omega Plate Reader (BMG labtech).

Western Blot Analysis

Protein isolation and Western blot analysis were performed as previously described (24, 25, 30). To obtain total protein cell lysates, cells were washed and lysed with radioimmunoprecipitation assay (RIPA) buffer (20 mM Tris·HCl, pH 7.6, 150 mM NaCl, 5 mM EDTA, 1% NP-40 (nonyl phenoxypolyethoxylethanol), 1 mM phenylmethylsulfonyl fluoride (PMSF), 1× Protease Inhibitors Mix, 1 mM Na_3VO_4, and 1 mM NaF). Cell lysates were sonicated with the "Ultrasonic Processor" (Sonics, Vibra Cell). Protein quantification was carried out using Micro BCATM Protein Assay Kit (Thermo Scientific) according to the manufacturer's protocol. SDS gel electrophoresis was performed with 25 μg of protein lysate were loaded on 10% or 12% acrylamide gels. Primary antibodies were incubated overnight at 4°C or for 1 h at room temperature. After washing was completed, specific horseradish peroxidase coupled secondary antibodies were applied for 1 h at room temperature and SuperSignal West Pico Chemiluminescent Substrate (Thermo Scientific) was used to develop signals. For following antibody incubations,

antibodies were stripped with RestoreTM PLUS Western Blot Stripping Buffer (Thermo Scientific). To verify equal loading of samples, expression of the housekeeping proteins β-actin or tubulin was detected. All primary and secondary antibodies are listed in Supplemental Table S2 and antibody specificity was validated by performing Western blot analysis.

Quantitative Real-Time PCR (qPCR)

RNA was isolated from hHSC using RNeasy mini Kit (Qiagen) according to the manufacturer's protocol and as previously described (24, 25, 30). Purity and RNA concentration were measured with Nanodrop spectrophotometer (Thermo Scientific) and cDNA was synthesized with MultiScribe reverse transcriptase, random primers, deoxyribose nucleoside triphosphate (dNTP) mix, and RNase inhibitor (all Applied Biosystems). Gene expression was measured via quantitative real-time PCR (qPCR) using Taqman gene assays (Supplemental Table S3) and 7500 Fast Real-Time PCR System (all Applied Biosystems). To quantify gene expression, the comparative CT method was used as described previously (24, 25, 30) using glyceraldehyde 3-phosphate dehydrogenase (GAPDH) as internal control.

Statistical Analysis

Data visualization and statistical analysis were performed using R software version 3.5.1 (R Foundation for Statistical Computing, Vienna, Austria, https://www.R-project.org), Microsoft Excel or Graph Pad Prism. Values are expressed as means ± standard deviation (SD), or means ± 95% confidence interval as indicated in the figures. Statistical significance was analyzed using unpaired, nonparametric *t* test, or ANOVA. Differences of mRNA expression levels between groups were assessed using Wilcoxon signed-rank test to compare two groups or Kruskal–Wallis test for post hoc analysis to compare more than two groups. Spearman's rank-order correlation was used to test the association between continuous variables. P value <0.05 was considered as significant.

RESULTS

HCC-Conditioned Medium Induces an Activated Phenotype and Activation of the AMPK Pathway in hHSC

To investigate the interaction between primary hHSC and HCC cells, we incubated three different hHSC preparations (i.e., cells obtained from three different donors) for 24 h with conditioned medium obtained from the hepatoblastoma cell line HepG2 (*TP53* gene wild-type cells with *CTNNB1* exon3 deletion activating β-catenin) and the HCC cell line PLC/PRF/5 (*TP53* mutation bearing cells with high levels of β-catenin protein expression) (31). Both HCC cell lines belong to transcriptomic class 1 classification including the most differentiated liver cancer cell lines with epithelial features (27). As shown in Fig. 1*A*, conditioned medium of PLC/PRF/5 and HepG2 cells induced a significant increase in expression of several genes associated with hHSC activation, including the collagen crosslinking enzyme lysyl oxidase (LOX) as well as the inflammatory genes IL-1β, IL-8, and CCL2 in a cancer cell type-specific manner. In contrast, 24 h treatment with HCC cell-conditioned medium had no effect on TIMP1 and MMP2 expression and resulted in downregulation of collagen 1A1 and IL-6 gene expression (Fig. 1*A*). Moreover, hHSC proliferation was significantly increased following incubation with HepG2 conditioned medium compared with serum-free medium (Fig. 1*B*), whereas hHSC proliferation remained unchanged when treated with conditioned medium of PLC/PRF/5 cells. As HepG2 cells are hepatoblastoma cells, further differences in the potential of HCC cells to induce hHSC proliferation were confirmed employing conditioned medium of additional HCC cell lines. Thus, HCC cell lines characterized by, among numerous other mutations (31–33), various mutations in cell-cycle regulating genes, such as p53 (PLC/PRF/5, Huh-7, Mahlavu) and β-catenin (HepG2, Huh-6, SNU398) were investigated. Similar to HepG2 cells, conditioned medium of Huh-6 and Huh-7 cells induced hHSC proliferation in vitro (Fig. 1*C*). In contrast, hHSC proliferation was unchanged following incubation with conditioned medium of SNU398 or Mahlavu cells (Fig. 1*C*), indicating that diverse HCC cell lines differentially affect hHSC proliferation. Overall, these data further confirm that the dysregulation of the cancer cell secretome plays a key role, not only in tumor transformation/progression but also affects the stromal cells in an HCC cell line-specific manner (34–36). It has been shown previously that cell proliferation is regulated via AMPK and that activation of AMPK in HSC leads to inhibition of PDGF-BB-induced proliferation (9, 19). AMPK activation is characterized by phosphorylation of AMPK at threonine residue 172 of its catalytic subunit α (AMPK-Thr^{172}), whereas phosphorylation of AMPK-$Ser^{485/491}$ results in inhibition of AMPK activity (37, 38) (Fig. 1*E*). To test whether activation of the AMPK pathway is associated with the induction of hHSC proliferation by HCC cells, activation of AMPK and its upstream kinase LKB1 were analyzed in hHSC after 24 h incubation with HCC cell line conditioned medium. PLC/PRF/5 cell-conditioned medium induced a strong phosphorylation of AMPK at Thr^{172} and only mild phosphorylation at AMPK-$Ser^{485/491}$ when compared to treatment with serum-free medium (SFM), indicating overall activation of AMPK (Fig. 1*D*; Supplemental Fig. S1*A*). In contrast, conditioned medium of HepG2 cells induced a mild phosphorylation of AMPK-Thr^{172} associated with a strong phosphorylation of AMPK-$Ser^{485/491}$, suggesting an overall inhibition of AMPK activity (Fig. 1*D*; Supplemental Fig. S1*A*). Phosphorylation of the AMPK upstream kinase LKB1 that regulates phosphorylation of AMPK-Thr^{172} was strongly reduced after treatment with the conditioned media of both HCC cell lines, compared with serum-free medium (Fig. 1*D*; Supplemental Fig. S1*A*), suggesting that phosphorylation of AMPK-Thr^{172} is regulated differently in hHSC treated with conditioned media. Similar to conditioned medium of PLC/PRF/5 cells, conditioned medium of the cancer cell lines SNU398 and Mahlavu-induced AMPK activation in hHSC, as suggested by the strong phosphorylation of AMPK-Thr^{172}, while phosphorylation of AMPK-Thr^{172} was only mildly induced or absent following incubation with Huh-6 and Huh-7 conditioned medium (Supplemental Fig. S1*B*). Overall, these results demonstrate the ability of HCC cells to induce hHSC activation, as well as activation of the AMPK pathway in hHSC, with HCC cell line-specific features.

AJP-Gastrointest Liver Physiol • doi:10.1152/ajpgi.00262.2020 • www.ajpgi.org

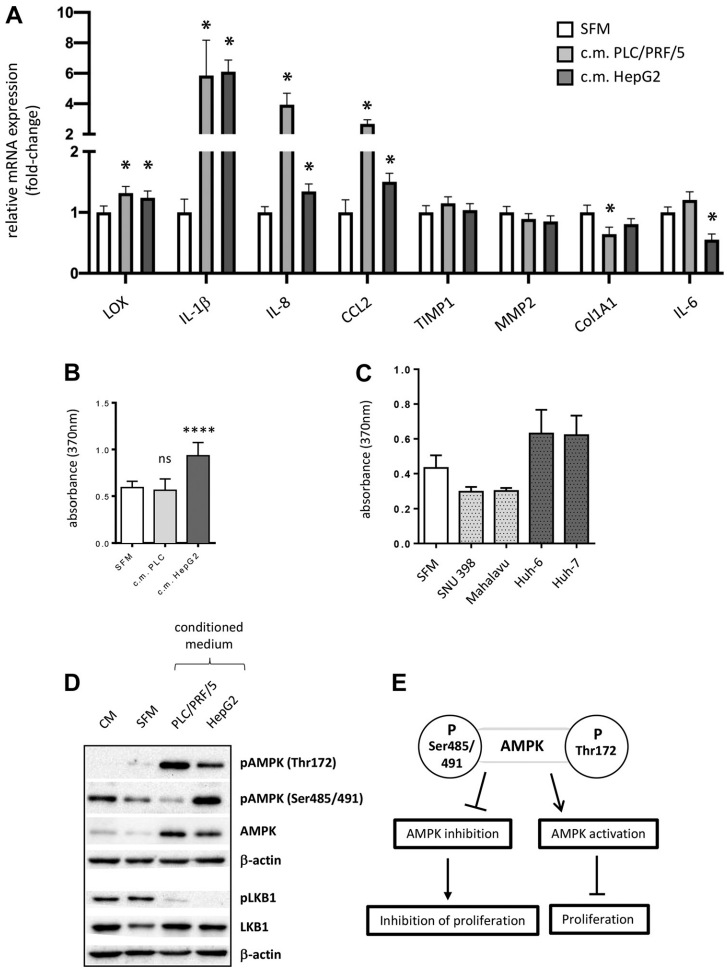

Figure 1. HCC-conditioned medium activates hHSC and affects the AMPK pathway in hHSC. Gene expression (*A*) and proliferation response (*B*) in hHSC following treatment with conditioned medium of HepG2 or PLC/PRF/5 cells for 24 h. *C*: proliferation of hHSC following 24 h treatment with different HCC-conditioned media. *D*: AMPK phosphorylation profile expression in hHSC after exposure with HepG2 or PLC/PRF/5 conditioned medium for 24 h. *E*: schematic of AMPK phosphorylation sites and AMPK activation/inhibition. *A*: data represent means ± 95% confidence interval, $^{*}P = 0.05$, pooled data of three independent experiments (see MATERIALS AND METHODS for statistical tests). *B–D*: representative data of four independent experiments (one-way ANOVA), data represent means ± SD, $^{****}P < 0.0001$, ns = not significant versus SFM. AMPK, adenosine monophosphate-activated kinase; CM, complete medium; hHSC, human hepatic stellate cell; HCC, hepatocellular carcinoma; SFM, serum-free medium.

AICAR and Compound C Inhibit hHSC Activation Induced by HCC Cells

We next investigated the effect of the pharmacological agents AICAR (39, 40) and Compound C (18), known to affect AMPK signaling. We first assessed the effect of both pharmacological agents on AMPK activation/phosphorylation in hHSC, as well as their effect on metabolic activity, proliferation, and hHSC gene expression. We observed an increase in AMPK phosphorylation at Thr^{172} in hHSC treated with AICAR, whereas p-AMPK-Thr^{172} was absent in hHSC exposed to Compound C (Fig. 2*A*). Further, we did not observe changes in phosphorylation of AMPK-$Ser^{485/491}$ following treatment with AICAR or Compound C compared to the untreated control (Fig. 2*A*), suggesting activation of AMPK through AICAR but not Compound C. The metabolic activity and proliferation in hHSC were significantly inhibited by both pharmacological agents in a dose-dependent manner, indicating that both AICAR and Compound C can inhibit hHSC activation (Fig. 2*B* – 2*C*) without inducing cell death as assessed by cell death ELISA (Fig. 2*D*).

We next investigated the effect of both pharmacological agents on HCC-induced hHSC activation by treating hHSC with conditioned medium of HepG2 or PLC/PRF/5 cells and AICAR or Compound C in parallel. As demonstrated in Fig. 2*E*, treatment with AICAR was sufficient to abrogate the induction of inflammatory gene expression by HepG2 and PLC/PRF/5 conditioned medium in hHSC, while expression

of LOX was unchanged. This effect was less prominent in hHSC exposed to Compound C (Supplemental Fig. S2*A*). Moreover, both AICAR and Compound C were able to reverse HepG2-induced proliferation in hHSC (Fig. 2*F*). Similarly, proliferation of HepG2 and PLC/PRF/5 cells treated with conditioned medium of hHSC was inhibited following treatment with AICAR and Compound C (Supplemental Fig. S2, *B* and *C*). These data indicate that both AICAR and Compound C inhibit the cross talk between HCC and hHSC and vice versa. Next, protein expression analysis was performed and

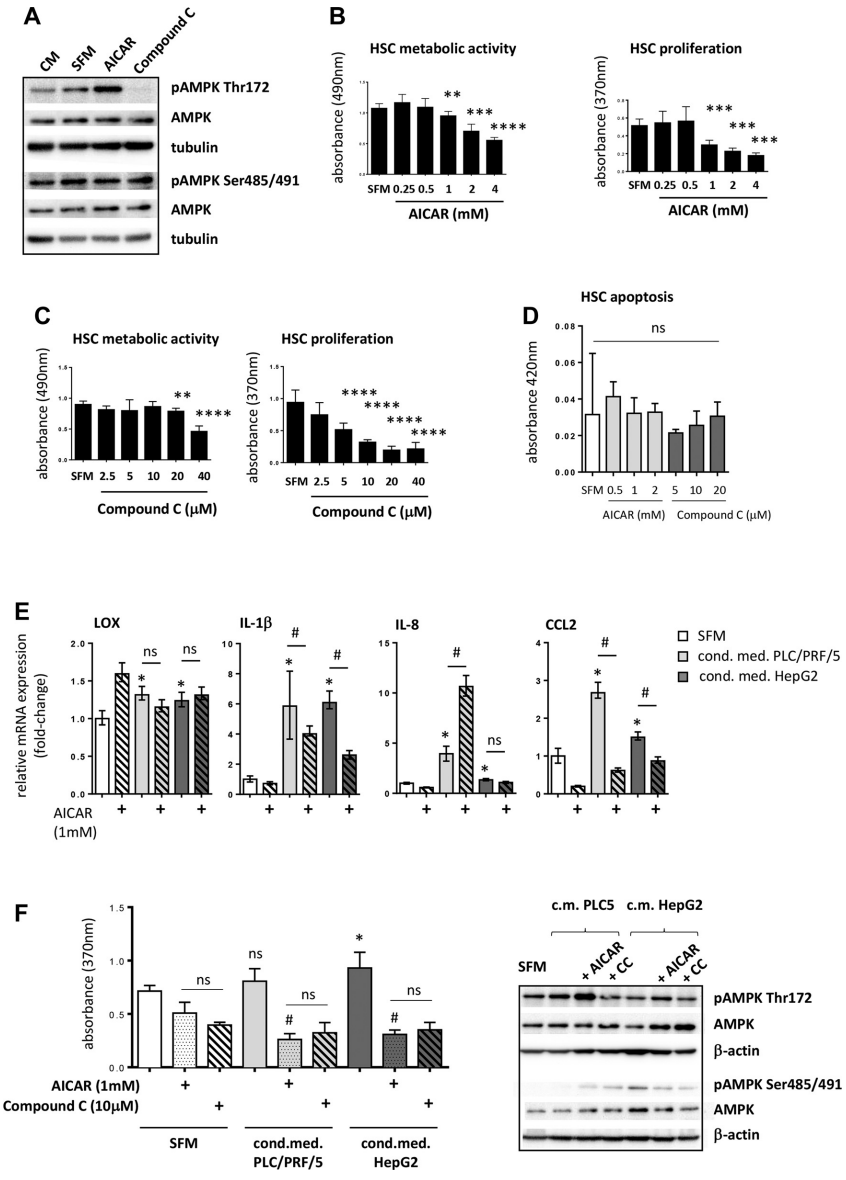

AJP-Gastrointest Liver Physiol • doi:10.1152/ajpgi.00262.2020 • www.ajpgi.org

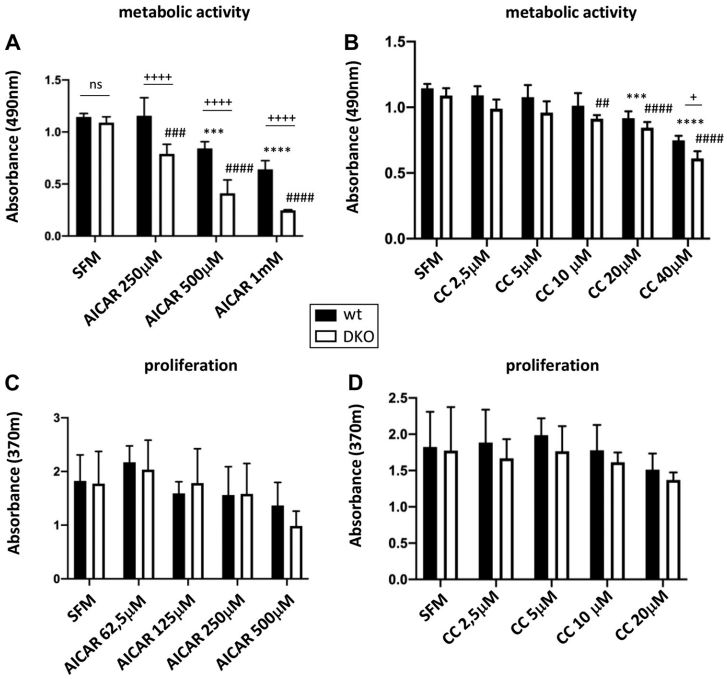

Figure 3. AICAR and Compound C inhibit hHSC metabolic activity and proliferation independently of AMPK. Metabolic activity (*A* and *B*) and proliferation (*C* and *D*) in wt and AMPK$^{\alpha1/\alpha2-/-}$ (DKO) MEFs following 24 h treatment with AICAR and Compound C. *A–D*: data represent means ± SD ***$P <$ 0.001, ****$P <$ 0.0001 versus SFM (wt), ##$P <$ 0.01, ###$P <$ 0.001, ####$P <$ 0.0001 versus SFM (AMPK$^{\alpha1/\alpha2-/-}$), +$P <$ 0.05, ++++$P <$ 0.0001 as indicated, representative data of four independent experiments (one-way ANOVA). AICAR, 5-aminoimidazole-4-carboxamide-1-β-d-ribofuranosid; AMPK, adenosine monophosphate-activated kinase; DKO, AMPK$^{\alpha1/\alpha2-/-}$; hHSC, human hepatic stellate cell; SFM, serum-free medium.

showed that AICAR could induce p-AMPK-Thr^{172} expression in hHSC treated with conditioned medium of PLC/PRF/5 and HepG2 cells. These effects were not observed when hHSC were exposed to Compound C in combination with HCC conditioned medium (Fig. 2*F*), indicating that the inhibitory effect of Compound C might be AMPK independent. Taken together, these data show that both AICAR and Compound C are potent inhibitors of hHSC activation and are able to reverse HCC-induced hHSC proliferation and activation in vitro.

AICAR and Compound C Inhibit MEF Proliferation in an AMPK-Independent Manner

Although AMPK is known as a crucial regulator of cell proliferation, pharmacological AMPK-modulating agents have been shown to act both in an AMPK-dependent and -independent manner (13, 41–44). Likewise, the previous set of data suggested that inhibition of hHSC proliferation and metabolic activity by AICAR and Compound C (Fig. 2) may be driven by both AMPK-dependent and AMPK-independent signals. To further test this hypothesis, we employed mouse embryonic fibroblasts (MEFs) deficient of both existing isotypes of the catalytic AMPK isoform α (AMPK$^{\alpha1/\alpha2-/-}$ i.e., DKO) and wild-type (wt) MEFs (29). Cells were treated with AICAR or Compound C for 24 hr and a significant, dose-dependent reduction of metabolic activity was observed in wt MEFs and AMPK$^{\alpha1/\alpha2-/-}$ MEFs (Fig. 3, *A* and *B*). Moreover, AICAR and Compound C showed a trend to inhibit cell proliferation in wt MEFs and AMPK$^{\alpha1/\alpha2-/-}$ MEFs (Fig. 3, *C* and *D*).

AICAR and Compound C Regulate hHSC Cell Proliferation through AMPK-Dependent and AMPK-Independent Mechanisms

We next aimed at unraveling the pathways and mechanisms through which AICAR and Compound C inhibited

Figure 2. AICAR and Compound C reverse HCC-induced hHSC activation. *A*: AMPK phosphorylation profile in hHSC treated with AICAR and Compound C. Human HSC metabolic activity and proliferation following 24 h treatment with AICAR (0.25–4 mM) (*B*) or Compound C (2.5–40 µM) (*C*). *D*: quantification of nucleosome expression by ELISA in hHSC following 24 h treatment with AICAR or Compound C. Gene expression (*E*), proliferation and protein expression (*F*) in hHSC following 24 h treatment with PLC/PRF/5 or HepG2 conditioned medium and AICAR (1 mM) or Compound C (10 µM). *B–D* and *F*: data represent means ± SD, *$P <$ 0.05, **$P <$ 0.01, ***$P <$ 0.001, ****$P <$ 0.0001 versus SFM and #$P <$ 0.05 versus non-AICAR-treated control. *E*: data represent means ± 95% confidence interval, *P = 0.05 versus serum-free medium, #P = 0.05 versus non-AICAR-treated control. *B* and *C*: n = 8 (t test vs. SFRM); *D* and *E*: n = 3 (one-way ANOVA); *F*: n = 4 (one-way ANOVA). AICAR, 5-aminoimidazole-4-carboxamide-1-β-d-ribofuranosid; c.m., conditioned medium; AMPK, adenosine monophosphate-activated kinase; CC, Compound C; CM, complete medium; ELISA, enzyme-linked immunosorbent assay; hHSC, human hepatic stellate cell; HCC, hepatocellular carcinoma; SFM, serum-free medium.

proliferation of hHSC and MEFs and their dependency on AMPK. First, cell cycle analysis was performed on hHSC treated with 1 mM AICAR or 10 μM Compound C for 24 hr. As shown in Fig. 4*A*, both AICAR and Compound C induced cell cycle arrest in hHSC in the S-phase. When analyzing the cell cycle in MEFs treated with AICAR or Compound C, we surprisingly observed inhibition of the cell cycle in both wt and AMPK$^{\alpha1/\alpha2-/-}$ MEFs, with AICAR inhibiting the cell cycle in the S-phase and Compound C in the G1 phase, respectively (Fig. 4*B*). These data suggest that both Compound C and AICAR can induce cell cycle arrest independently of AMPK.

Next, the mammalian target of rapamycin (mTOR), a critical regulator of cell metabolism and proliferation, was investigated to test another signaling pathway by which AICAR and Compound C may inhibit cell proliferation. Although mTOR is downstream of AMPK (12), the pathway can alternatively be regulated through various other pathways (45). The mTOR complex 1 (mTORC1) mediates its effects through phosphorylation of its downstream targets eukaryotic initiation factor 4E-binding protein 1 (4E-BP1) and the p70 ribosomal S6 kinase (S6) (46). Thus, hHSC were treated with 1 mM AICAR or 10 μM Compound C for 24 h, and

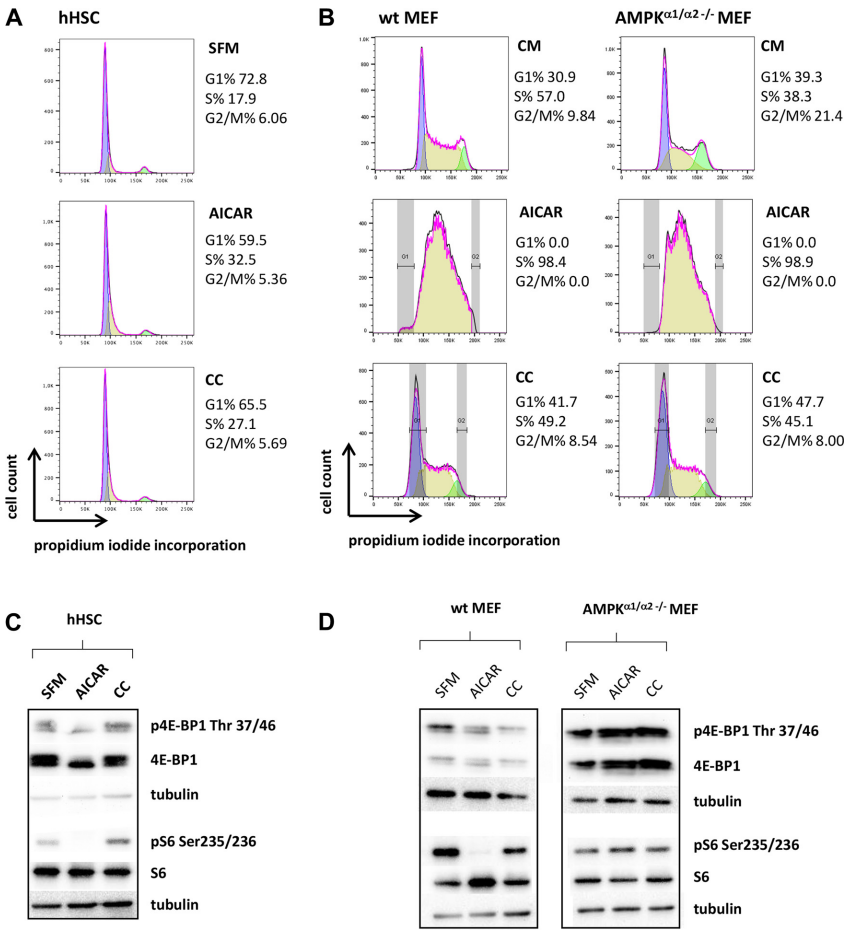

Figure 4. AICAR and Compound C inhibit hHSC proliferation through various mechanisms. *A*: cell cycle analysis in hHSC following treatment with 1 mM AICAR or 10 μM Compound C for 24 h. *B*: cell cycle analysis in wt and AMPKα1/α2$^{-/-}$ MEFs following treatment with 0.5 mM AICAR and 10 μM Compound C for 24 h. *C*: protein expression in hHSC following treatment with 1 mM AICAR or 10 μM Compound C for 24 h. *D*: protein expression in wt and AMPKα1/α2$^{-/-}$ MEFs following 24 h treatment with 0.25 mM AICAR and 10 μM Compound C. *A*–*D*: Representative data of at least three independent experiments. AICAR, 5-aminoimidazole-4-carboxamide-1-β-d-ribofuranosid; AMPKα1α2, AMP-activated protein kinase subunit α1α2-deficient; CC, Compound C; CM, complete medium; hHSC, human hepatic stellate cell; MEF, mouse embryonic fibroblasts; SFM, serum-free medium; wt, wild type.

AJP-Gastrointest Liver Physiol • doi:10.1152/ajpgi.00262.2020 • www.ajpgi.org

phosphorylation of S6 and 4E-BP1 proteins was assessed. Figure 4*C* demonstrates that phosphorylation of 4E-BP1 was mildly reduced, whereas phosphorylation of S6 was abrogated following treatment with AICAR, but not upon Compound C exposure (Supplemental Fig. S3*A*). These data show that AICAR, but not Compound C, inhibits cell proliferation through mTORC1 inhibition in hHSC. To further test whether AICAR inhibited mTORC1 in an AMPK-dependent manner, wt MEFs and AMPK$^{\alpha1/\alpha2-/-}$ MEFs were treated with AICAR for 24 h. As shown in Fig. 4*D*, phosphorylation of 4E-BP1 was slightly reduced, and phosphorylation of S6 was abrogated in AICAR-treated wt MEFs. In contrast, such reduction of 4E-BP1 and S6 phosphorylation did not occur in AMPK$^{\alpha1/\alpha2-/-}$ MEFs (Fig. 4*D*; Supplemental Fig. S3*A*), indicating that AICAR inhibits mTORC1 in wt MEFs and hHSC, in an AMPK-dependent manner. The data further show that Compound C only mildly reduced phosphorylation of 4E-BP1 in wt MEFs and that S6 phosphorylation was unchanged in wt MEFs and AMPK$^{\alpha1/\alpha2-/-}$ MEFs, clearly indicating that Compound C does not affect the mTORC1 pathway in MEFs or hHSC (Fig. 4*D*). Overall, these data show that both AICAR and Compound C inhibit cell proliferation through different pathways involving both AMPK-dependent and -independent mechanisms.

AMPK Gene Expression Is Overexpressed in a Subset of Patients with HCC

To further investigate possible changes in AMPK gene expression during the process of HCC, we analyzed the gene expression level of both isotypes of the catalytic AMPK α isoforms, that is, AMPKα1 (*PRKAA1*) and AMPKα2 (*PRKAA2*) in two independent cohorts of HCC tissue, that is, the TCGA and LICA-FR (47). In both cohorts, samples were excluded when carrying both the *TP53* and *CTNNB1* gene mutations. The main difference between both cohorts concerns etiology, that is, the TCGA cohort is enriched by patients with hepatitis B virus and contains a lower amount of patients featuring the CTNNB1 mutation rate. In contrast, there is no significant difference in the METAVIR fibrosis score between the two cohorts (Supplemental Table S1).

A correlation analysis was performed and showed that *PRKAA1* and *PRKAA2* expression levels are not associated (Fig. 5*A*; LICA-FR: $R = -0.101$, P value = ns and TCGA: $R = -0.026$, P value = ns). Next, *PRKAA1* and *PRKAA2* expressions were analyzed and no significant correlation was found in tumors carrying the *TP53* mutation (Supplemental Fig. S4). In contrast, a significant association was demonstrated between *PRKAA1* and *CTNNB1* mutation in the TCGA data set but not in LICA-FR, whereas a significant association was demonstrated between *PRKAA2* expression and tumors carrying the *CTNNB1* gene mutation in both cohorts (Fig. 5*B*). Importantly, a positive correlation was observed between *PRKAA2* expression and *CTNNB1* target genes such as glutamate-ammonia ligase (GLUL), leucine-rich repeat containing G protein-coupled receptor 5 (LGR5), and Laminin Subunit Alpha 3 (LAMA3) in both data sets confirming that *PRKAA2* is a potential CTNNB1 target gene (Fig. 5*C*).

Furthermore, both *PRKAA1* and *PRKAA2* expressions were compared in both data sets by using Edmondson grading (I–II and III–IV) and the previous described unsupervised transcriptome analysis (23), which classifies human HCC tumors into six subgroups (G1–G6). *PRKAA1* gene expression showed no significant correlation with different degrees in Edmondson grading (I–II and III–IV) (Supplemental Fig. S5*A* and S5*E*) and G1 versus G6 subgroups (Supplemental Fig. S5*B* and S5*F*) in both data sets. In contrast, *PRKAA2* expression showed significant differences between grade I–II versus III–IV ($P = 0.011$, LICA-FR data set; Supplemental Fig. S5*C*), whereas no significant correlation was found in the TCGA data set. Notably, in both data sets, a high *PRKAA2* expression was found in G5-G6 subgroups in line with its association with *CTNNB1* gene mutations (Supplemental Fig. S5, *D* and *H*).

Furthermore, IHC for the detection of AMPKα1 was performed on formalin-fixed paraffin-embedded human liver sections from histologically normal liver, cirrhotic liver without HCC, and HCC in the context of a cirrhotic liver (Supplemental Fig. S6). AMPKα1 weakly stained the hepatocyte membranes in both normal liver tissue and cirrhotic liver tissue without HCC (Supplemental Fig. S6*A* and S6*B*). Similar localization was observed in cirrhotic tissue surrounding the HCC lesion. AMPKα1 staining showed a stronger membrane staining with some cytoplasm staining in the HCC tumor tissue of patients with grade 1 (Supplemental Fig. S6*C*). Further, the tumor tissue of grade 2 classified patients showed a strong cytoplasmic staining for AMPKα1, which appeared even stronger in the HCC tissue classified as grade 3 (Supplemental Fig. S6, *D* and *E*).

Overall, these data, although reflecting the heterogeneity in human HCC (2), suggest an important role for AMPK modulation for the development of novel therapeutic strategies against HCC.

DISCUSSION

HCC is one of the leading causes of cancer death worldwide (1, 48). In spite of the recent progress in treatment options for HCC with the introduction of new multikinase inhibitors and immunotherapy (49), the identification of new therapeutic targets, more widely reflecting HCC biology, represents a current crucial effort in oncology.

The tumor microenvironment plays a crucial role in HCC development and progression (2, 6), as over 80% of HCC develop on the background of liver fibrosis and cirrhosis (50). In this context, genetic alterations and deregulation of signaling pathways are the result of chronic hepatocellular necrosis, inflammation, oxidative stress, and a dysregulated extracellular matrix (ECM) deposition, which further favor cancer development (6, 51). Moreover, in a previous study, we identified, by proteomic analysis, specific enriched proteins in the human cirrhotic ECM in comparison to healthy ECM proteins. Culturing the cells in a stiffer cirrhotic 3D microenvironment demonstrated the unique upregulation in genes related to epithelial to mesenchymal transition (EMT) and TGFβ signaling. Further demonstrating that the inherent features of the human cirrhotic liver ECM are key procarcinogenic components in HCC (52). One of the key hallmarks of the development of liver fibrosis is the activation of HSC (3). Recent evidence showed that the bidirectional cross talk between activated HSC and HCC cells promotes HCC cell proliferation and tumor growth (7, 8), in

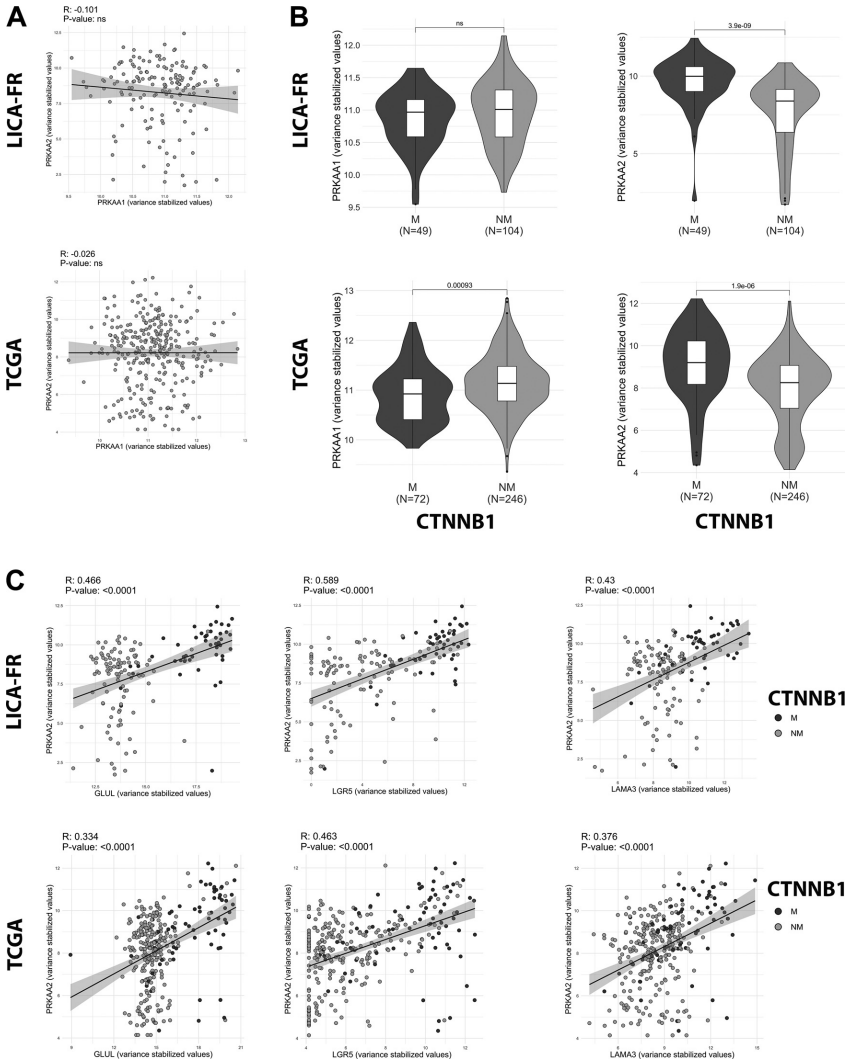

Figure 5. Validation of AMPK gene expression in a subset of HCC patients. Gene expression levels of AMPKα1 (*PRKAA1*) and AMPKα2 (*PRKAA2*) were investigated in two independent cohorts of HCC (TCGA and LICA-FR). *A*: correlation analysis showed that *PRKAA1* and *PRKAA2* expression levels are not associated (Spearman's $R = -0.101$ LICA-FR, P value = ns and Spearman's R = −0.026, P value = ns in TCGA). *B*: a significant association was observed between *PRKAA1* and *CTNNB1* gene mutations in the TCGA cohort but not in the LICA-FR data set. A significant association was demonstrated between *PRKAA2* expression and tumors carrying the *CTNNB1* gene mutation in both cohorts (Wilcoxon signed-rank test). *C*: a positive correlation was observed between *PRKAA2* expression and *CTNNB1* target genes such as *GLUL*, *LGR5*, and *LAMA3* in both data sets confirming that *PRKAA2* is a potential CTNNB1 target gene (Spearman's rank-order correlation, P value < 0.0001 (M, mutant, NM, nonmutant). AICAR, 5-aminoimidazole-4-carboxamide-1-β-d-ribofuranoside; AMPKα1α2, AMP-activated protein kinase subunit α1α2-deficient; CC, Compound C; CM, complete medium; GLUL, glutamate–ammonia ligase; hHSC, human hepatic stellate cell; HCC, hepatocellular carcinoma; LGR5, leucine rich repeat containing G protein-coupled receptor 5; LAMA3, laminin subunit α 3.

AJP-Gastrointest Liver Physiol • doi:10.1152/ajpgi.00262.2020 • www.ajpgi.org

addition to favoring a proinflammatory and profibrogenic microenvironment (8). Here, we investigated the potential paracrine effect of different HCC cell lines to activate primary human HSC and the possible implication of AMPK in the HCC-induced activation of hHSC. As HCC is known to be a highly heterogeneous cancer (20, 21), several HCC cell lines were investigated in this study. These cell lines are characterized by different mutations in cell cycle regulating genes such as p53 (PLC/PRF/5, Huh-7, Mahlavu) and β-catenin (HepG2, Huh-6, SNU398) (31–33) and express a characteristic secretome (34–36). Besides exerting different effects on hHSC proliferation and gene expression, HCC conditioned media differentially activated the AMPK pathway in hHSC, again emphasizing the complexity of HCC heterogeneity by possibly affecting the stromal compartment through AMPK induction. Indeed, when data mining two independent cohorts of HCC tissues, that is, the TCGA and LICA-FR, we showed no significant correlation between tumors carrying the *TP53* mutation and both catalytic AMPKα isoforms, whereas a significant correlation was found between tumors carrying the *CTNNB1* gene mutation and the AMPKα isoforms. It is known that *CTNNB1* and *TP53* mutations are affecting 25%–30% of HCC patients and both mutations are defined by different subgroups in HCC and correlate with better or worse patient outcome, respectively (20, 23, 27). Another layer of complexity may emerge knowing that in certain cancer cell lines and primary tumors a correlation has been demonstrated between *PRKAA1* gene copy number and mRNA expression suggesting that gene amplification does lead to increased expression, whereas the frequency of alterations in the *PRKAA2* gene in cancer is lower overall (53, 54). Moreover, recent studies have shown that the liver microenvironment may play a crucial role in NAFLD/NASH toward HCC progression. Such changes in HCC incidence are affected by obesity, type 2 diabetes, and NAFLD, which is the most common liver disease and marked by aberrant AMPK activity (55, 56). Indeed, in a previous study, an unbiased transcriptomic and ingenuity pathway analysis revealed no AMPK-related pathway enrichment in patients with NAFLD. Nevertheless, a list of AMPK-related genes, unbiasedly generated by means of STRING analysis and UCSC Genome Browser data mining tool goldenPath, showed to be significantly affected in the RNA sequence data of patients with NAFLD versus healthy controls. Several AMPK subunits such as *PRKAB1*, *PRKAB2*, and *PRKAG1* were significantly downregulated in patients with NAFLD. Most strikingly, a perturbation was found in many AMPK pathway genes such as TBC1D1, SLC2A4/GLUT4, AKT1/2, and genes involved in the regulation of lipid metabolism and activation/phosphorylation of AMPK such as Sirt3 and TSC2 in patients with NAFLD (57).

AMPKα1 is widely expressed across tissues, whereas AMPKα2 is more restricted in its tissue-and intracellular distribution (54, 58). Both AMPKα isoforms are expressed in human healthy and diseased liver tissue (53, 57, 59). Furthermore, we demonstrated that primary hHSC expresses more isoform AMPKα1 than AMPKα2 (39). Besides changes of AMPKα1/α2 gene expression in HCC, posttranslational modifications, such as the phosphorylation of AMPK is important in the development/progression of HCC as was demonstrated by Jiang et al. (60), that the risk of HCC occurrence was significantly higher in patients with a low expression of p-AMPK. In this study, we demonstrate that HCC-induced activation of hHSC can involve AMPK and its phosphorylation. Importantly, the catalytic AMPK subunit α can be phosphorylated at different phosphorylation sites (61). While phosphorylation at Thr^{172} activates AMPK (62), phosphorylation at $Ser^{485/491}$ inhibits its activity and favors dephosphorylation at Thr-172 (38, 63). We demonstrate that, depending on the HCC cell line used, either phosphorylation of AMPK-$Ser^{485/491}$ or phosphorylation of AMPK-Thr^{172} can be achieved by HCC cells. This further resulted in differences observed in hHSC proliferation.

In this study, we also provide new evidence for the possible working mechanisms of pharmacological agents known as AMPK activators and inhibitors in the cross talk between hHSC and HCC. Here, we demonstrate that the AMPK activator AICAR inhibits both the proliferation and the profibrogenic and proinflammatory phenotype of primary human HSC in a dose-dependent manner under basal conditions and after exposure to HCC conditioned medium. Indeed, pharmacologically induced AMPK activation has been shown to exert anti-HCC properties by inhibiting proliferation through AICAR (10, 17), and the incidence of several tumor types, including HCC, has been shown to be lower in patients treated with the AMPK activator and oral antidiabetic drug metformin (15). Our data reinforce the concept that AMPK activation may be beneficial for tumor–stromal interactions in HCC, as it can target both hHSC and HCC cells. Therefore, our data add new evidence about pharmacological AMPK activators and their effect on HCC-induced proliferation in primary hHSC.

Next, we demonstrate in more detail an AMPK-dependent but also AMPK-independent working mechanisms of Compound C, a known AMPK inhibitor, which inhibits proliferation and induces cancer cell death (13, 64, 65). Treatment with Compound C showed significant, dose-dependent antiproliferative effects on hHSC to the same extent as the AMPK activator AICAR without affecting the inhibitory phosphorylation of AMPK-$Ser^{485/491}$, suggesting AMPK-independent effects. Indeed, recent evidence suggests that Compound C exerts AMPK-independent antiproliferative effects in different cancers, by inducing apoptosis, inhibiting Akt and the mTOR signaling pathway, as well as induction of cell cycle arrest (13, 18). Unlike in cancer cells (13, 65), Compound C did not induce apoptosis in primary human HSC and did not modulate mTOR signaling pathway. However, we show that Compound C induces cell cycle arrest in the S-phase in hHSC and the G1-phase in MEFs and independently of AMPK. Moreover, we show that treatment with AICAR inhibits the mTORC1 pathway in primary hHSC and in wt MEFs in an AMPK-dependent manner. Overall, our data show that AICAR and Compound C inhibit hHSC proliferation through different mechanisms, some of which are AMPK dependent.

This study clearly demonstrates the existence of a cross talk between human HCC cells and primary human HSC which affects hHSC activation, as well as activation of the AMPK pathway in hHSC, pointing toward a role for AMPK in tumor–stromal interactions in HCC development. Moreover, the data show that pharmacological AMPK activation of the

antiproliferative pharmacological compounds AICAR and Compound C could represent a novel approach for anticancer and antifibrotic therapy.

ACKNOWLEDGMENTS

The results shown here are part based upon data generated by the TCGA https://www.cancer.gov/tcga and https://icgcportal.genomics.cn/projects/LICA-FR. We thank Brian Davidson, Barry Fuller, and Amir Gander (Tissue Access for Patient Benefit) and the NHSBT, for providing tissue samples for our research.

GRANTS

This research was funded by Grants from the NIHR UCLH BRC (to M. Pinzani and K. Rombouts), the Royal Free Charity (to M. Pinzani). L. Ghemtio gratefully acknowledges the support of The Drug Discovery and Chemical Biology—Biocenter Finland and The CSC—IT Center for Science Ltd. (Helsinki, Finland) for organizing computational resources. J. Zucman-Rossi group was supported by INSERM, Ligue Nationale contre le Cancer (Equipe Labellisée), Labex Oncolmmunology (investissement d'avenir), grant IREB, Coup d'Elan de la Fondation Bettencourt-Schueller, the SIRIC CARPEM, Raymond Rosen Award from the Fondation pour le Recherche Médicale, Prix René, and Andrée Duquesne—Comité de Paris Ligue Contre le Cancer and Fondation Mérieux. S. Caruso was supported by a funding from Labex Oncolmunology and CARPEM. G. Marrone received funding through a postdoctoral Fellowship by the European Association for the Study of the Liver (EASL). K. Böttcher received funding through a Physician–Scientist Fellowship by the European Association for the Study of the Liver (EASL).

DISCLAIMERS

The funders had no role in the design of the study; in the collection, analyses, or interpretation of data; in the writing of the manuscript, or in the decision to publish the results.

DISCLOSURES

L. Longato and G. Mazza are now full-time employees at Engitix Ltd., and L. Longato, G. Mazza, M. Pinzani, and K. Rombouts own shares in Engitix Therapeutics Ltd., A.H., T.V.L., M. P., and K.R. receive consultancies from Engitix Ltd. None of the other authors has any conflicts of interest, financial or otherwise, to disclose.

AUTHOR CONTRIBUTIONS

K.R. conceived and designed research; K.B., K.R., L.L., G. Marrone, G. Mazza, L.G., A.H., T.L., and S.C. performed experiments; K.B., K.R., L.L., G. Marrone, G. Mazza, L.G., A.H., T.L., and S.C. analyzed data; K.B., J.Z., M.P., K.R., L.L., G. Marrone, G. Mazza, L.G., S.C., and B.V. interpreted results of experiments; K.B. and K.R. prepared figures; K.B. and K.R. drafted manuscript; K.B., J.Z., M.P., K.R., L.L., A.H., T.L., and B.V. edited and revised manuscript; K.B., J.Z., M.P., K.R., G. Marrone, G. Mazza, L.G., A.H., T.L., S.C., and B.V. approved final version of manuscript.

REFERENCES

1. **Ferlay J**, **Soerjomataram I**, **Dikshit R**, **Eser S**, **Mathers C**, **Rebelo M**, **Parkin DM**, **Forman D**, **Bray F.** Cancer incidence and mortality worldwide: sources, methods and major patterns in GLOBOCAN 2012. *Int J Cancer* 136: E359–E386, 2015. doi:10.1002/ijc.29210.
2. **Llovet JM**, **Zucman-Rossi J**, **Pikarsky E**, **Sangro B**, **Schwartz M**, **Sherman M**, **Gores G.** Hepatocellular carcinoma. *Nat Rev Dis Primers* 2: 16018, 2016. doi:10.1038/nrdp.2016.18.
3. **Pinzani M.** Pathophysiology of liver fibrosis. *Dig Dis* 33: 492–497, 2015. doi:10.1159/000374096.
4. **Rombouts K.** Hepatic stellate cell culture models. In: *Stellate Cells in Health and Disease*, edited by Gandhi CRaPM**.** Cambridge, MA: Academic Press Elsevier, 2015, p. 15–27.
5. **Trautwein C**, **Friedman SL**, **Schuppan D**, **Pinzani M.** Hepatic fibrosis: concept to treatment. *J Hepatol* 62: S15–S24, 2015. doi:10.1016/j.jhep.2015.02.039.
6. **Carloni V**, **Luong TV**, **Rombouts K.** Hepatic stellate cells and extracellular matrix in hepatocellular carcinoma: more complicated than ever. *Liver Int* 34: 834–843, 2014. doi:10.1111/liv.12465.
7. **Amann T**, **Bataille F**, **Spruss T**, **Muhlbauer M**, **Gabele E**, **Scholmerich J**, **Kiefer P**, **Bosserhoff AK**, **Hellerbrand C.** Activated hepatic stellate cells promote tumorigenicity of hepatocellular carcinoma. *Cancer Sci* 100: 646–653, 2009. doi:10.1111/j.1349-7006.2009.01087.x.
8. **Coulouarn C**, **Corlu A**, **Glaise D**, **Guenon I**, **Thorgeirsson SS**, **Clement B.** Hepatocyte-stellate cell cross-talk in the liver engenders a permissive inflammatory microenvironment that drives progression in hepatocellular carcinoma. *Cancer Res* 72: 2533–2542, 2012. doi:10.1158/0008-5472.CAN-11-3317.
9. **Mihaylova MM**, **Shaw RJ.** The AMPK signalling pathway coordinates cell growth, autophagy and metabolism. *Nat Cell Biol* 13: 1016–1023, 2011. doi:10.1038/ncb2329.
10. **Lee CW**, **Wong LL**, **Tse EY**, **Liu HF**, **Leong VY**, **Lee JM**, **Hardie DG**, **Ng IO**, **Ching YP.** AMPK promotes p53 acetylation via phosphorylation and inactivation of SIRT1 in liver cancer cells. *Cancer Res* 72: 4394–4404, 2012. doi:10.1158/0008-5472.CAN-12-0429.
11. **Short JD**, **Houston KD**, **Dere R**, **Cai SL**, **Kim J**, **Johnson CL**, **Broaddus RR**, **Shen J**, **Miyamoto S**, **Tamanoi F**, **Kwiatkowski D**, **Mills GB**, **Walker CL.** AMP-activated protein kinase signaling results in cytoplasmic sequestration of p27. *Cancer Res* 68: 6496–6506, 2008. doi:10.1158/0008-5472.CAN-07-5756.
12. **Gwinn DM**, **Shackelford DB**, **Egan DF**, **Mihaylova MM**, **Mery A**, **Vasquez DS**, **Turk BE**, **Shaw RJ.** AMPK phosphorylation of raptor mediates a metabolic checkpoint. *Mol Cell* 30: 214–226, 2008. doi:10.1016/j.molcel.2008.03.003.
13. **Liu X**, **Chhipa RR**, **Nakano I**, **Dasgupta B.** The AMPK inhibitor compound C is a potent AMPK-independent antiglioma agent. *Mol Cancer Ther* 13: 596–605, 2014. doi:10.1158/1535-7163.MCT-13-0579.
14. **Steinberg GR**, **Carling D.** AMP-activated protein kinase: the current landscape for drug development. *Nat Rev Drug Disc* 18: 527–551, 2019. doi:10.1038/s41573-019-0019-2.
15. **Chen HP**, **Shieh JJ**, **Chang CC**, **Chen TT**, **Lin JT**, **Wu MS**, **Lin JH**, **Wu CY.** Metformin decreases hepatocellular carcinoma risk in a dose-dependent manner: population-based and in vitro studies. *Gut* 62: 606–615, 2013. doi:10.1136/gutjnl-2011-301708.
16. **Qu H**, **Yang X.** Metformin inhibits angiogenesis induced by interaction of hepatocellular carcinoma with hepatic stellate cells. *Cell Biochem Biophys* 71: 931–936, 2015. doi:10.1007/s12013-014-0287-8.
17. **Cheng J**, **Huang T**, **Li Y**, **Guo Y**, **Zhu Y**, **Wang Q**, **Tan X**, **Chen W**, **Zhang Y**, **Cheng W**, **Yamamoto T**, **Jing X**, **Huang J.** AMP-activated protein kinase suppresses the in vitro and in vivo proliferation of hepatocellular carcinoma. *PLoS One* 9: e93256, 2014. doi:10.1371/journal.pone.0093256.
18. **Adachi M**, **Brenner DA.** High molecular weight adiponectin inhibits proliferation of hepatic stellate cells via activation of adenosine monophosphate-activated protein kinase. *Hepatology* 47: 677–685, 2008. doi:10.1002/hep.21991.
19. **Caligiuri A**, **Bertolani C**, **Guerra CT**, **Aleffi S**, **Galastri S**, **Trappoliere M**, **Vizzutti F**, **Gelmini S**, **Laffi G**, **Pinzani M**, **Marra F.** Adenosine monophosphate-activated protein kinase modulates the activated phenotype of hepatic stellate cells. *Hepatology* 47: 668–676, 2008. doi:10.1002/hep.21995.
20. **Calderaro J**, **Ziol M**, **Paradis V**, **Zucman-Rossi J.** Molecular and histological correlations in liver cancer. *J Hepatol* 71: 616–630, 2019. doi:10.1016/j.jhep.2019.06.001.
21. **Dhanasekaran R**, **Nault JC**, **Roberts LR**, **Zucman-Rossi J.** Genomic medicine and implications for hepatocellular carcinoma prevention

and therapy. *Gastroenterology* 156: 492–509, 2019. doi:10.1053/j.gastro.2018.11.001.

22. **Hirsch TZ**, **Negulescu A**, **Gupta B**, **Caruso S**, **Noblet B**, **Couchy G**, **Bayard Q**, **Meunier L**, **Morcrette G**, **Scoazec JY**, **Blanc JF**, **Amaddeo G**, **Nault JC**, **Bioulac-Sage P**, **Ziol M**, **Beaufrere A**, **Paradis V**, **Calderaro J**, **Imbeaud S**, **Zucman-Rossi J.** BAP1 mutations define a homogeneous subgroup of hepatocellular carcinoma with fibrolamellar-like features and activated PKA. *J Hepatol* 72: 924–936, 2020. doi:10.1016/j.jhep.2019.12.006.
23. **Boyault S**, **Rickman DS**, **de RA**, **Balabaud C**, **Rebouissou S**, **Jeannot E**, **Herault A**, **Saric J**, **Belghiti J**, **Franco D**, **Bioulac-Sage P**, **Laurent-Puig P**, **Zucman-Rossi J.** Transcriptome classification of HCC is related to gene alterations and to new therapeutic targets. *Hepatology* 45: 42–52, 2007. doi:10.1002/hep.21467.
24. **Marrone G**, **De CF**, **Bottcher K**, **Levi A**, **Dhar D**, **Longato L**, **Mazza G**, **Zhang Z**, **Marrali M**, **Iglesias AF**, **Hall A**, **Luong TV**, **Viollet B**, **Pinzani M**, **Rombouts K.** The AMPK-v-ATPase-pH axis: a key regulator of the pro-fibrogenic phenotype of human hepatic stellate cells. *Hepatology* 68: 1140–1153, 2018.doi:10.1002/hep.30029.
25. **Longato L**, **Andreola F**, **Davies SS**, **Roberts JL**, **Fusai G**, **Pinzani M**, **Moore K**, **Rombouts K.** Reactive gamma-ketoaldehydes as novel activators of hepatic stellate cells in vitro. *Free Radic Biol Med* 102: 162–173, 2017. doi:10.1016/j.freeradbiomed.2016.11.036.
26. **Rombouts K**, **Carloni V.** Determination and characterization of tetraspanin-associated phosphoinositide-4 kinases in primary and neoplastic liver cells. *Methods Mol Biol* 1376: 203–212, 2016. doi:10.1007/978-1-4939-3170-5_17.
27. **Caruso S**, **Calatayud AL**, **Pilet J**, **La Bella T**, **Rekik S**, **Imbeaud S**, **Letouze E**, **Meunier L**, **Bayard Q**, **Rohr-Udilova N**, **Peneau C**, **Grasl-Kraupp B**, **de Koning L**, **Ouine B**, **Bioulac-Sage P**, **Couchy G**, **Calderaro J**, **Nault JC**, **Zucman-Rossi J**, **Rebouissou S.** Analysis of liver cancer cell lines identifies agents with likely efficacy against hepatocellular carcinoma and markers of response. *Gastroenterology* 157: 760–776, 2019. doi:10.1053/j.gastro.2019.05.001.
28. **Uphoff CC**, **Drexler HG.** Detection of mycoplasma contaminations in cell cultures by PCR analysis. *Hum Cell* 12: 229–236, 1999.
29. **Laderoute KR**, **Amin K**, **Calaoagan JM**, **Knapp M**, **Le T**, **Orduna J**, **Foretz M**, **Viollet B.** 5'-AMP-activated protein kinase (AMPK) is induced by low-oxygen and glucose deprivation conditions found in solid-tumor microenvironments. *Mol Cell Biol* 26: 5336–5347, 2006. doi:10.1128/MCB.00166-06.
30. **Bottcher K**, **Rombouts K**, **Saffioti F**, **Roccarina D**, **Rosselli M**, **Hall A**, **Luong T**, **Tsochatzis EA**, **Thorburn D**, **Pinzani M.** MAIT cells are chronically activated in patients with autoimmune liver disease and promote pro-fibrogenic hepatic stellate cell activation. *Hepatology* 68: 172–186, 2018. doi:10.1002/hep.29782.
31. **Cagatay T**, **Ozturk M.** P53 mutation as a source of aberrant beta-catenin accumulation in cancer cells. *Oncogene* 21: 7971–7980, 2002. doi:10.1038/sj.onc.1205919.
32. **Forbes SA**, **Bhamra G**, **Bamford S**, **Dawson E**, **Kok C**, **Clements J**, **Menzies A**, **Teague JW**, **Futreal PA**, **Stratton MR.** The Catalogue of Somatic Mutations in Cancer (COSMIC). *Curr Protoc Hum Genet Chapter* 10: 11, 2008.
33. **Rebouissou S**, **La Bella T**, **Rekik S**, **Imbeaud S**, **Calatayud AL**, **Rohr-Udilova N**, **Martin Y**, **Couchy G**, **Bioulac-Sage P**, **Grasl-Kraupp B**, **de Koning L**, **Ganne-Carrie N**, **Nault JC**, **Ziol M**, **Zucman-Rossi J.** Proliferation markers are associated with MET expression in hepatocellular carcinoma and predict tivantinib sensitivity in vitro. *Clin Cancer Res* 23: 4364–4375, 2017. doi:10.1158/1078-0432.CCR-16-3118.
34. **Brown KJ**, **Formolo CA**, **Seol H**, **Marathi RL**, **Duguez S**, **An E**, **Pillai D**, **Nazarian J**, **Rood BR**, **Hathout Y.** Advances in the proteomic investigation of the cell secretome. *Expert Rev Proteomics* 9: 337–345, 2012. doi:10.1586/epr.12.21.
35. **Li X**, **Jiang J**, **Zhao X**, **Wang J**, **Han H**, **Zhao Y**, **Peng B**, **Zhong R**, **Ying W**, **Qian X.** N-glycoproteome analysis of the secretome of human metastatic hepatocellular carcinoma cell lines combining hydrazide chemistry, HILIC enrichment and mass spectrometry. *PLoS One* 8: e81921, 2013. doi:10.1371/journal.pone.0081921.
36. **Xiang Y**, **Liu Y**, **Yang Y**, **Hu H**, **Hu P**, **Ren H**, **Zhang D.** A secretomic study on human hepatocellular carcinoma multiple drug-resistant cell lines. *Oncol Rep* 34: 1249–1260, 2015. doi:10.3892/or.2015.4106.
37. **Hawley SA**, **Davison M**, **Woods A**, **Davies SP**, **Beri RK**, **Carling D**, **Hardie DG.** Characterization of the AMP-activated protein kinase kinase from rat liver and identification of threonine 172 as the major site at which it phosphorylates AMP-activated protein kinase. *J Biol Chem* 271: 27879–27887, 1996. doi:10.1074/jbc.271.44.27879.
38. **Horman S**, **Vertommen D**, **Heath R**, **Neumann D**, **Mouton V**, **Woods A**, **Schlattner U**, **Wallimann T**, **Carling D**, **Hue L**, **Rider MH.** Insulin antagonizes ischemia-induced Thr172 phosphorylation of AMP-activated protein kinase alpha-subunits in heart via hierarchical phosphorylation of Ser485/491. *J Biol Chem* 281: 5335–5340, 2006. doi:10.1074/jbc.M506850200.
39. **Corton JM**, **Gillespie JG**, **Hawley SA**, **Hardie DG.** 5-aminoimidazole-4-carboxamide ribonucleoside: a specific method for activating AMP-activated protein kinase in intact cells? *Eur J Biochem* 229: 558–565, 1995. doi:10.1111/j.1432-1033.1995.tb20498.x.
40. **Sun Y**, **Connors KE**, **Yang DQ.** AICAR induces phosphorylation of AMPK in an ATM-dependent, LKB1-independent manner. *Mol Cell Biochem* 306: 239–245, 2007. doi:10.1007/s11010-007-9575-6.
41. **Liu X**, **Chhipa RR**, **Pooya S**, **Wortman M**, **Yachyshin S**, **Chow LM**, **Kumar A**, **Zhou X**, **Sun Y**, **Quinn B**, **McPherson C**, **Warnick RE**, **Kendler A**, **Giri S**, **Poels J**, **Norga K**, **Viollet B**, **Grabowski GA**, **Dasgupta B.** Discrete mechanisms of mTOR and cell cycle regulation by AMPK agonists independent of AMPK. *Proc Natl Acad Sci USA* 111: E435–E444, 2014. doi:10.1073/pnas.1311121111.
42. **Rattan R**, **Giri S**, **Singh AK**, **Singh I.** 5-Aminoimidazole-4-carboxamide-1-beta-D-ribofuranoside inhibits cancer cell proliferation in vitro and in vivo via AMP-activated protein kinase. *J Biol Chem* 280: 39582–39593, 2005. doi:10.1074/jbc.M507443200.
43. **Vucicevic L**, **Misirkic M**, **Janjetovic K**, **Harhaji-Trajkovic L**, **Prica M**, **Stevanovic D**, **Isenovic E**, **Sudar E**, **Sumarac-Dumanovic M**, **Micic D**, **Trajkovic V.** AMP-activated protein kinase-dependent and -independent mechanisms underlying in vitro antiglioma action of compound C. *Biochem Pharmacol* 77: 1684–1693, 2009. doi:10.1016/j.bcp.2009.03.005.
44. **Vucicevic L**, **Misirkic M**, **Janjetovic K**, **Vilimanovich U**, **Sudar E**, **Isenovic E**, **Prica M**, **Harhaji-Trajkovic L**, **Kravic-Stevovic T**, **Bumbasirevic V**, **Trajkovic V.** Compound C induces protective autophagy in cancer cells through AMPK inhibition-independent blockade of Akt/mTOR pathway. *Autophagy* 7: 40–50, 2011. doi:10.4161/auto.7.1.13883.
45. **Saxton RA**, **Sabatini DM.** mTOR signaling in growth, metabolism, and disease. *Cell* 169: 361–371, 2017. doi:10.1016/j.cell.2017.03.035.
46. **Laplante M**, **Sabatini DM.** mTOR signaling at a glance. *J Cell Sci* 122: 3589–3594, 2009. doi:10.1242/jcs.051011.
47. **Bayard Q**, **Meunier L**, **Peneau C**, **Renault V**, **Shinde J**, **Nault JC**, **Mami I**, **Couchy G**, **Amaddeo G**, **Tubacher E**, **Bacq D**, **Meyer V**, **La Bella T**, **Debaillon-Vesque A**, **Bioulac-Sage P**, **Seror O**, **Blanc JF**, **Calderaro J**, **Deleuze JF**, **Imbeaud S**, **Zucman-Rossi J**, **Letouze E.** Cyclin A2/E1 activation defines a hepatocellular carcinoma subclass with a rearrangement signature of replication stress. *Nat Commun* 9: 5235, 2018. doi:10.1038/s41467-018-07552-9.
48. **Jemal A**, **Bray F**, **Center MM**, **Ferlay J**, **Ward E**, **Forman D.** Global cancer statistics. *CA Cancer J Clin* 61: 69–90, 2011. [Erratum in *CA Cancer J Clin* 61: 134, 2011]. doi:10.3322/caac.20107.
49. **Llovet JM**, **Montal R**, **Sia D**, **Finn RS.** Molecular therapies and precision medicine for hepatocellular carcinoma. *Nat Rev Clin Oncol* 15: 599–616, 2018. doi:10.1038/s41571-018-0073-4.
50. **Thorgeirsson SS**, **Grisham JW.** Molecular pathogenesis of human hepatocellular carcinoma. *Nat Genet* 31: 339–346, 2002. doi:10.1038/ng0802-339.
51. **Hernandez-Gea V**, **Toffanin S**, **Friedman SL**, **Llovet JM.** Role of the microenvironment in the pathogenesis and treatment of hepatocellular carcinoma. *Gastroenterology* 144: 512–527, 2013. doi:10.1053/j.gastro.2013.01.002.
52. **Mazza G**, **Telese A**, **Al-Akkad W**, **Frenguelli L**, **Levi A**, **Marrali M**, **Longato L**, **Thanapirom K**, **Vilia MG**, **Lombardi B**, **Crowley C**, **Crawford M**, **Karsdal MA**, **Leeming DJ**, **Marrone G**, **Bottcher K**, **Robinson B**, **Del Rio Hernandez A**, **Tamburrino D**, **Spoletini G**, **Malago M**, **Hall AR**, **Godovac-Zimmermann J**, **Luong TV**, **De Coppi P**, **Pinzani M**, **Rombouts K.** Cirrhotic human liver extracellular matrix 3D scaffolds promote Smad-dependent TGF-beta1 epithelial mesenchymal transition. *Cells* 9: 83, 2019. doi:10.3390/cells9010083.
53. **Cerami E**, **Gao J**, **Dogrusoz U**, **Gross BE**, **Sumer SO**, **Aksoy BA**, **Jacobsen A**, **Byrne CJ**, **Heuer ML**, **Larsson E**, **Antipin Y**, **Reva B**,

Goldberg AP, **Sander C**, **Schultz N.** The cBio cancer genomics portal: an open platform for exploring multidimensional cancer genomics data. *Cancer Discov* 2: 401–404, 2012. [Erratum in *Cancer Discov* 2: 960, 2012]. doi:10.1158/2159-8290.CD-12-0095.

54. **Kazgan N**, **Williams T**, **Forsberg LJ**, **Brenman JE.** Identification of a nuclear export signal in the catalytic subunit of AMP-activated protein kinase. *Mol Biol Cell* 21: 3433–3442, 2010. doi:10.1091/mbc.e10-04-0347.
55. **Piscaglia F**, **Svegliati-Baroni G**, **Barchetti A**, **Pecorelli A**, **Marinelli S**, **Tiribelli C**, **Bellentani S.** and **Group H-NIS.** Clinical patterns of hepatocellular carcinoma in nonalcoholic fatty liver disease: a multicenter prospective study. *Hepatology* 63: 827–838, 2016. doi:10.1002/hep.28368.
56. **Zhao P**, **Saltiel AR.** From overnutrition to liver injury: AMP-activated protein kinase in nonalcoholic fatty liver diseases. *J Biol Chem* 295: 12279–12289, 2020. doi:10.1074/jbc.REV120.011356.
57. **Zanieri F**, **Levi A**, **Montefusco D**, **Longato L**, **De Chiara F**, **Frenguelli L**, **Omenetti S**, **Andreola F**, **Luong TV**, **Massey V**, **Caballeria J**, **Fondevila C**, **Shanmugavelandy SS**, **Fox T**, **Mazza G**, **Argemi J**, **Bataller R**, **Cowart LA**, **Kester M**, **Pinzani M**, **Rombouts K.** Exogenous liposomal ceramide-C6 ameliorates lipidomic profile, energy homeostasis, and anti-oxidant systems in NASH. *Cells* 9: 1237, 2020. doi:10.3390/cells9051237.
58. **Ross FA**, **MacKintosh C**, **Hardie DG.** AMP-activated protein kinase: a cellular energy sensor that comes in 12 flavours. *FEBS J* 283: 2987–3001, 2016. doi:10.1111/febs.13698.
59. **Qiu SL**, **Xiao ZC**, **Piao CM**, **Xian YL**, **Jia LX**, **Qi YF**, **Han JH**, **Zhang YY**, **Du J.** AMP-activated protein kinase alpha2 protects against liver injury from metastasized tumors via reduced glucose deprivation-induced oxidative stress. *J Biol Chem* 289: 9449–9459, 2014. doi:10.1074/jbc.M113.543447.
60. **Jiang X**, **Tan HY**, **Teng S**, **Chan YT**, **Wang D**, **Wang N.** The role of AMP-activated protein kinase as a potential target of treatment of hepatocellular carcinoma. *Cancers (Basel)* 11: 647, 2019. doi:10.3390/cancers11050647.
61. **Woods A**, **Vertommen D**, **Neumann D**, **Turk R**, **Bayliss J**, **Schlattner U**, **Wallimann T**, **Carling D**, **Rider MH.** Identification of phosphorylation sites in AMP-activated protein kinase (AMPK) for upstream AMPK kinases and study of their roles by site-directed mutagenesis. *J Biol Chem* 278: 28434–28442, 2003. doi:10.1074/jbc.M303946200.
62. **Suter M**, **Riek U**, **Tuerk R**, **Schlattner U**, **Wallimann T**, **Neumann D.** Dissecting the role of 5'-AMP for allosteric stimulation, activation, and deactivation of AMP-activated protein kinase. *J Biol Chem* 281: 32207–32216, 2006. doi:10.1074/jbc.M606357200.
63. **Hurley RL**, **Barre LK**, **Wood SD**, **Anderson KA**, **Kemp BE**, **Means AR**, **Witters LA.** Regulation of AMP-activated protein kinase by multisite phosphorylation in response to agents that elevate cellular cAMP. *J Biol Chem* 281: 36662–36672, 2006. doi:10.1074/jbc.M606676200.
64. **Huang SW**, **Wu CY**, **Wang YT**, **Kao JK**, **Lin CC**, **Chang CC**, **Mu SW**, **Chen YY**, **Chiu HW**, **Chang CH**, **Liang SM**, **Chen YJ**, **Huang JL**, **Shieh JJ.** p53 modulates the AMPK inhibitor compound C induced apoptosis in human skin cancer cells. *Toxicol Appl Pharmacol* 267: 113–124, 2013. doi:10.1016/j.taap.2012.12.016.
65. **Yang WL**, **Perillo W**, **Liou D**, **Marambaud P**, **Wang P.** AMPK inhibitor compound C suppresses cell proliferation by induction of apoptosis and autophagy in human colorectal cancer cells. *J Surg Oncol* 106: 680–688, 2012. doi:10.1002/jso.23184.

HEPATOLOGY

HEPATOLOGY, VOL. 00, NO. 00, 2018

MAIT Cells Are Chronically Activated in Patients With Autoimmune Liver Disease and Promote Profibrogenic Hepatic Stellate Cell Activation

Katrin Böttcher,[1,2] Krista Rombouts,[1] Francesca Saffioti,[1-3] Davide Roccarina,[1,2] Matteo Rosselli,[1,2] Andrew Hall,[1] TuVinh Luong,[1,2] Emmanuel A. Tsochatzis,[1,2] Douglas Thorburn,[1,2] and Massimo Pinzani[1,2]

Autoimmune liver diseases (AILDs) are chronic liver pathologies characterized by fibrosis and cirrhosis due to immune-mediated liver damage. In this study, we addressed the question whether mucosal-associated invariant T (MAIT) cells, innate-like T cells, are functionally altered in patients with AILD and whether MAIT cells can promote liver fibrosis through activation of hepatic stellate cells (HSCs). We analyzed the phenotype and function of MAIT cells from AILD patients and healthy controls by multicolor flow cytometry and investigated the interaction between human MAIT cells and primary human hepatic stellate cells (hHSCs). We show that MAIT cells are significantly decreased in peripheral blood and liver tissue of patients with AILD. Notably, MAIT cell frequency tended to decrease with increasing fibrosis stage. MAIT cells from AILD patients showed signs of exhaustion, such as impaired interferon-γ (IFN-γ) production and high *ex vivo* expression of the activation and exhaustion markers CD38, HLA-DR, and CTLA-4. Mechanistically, this exhausted state could be induced by repetitive stimulation of MAIT cells with the cytokines interleukin (IL)-12 and IL-18, leading to decreased IFN-γ and increased exhaustion marker expression. Of note, repetitive stimulation with IL-12 further resulted in expression of the profibrogenic cytokine IL-17A by otherwise exhausted MAIT cells. Accordingly, MAIT cells from both healthy controls and AILD patients were able to induce an activated, proinflammatory and profibrogenic phenotype in hHSCs *in vitro* that was partly mediated by IL-17. *Conclusion:* Our data provide evidence that MAIT cells in AILD patients have evolved towards an exhausted, profibrogenic phenotype and can contribute to the development of HSC-mediated liver fibrosis. These findings reveal a cellular and molecular pathway for fibrosis development in AILD that could be exploited for antifibrotic therapy. (HEPATOLOGY 2018; 00:000-000).

Mucosal-associated invariant T (MAIT) cells are innate-like T cells characterized by an evolutionarily conserved semi-invariant T cell receptor (TCR) consisting of an invariant α chain (Vα7.2-Jα33/Ja20/Jα12 in humans) and varying β chains,[1,2] as well as high expression of the C-type lectin CD161.[3] Human MAIT cells are abundant in peripheral blood, but particularly enriched in liver tissue, representing up to 30% of hepatic $CD3^+$ T cells.[3,4] The ability of MAIT cells to recognize microbial-derived vitamin B metabolites presented on the major histocompatibility complex class I–related

Abbreviations: AIH, autoimmune hepatitis; AILD, autoimmune liver disease; ANOVA, analysis of variance; HSC, hepatic stellate cell; hHSC, primary human hepatic stellate cell; IFN-γ, interferon-γ; IL, interleukin; MAIT cell, mucosal-associated invariant T cell; PBC, primary biliary cholangitis; NASH, nonalcoholic steatohepatitis; PBMC, peripheral blood mononuclear cell; PMA, phorbol 12-myristate 13-acetate; PSC, primary sclerosing cholangitis; RORγT, retinoic acid–related orphan receptor γT; SD, standard deviation; SEM, standard error of the mean; STAT, signal transducer and activator of transcription; TCR, T cell receptor; TIMP-1, tissue inhibitor of metalloproteinase 1; TNF-α, tumor necrosis factor α.

Received August 1, 2017; accepted January 9, 2018.

Additional Supporting Information may be found at onlinelibrary.wiley.com/doi/10.1002/hep.29782/suppinfo.

This work was supported by grants from the NIHR UCLH BRC and the Royal Free Charity (to M.P.) and Innovate UK (to K.R.) as well as a Physician-Scientist Fellowship by the European Association for the Study of the Liver (to K.B.).

View this article online at wileyonlinelibrary.com.

DOI 10.1002/hep.29782

Potential conflicts of interest: Nothing to report.

molecule MR1[5] allows MAIT cells to detect various strains of bacteria and yeasts *in vitro* and *in vivo*.[6,7] In line with their innate-like nature, MAIT cells are also activated by the proinflammatory cytokines interleukin (IL)-12 and IL-18 in a TCR-independent manner.[8] Once activated, MAIT cells exert cytotoxic properties and secrete proinflammatory cytokines such as IL-17 and IFN-γ.[3,6] In addition to their role in mediating antimicrobial defense, MAIT cells have been implicated in the development of noninfectious diseases, including autoimmune diseases such as multiple sclerosis[9,10] and inflammatory bowel disease,[11] suggesting that MAIT cells can orchestrate inflammatory responses in absence of infection. Autoimmune liver diseases (AILD) (e.g., primary sclerosing cholangitis [PSC], primary biliary cholangitis [PBC], and autoimmune hepatitis [AIH]) are characterized by chronic hepatic inflammation, which eventually leads to the development of liver fibrosis and cirrhosis and is associated with a high risk of morbidity and mortality.[12] The pathogenesis of AILD is poorly understood, although it is becoming increasingly clear that environmental triggers and genetic aberrations of immunoregulatory pathways contribute to chronic inflammation and T cell–mediated damage in the liver.[12] Genome-wide association studies recently demonstrated that variations in the *IL-12* pathway are associated with the development of PBC.[13] A potential role of IL-12 in AILD development is further supported by murine studies, in which deletion of the IL-12 subunit p40 ameliorated the development of autoimmune cholangitis,[14] and overexpression of IL-12 resulted in development of an AIH-resembling liver inflammation.[15] Central to the development of liver fibrosis by inflammation is the activation of hepatic stellate cells (HSCs), nonparenchymal liver cells that transform into extracellular matrix secreting myofibroblasts following activation.[16] HSC activation and the subsequent development of liver fibrosis are mediated by IL-17 in murine models, evident by ameliorated liver fibrosis in IL-17RA$^{-/-}$ mice *in vivo*, as well as increased collagen secretion and expression of α smooth muscle actin, IL-6, and transforming growth factor β by IL-17–stimulated HSCs *in vitro*.[17,18]

However, whether MAIT cell–derived IL-17A can mediate HSC activation in humans remains unclear. Here, we investigated the role of human MAIT cells in fibrosis development and HSC activation in AILD. Our data show that MAIT cells are severely reduced in peripheral blood and liver tissue from AILD patients, and the remaining MAIT cells show features of chronic activation and functional exhaustion, which could be induced by long-term exposure to the proinflammatory cytokines IL-12 and IL-18. Despite their exhausted state, MAIT cells produce large amounts of IL-17A in response to repetitive stimulation with IL-12. MAIT cells are further able to activate HSCs, leading to HSC proliferation and the expression of profibrogenic and proinflammatory genes in HSCs in an IL-17 and cell–cell contact dependent manner. Our data reveal a crucial role of MAIT cells in liver fibrosis development and provide important mechanistic insights that will help to design novel therapeutic approaches targeting HSC activation in fibrosis.

Material and Methods

A complete description of the materials and methods used in this study is provided in the Supporting Information.

ETHICS STATEMENT

This study was fully approved by the Royal Free Hospital ethical board. All participants provided written informed consent before sample collection.

ARTICLE INFORMATION:

From the [1]Regenerative Medicine and Fibrosis Group, Institute for Liver and Digestive Health, University College London, Royal Free Campus, London, United Kingdom; [2]Sheila Sherlock Liver Centre, Royal Free Hospital, London, United Kingdom; and [3]Department of Clinical and Experimental Medicine, Division of Clinical and Molecular Hepatology, University Hospital of Messina, Messina, Italy.

ADDRESS CORRESPONDENCE AND REPRINT REQUESTS TO:

Katrin Böttcher, M.D., Ph.D.
UCL Institute for Liver and Digestive Health
Royal Free Hospital
Rowland Hill Street
London NW3 2PF, United Kingdom
E-mail: katrin.bottcher@ucl.ac.uk
Tel.: +44-20-7794-0500

PRIMARY CELL ISOLATION

All tissue samples were obtained from patients or healthy volunteers at the Royal Free Hospital (see Supporting Table S1 for patient information). Peripheral blood mononuclear cells (PBMCs) were isolated using Ficoll-Paque Plus (GE Healthcare, Uppsala, Sweden) gradient centrifugation. Liver-associated lymphocytes were isolated from cirrhotic liver tissue derived from explanted livers of patients with AILD, from wedge sections of patients undergoing liver surgery in the absence of background liver disease, or from healthy liver explants considered unsuitable for transplantation (enabled by NHSBT). Primary human HSCs (hHSCs) were isolated from wedge sections of human liver tissue as described previously.[19]

FLOW CYTOMETRIC ANALYSIS

Cells were stained for surface markers and intracellular markers (see Supporting Information for a full list of antibodies). Dead cells were excluded using a live/dead fixable UV dead cell stain kit (Invitrogen, Carlsbad, CA). For staining of intracellular markers, cells were fixed and permeabilized using an Intracellular Fixation & Permeabilization Buffer Set (ebioscience, San Diego, CA) or human FOXP3 buffer set (BD Biosciences, San Jose, CA). CountBright Absolute Counting Beads (Molecular Probes, Eugene, OR) were used to determine absolute numbers of MAIT cells in peripheral blood. Samples were acquired with LSRFortessa (BD Biosciences, San Jose, CA) and analyzed with FlowJo 10.0 (Treestar, Ashland, OR).

TRANSIENT ELASTOGRAPHY

Transient elastography was performed to measure liver stiffness using FibroScan (Echosens, Waltham, MA). Fibrosis stage was defined using the previously described cutoffs for stiffness: F0-1, <7.1 kPa; F2, 7.1-9.4 kPa; F3, 9.5-12.4 kPa; F4, >12.5 kPa.[20]

IN VITRO STIMULATION ASSAYS

PBMCs or purified Vα7.2$^+$ cells, enriched by magnetic cell separation (see Supporting Information) were stimulated *in vitro* with 50 ng/mL phorbol 12-myristate 13-acetate (PMA) and 1 μM ionomycin (both Sigma Aldrich, St. Louis, MO) or Dynabead Human T-activator CD3/CD28 (Invitrogen) for 16 hours. PMBCs or purified Vα7.2$^+$ cells were stimulated *in vitro* with 50 ng/mL IL-1β, IL-18 (R&D Systems, Minneapolis, MN) or IL-12 (Miltenyi Biotec, Bergisch Gladbach, Germany) for 24 hours (short-term stimulation) or every 24 hours for 72 hours (long-term, repetitive stimulation). Brefeldin A and Monensin (both ebioscience, San Diego, CA) were added for the last 4 hours of culture when intracellular cytokine expression was analyzed by flow cytometry.

IN VITRO COCULTURE OF MAIT CELLS AND HSCs

Vα7.2$^+$ cells were purified from PBMCs by way of magnetic cell separation and added to cultured primary human HSCs for 48 hours. Dynabead Human T-activator CD3/CD28 (Invitrogen) or 2 μg/mL IL-17RA/IL-17R antibody (R&D Systems) was added where indicated. After extensive washing to remove MAIT cells, HSC gene expression was determined by quantitative real-time polymerase chain reaction and HSC proliferation was assessed using a bromodeoxyuridine cell proliferation enzyme-linked immunosorbent assay (Roche, Basel, Switzerland).

STATISTICAL ANALYSIS

Statistical analyses were performed using Microsoft Excel or Graph Pad Prism. Values are expressed as the mean ± standard deviation (SD), mean ± standard error of the mean (SEM), or mean ± 95% confidence interval (CI) as indicated in the figures. Statistical significance was analyzed with the appropriate test as indicated in the figures.

Results

MAIT CELLS ARE SIGNIFICANTLY DECLINED AND PHENOTYPICALLY ALTERED IN AILD PATIENTS

Human MAIT cells are defined by expression of CD3, CD161, and Vα7.2 TCR[2,3] (Supporting Fig. S1a). To investigate the MAIT cell compartment in patients with PSC, PBC, and AIH, we first determined the frequency of CD3$^+$ CD161^{++} Vα7.2$^+$ MAIT cells (hereafter referred to as MAIT cells) by way of flow cytometry in peripheral blood and liver tissue of AILD patients and healthy controls. MAIT cells were severely reduced in frequency and absolute number in peripheral blood (Fig. 1a) and liver tissue (Fig. 1b) of AILD patients, regardless of the subtype of disease. Moreover, MAIT cell frequency was

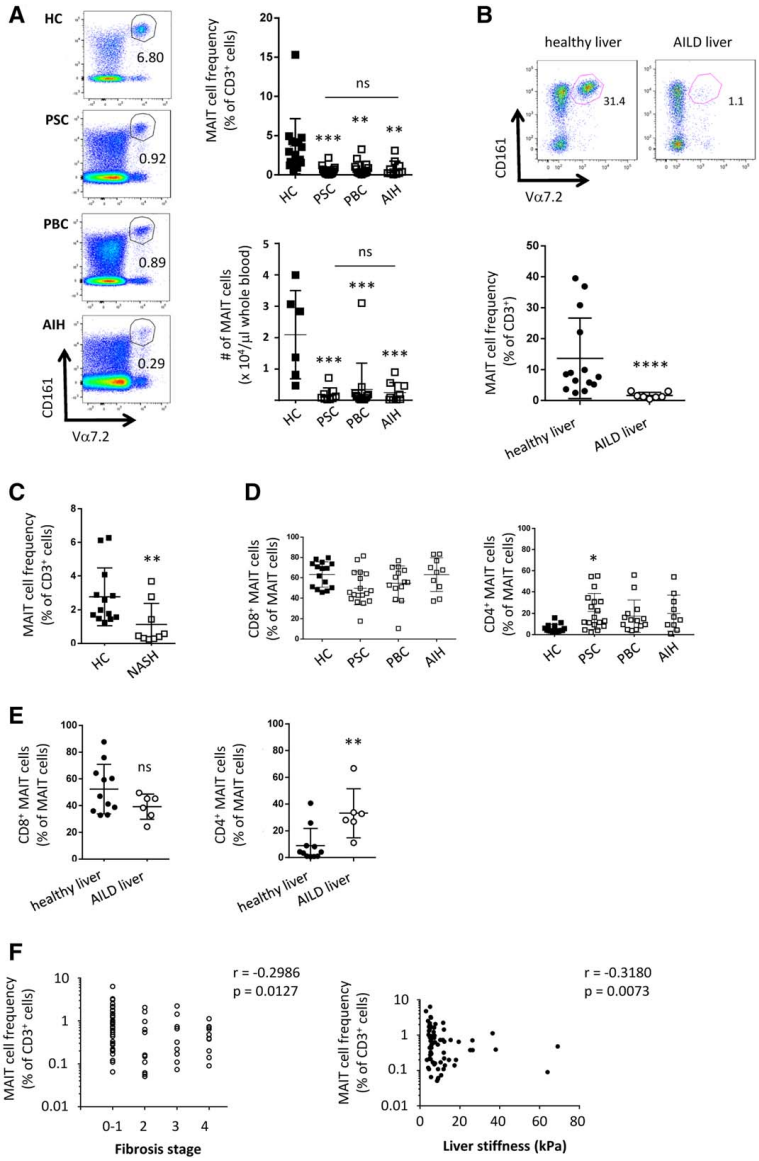

FIG. 1. MAIT cell frequency is significantly reduced in peripheral blood and liver tissue of patients with AILD. (a-c) MAIT cell frequency (HC, n = 15; PSC, n = 18; PBC, n = 14; AIH, n = 10) and absolute number in peripheral blood (a, c) and liver tissue (b). (d, e) Phenotype of MAIT cells in peripheral blood (d) and liver tissue (e). (f) Spearman correlation between MAIT cell frequency in peripheral blood of AILD patients and fibrosis stage or liver stiffness (n = 70). Data are presented as the mean ± SD and were pooled from four independent experiments. $^{*}P < 0.05$, $^{**}P < 0.01$, $^{***}P < 0.001$, $^{****}P < 0.0001$ versus healthy controls (HC). Data were assessed using one-way analysis of variance (ANOVA) with Tukey's multiple comparisons test (a, d) or Mann-Whitney test (b, c, e). ns, not significant.

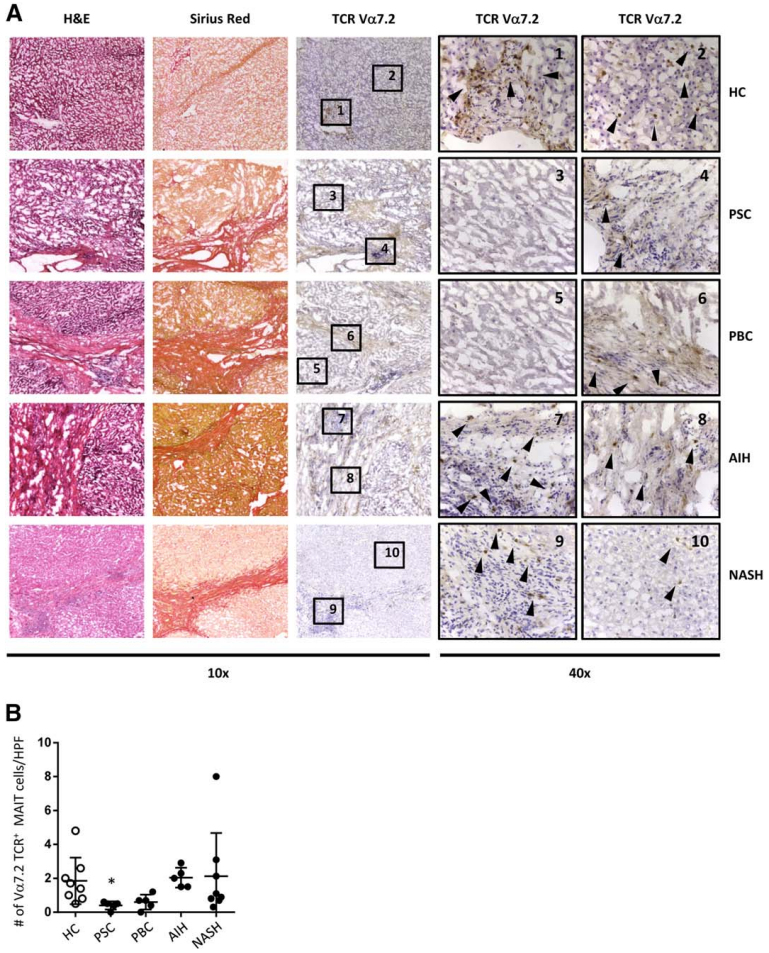

FIG. 2. MAIT cells localize around portal tracts and fibrotic septae in AILD livers. (a) Hematoxylin & eosin (H&E), Sirius Red, and immunohistochemistry of healthy and diseased liver tissue. (b) Number of Vα7.2$^+$ MAIT cells per high power field; each symbol represents one individual. Data are presented as the mean ± SD. $^*P < 0.05$ versus healthy controls (HC). Data were assessed using the Kruskal-Wallis test.

significantly decreased in peripheral blood of patients with nonalcoholic steatohepatitis (NASH) (Fig. 1c), suggesting that MAIT cells are decreased in various types of chronic liver disease. The significant decrease in frequency was specific to MAIT cells in AILD, because the frequency of other conventional and non-conventional lymphocyte populations was unchanged (Supporting Fig. S1b). MAIT cells can be divided into subsets based on CD4 and CD8 expression, with the majority of MAIT cells being CD8$^+$ or CD4/

$CD8^{-/-}$.[2] In AILD, all subsets of MAIT cells were significantly reduced in peripheral blood (Supporting Fig. S1c). $CD8^{+}$ MAIT cells represented the major subset in peripheral blood and liver tissue of healthy controls and AILD patients (Fig. 1d-e), although a relative increase of $CD4^{+}$ MAIT cells was observed (Fig. 1d-e) in AILD patients. Moreover, the frequency of MAIT cells in peripheral blood of AILD patients decreased with increasing fibrosis stage and liver tissue stiffness assessed by transient elastography (Fig. 1f), suggesting that the frequency of MAIT cells declines with disease progression in AILD. To analyze the localization of MAIT cells in the liver, Vα7.2 TCR was immunohistochemically detected in liver tissue of patients and controls. Whereas MAIT cells localized around the portal tracts and in the parenchyma in normal livers (Fig. 2a), MAIT cells were observed in inflammatory infiltrates around portal tracts and fibrotic septae in diseased livers (Fig. 2a). Quantification of $V\alpha7.2^{+}$ cells revealed a marked decrease of MAIT cell numbers in liver tissue of PSC and PBC patients compared to healthy controls, while MAIT cells were unchanged in highly inflamed AIH and NASH (Fig. 2b). Taken together, these data establish that the frequency of MAIT cells is severely reduced in peripheral blood and liver tissue of patients with AILD.

MAIT CELLS FROM AILD PATIENTS SHOW FEATURES OF CHRONIC ACTIVATION AND FUNCTIONAL EXHAUSTION

Because AILDs are characterized by chronic inflammation,[12] we next probed MAIT cells from patients with AILD for features of immune activation and exhaustion *ex vivo*. Whereas the surface expression of the inhibitory receptor PD-1 was comparable in MAIT cells from peripheral blood of patients and healthy controls (Supporting Fig. S2a), levels of CTLA-4 and TIM-3 were higher in MAIT cells from patients with AILD. Importantly, MAIT cells from AILD patients showed higher expression of CD39, a marker of terminal and irreversible T cell exhaustion.[21] In line with increased expression of exhaustion markers, MAIT cells from patients with AILD showed significantly higher levels of the activation marker CD38 and markedly increased expression of CD69 and HLA-DR (Fig. 3a), indicating that MAIT cells in peripheral blood of AILD patients are chronically activated. Mirroring the findings in MAIT cells from peripheral blood, hepatic MAIT cells from AILD patients showed significantly higher levels of CTLA-4 compared with healthy controls (Fig. 3b), while the levels of other activation and exhaustion markers were similar (Supporting Fig. S2b). Of note, MAIT cells isolated from peripheral blood of NAFLD/NASH patients showed increased expression of the activation and exhaustion markers PD-1, CD39, CD38, and HLA-DR as well (Supporting Fig. S2c), suggesting that MAIT cell activation also occurs in nonautoimmune liver disease. Because T cell exhaustion is associated with a loss of effector function,[22] we next assessed the ability of AILD MAIT to produce effector cytokines and cytolytic proteins in response to stimulation. Compared with healthy controls, IFN-γ production was significantly impaired in MAIT cells from patients with PBC, and markedly reduced in MAIT cells from patients with PSC and AIH following *in vitro* stimulation with PMA/ionomycin (Fig. 3c). Moreover, MAIT cells from AILD patients showed higher granzyme B levels at steady state, but failed to significantly up-regulate granzyme B expression upon CD3/CD28 bead stimulation, compared with healthy controls (Fig. 3d). In contrast, IL-17A and tumor necrosis factor α (TNF-α) production in response to such stimulation remained unchanged (Fig. 3e and Supporting Fig. S2d). These data strongly suggest that MAIT cells in AILD are highly activated and show signs of early functional exhaustion while maintaining their ability to express IL-17A and TNF-α. Correlation analyses further revealed a negative correlation between MAIT cell frequency in AILD and expression of activation markers such as CD38 and HLA-DR as well as exhaustion markers such as CTLA4, CD39, and TIM-3 (Fig. 3f and Supporting Fig. S2e). These data indicate that the low frequency of circulating MAIT cells in AILD patients may result from reduced survival of MAIT cells as a consequence of chronic activation and exhaustion *in vivo*.

LONG-TERM STIMULATION WITH IL-12 + IL-18 DRIVES MAIT CELL EXHAUSTION AND CELL DEATH

High expression of the cytokine receptors IL-12R and IL-18R by MAIT cells allows for TCR-independent stimulation of MAIT cells with IL-12 and IL-18 which results in IFN-γ expression.[8] In line with this, we observed high levels of IL-12R and IL-

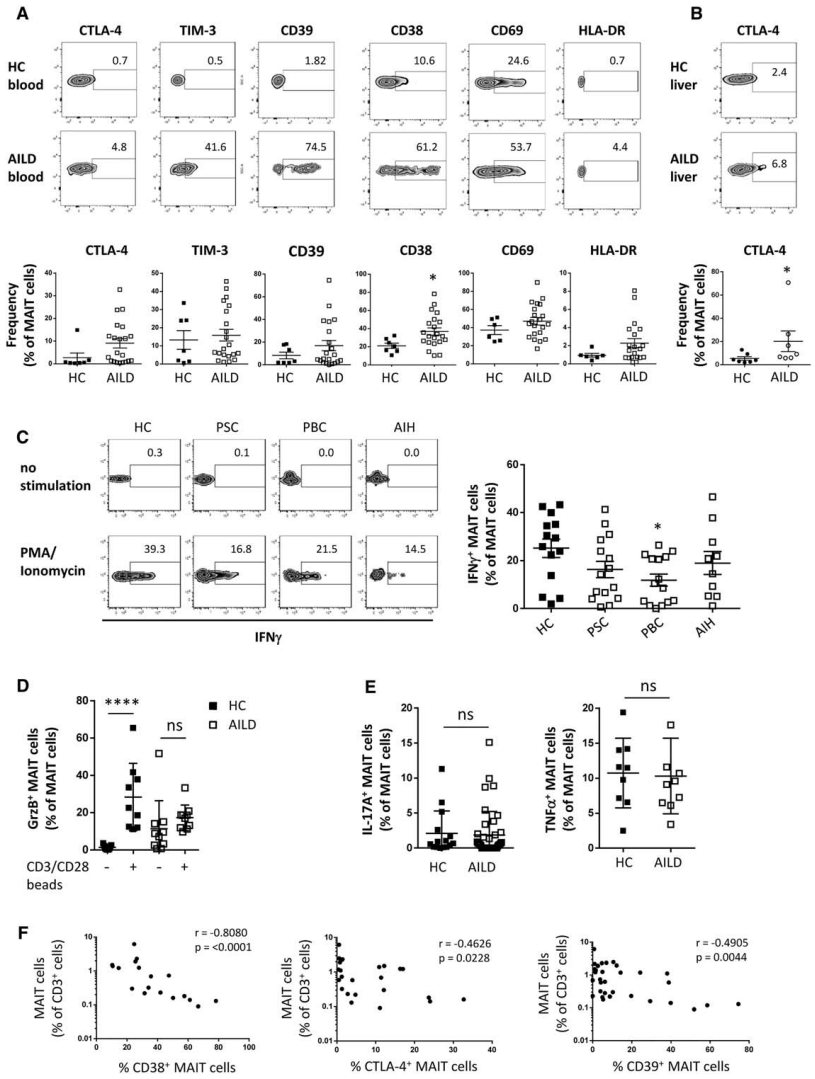

FIG. 3. AILD MAIT cells show signs of exhaustion and express IL-17A. *Ex vivo* expression of surface markers in MAIT cells from (a) peripheral blood and (b) liver. (c-e) Intracellular IFN-γ (c), granzyme B (d), IL-17A and TNF-α (e) expression in MAIT cells following in vitro PMA/ionomycin (c, e) or CD3/CD28 bead (d) stimulation for 16 hours. (e, f) Spearman correlation between MAIT cell frequency in peripheral blood of AILD patients and expression of activation markers and inhibitory receptors. Data are presented as the mean ± SEM (a,c), or mean ± SD (b, d, e) and were pooled from at least three independent experiments. $^{*}P < 0.05$ vs. healthy controls (HC), $^{****}P < 0.0001$ versus unstimulated control. Data were assessed using the Mann-Whitney test (a, b, e), or one-way ANOVA with Tukey's or Dunn's multiple comparisons test (c, d). ns, not significant.

18R expression on MAIT cells from peripheral blood and liver tissue of healthy controls and AILD patients (Supporting Fig. S3a-b). AILDs are characterized by persistent liver inflammation and high serum levels of proinflammatory cytokines such as IL-1β, IL-12, and IL-18.[23,24] We mimicked this chronic inflammatory setting by repetitively stimulating MAIT cells with IL-12, IL-18, and IL-1β *in vitro* and assessed their ability to express IFN-γ. Both short-term (24 hours) and repetitive, long-term (72 hours) in vitro stimulation with a combination of IL-12 and IL-18, but not IL-12 or IL-18 alone, induced a robust IFN-γ response in MAIT cells from healthy controls and AILD patients, which was not further exacerbated by additional IL-1β (Fig. 4a), demonstrating that the response to cytokine-mediated stimulation is maintained in MAIT cells from patients with AILD, despite their exhausted phenotype. To exclude effects from bystander immune cells in the stimulated PBMC pool on the induction of IFN-γ expression in MAIT cells, purified Vα7.2$^+$ MAIT cells from healthy controls were stimulated with IL-1β, IL-12, and IL-18 next. Like in PBMCs, IL-12 + IL-18 specifically induced expression of IFN-γ in purified MAIT cells (Fig. 4b), indicating that IL-12 + IL-18 can directly stimulate MAIT cell activation. Interestingly, IFN-γ expression of MAIT cells from healthy controls and AILD patients significantly decreased following repetitive, long-term stimulation with IL-12 + IL-18 in vitro (Fig. 4c), despite constant levels of IL-12 receptor expression (Supporting Fig. S4a). Because decreasing IFN-γ expression is a hallmark of T cell exhaustion, we next tested the expression of inhibitory receptors in cytokine-stimulated MAIT cells. Following repetitive stimulation with IL-12 + IL-18, we observed increased PD-1 and TIM-3 expression, as well as significantly higher expression of CD39 in MAIT cells from healthy controls (Fig. 4d) and AILD patients (Supporting Fig. S34b). Moreover, the frequency of live MAIT cells declined in response to repetitive stimulation with IL-12 + IL-18, whereas the frequency of CD3$^+$ cells remained constant (Supporting Fig. S4c), showing that MAIT cell loss was specific and not accompanied by general T cell death in culture. These data suggest that repetitive stimulation with the proinflammatory cytokines IL-12 + IL-18 can to drive MAIT cell exhaustion and cell death *in vitro*. To investigate possible mechanisms of MAIT cell exhaustion in AILD *in vivo*, we analyzed CD3 expression in hepatic MAIT cells as a surrogate marker for antigen exposure.[25] Indeed, hepatic AILD MAIT cells showed significantly lower expression of CD3 compared with healthy controls (Fig. 4e), suggesting that MAIT cells are chronically exposed to their cognate antigen in AILD livers *in vivo*. Of note, exposure to bacterial antigens has been shown to induce downregulation of the transcription factors eomesodermin and T-bet in MAIT cells, which has been linked to MAIT cell exhaustion.[26] We therefore analyzed T-bet and eomesodermin expression in MAIT cells *ex vivo*. Indeed, MAIT cells from peripheral blood of AILD patients expressed significantly lower levels of eomesodermin and lower levels of T-bet compared with healthy controls (Fig. 4f). These data suggest that MAIT cell exhaustion in AILD might be induced by chronic exposure to both inflammatory cytokines and bacterial antigen and may be regulated by downregulation of T-bet and eomesodermin.

REPETITIVE IL-12 STIMULATION SIGNIFICANTLY INDUCES THE EXPRESSION OF THE PROFIBROGENIC CYTOKINE IL-17A IN MAIT CELLS

Previous reports have described the induction of IFN-γ expression in MAIT cells in a PBMC pool by IL-12 + IL-18.[8,27] However, to our knowledge there is no evidence for cytokine-mediated stimulation of IL-17A expression, which has been shown to contribute to fibrosis development in animal models and to stimulate HSC activation in vitro.[17,18] Interestingly, no IL-17A expression was detected in MAIT cells after short-term (24 hours) cytokine stimulation (Fig. 5a). In contrast, repetitive, long-term (72 hours) stimulation with IL-12 alone or in combination with other cytokines resulted in a significant increase in IL-17A$^+$ MAIT cells from healthy controls (Fig. 5b). Similarly, repetitive stimulation of purified MAIT cells with IL-12 significantly induced IL-17A expression in MAIT cells (Fig. 5c), demonstrating that the observed IL-17A expression resulted from direct IL-12 signaling on MAIT cells. Along these lines, long-term stimulation with IL-12 induced IL-17A expression in MAIT cells from AILD patients (Fig. 5d), which was indistinguishable from IL-17A expression in MAIT cells from healthy controls (Fig. 5e). These data demonstrate that MAIT cells from AILD patients, despite their exhausted phenotype, produce IL-17A in response to repetitive stimulation with inflammatory cytokines. To elucidate a mechanism through which

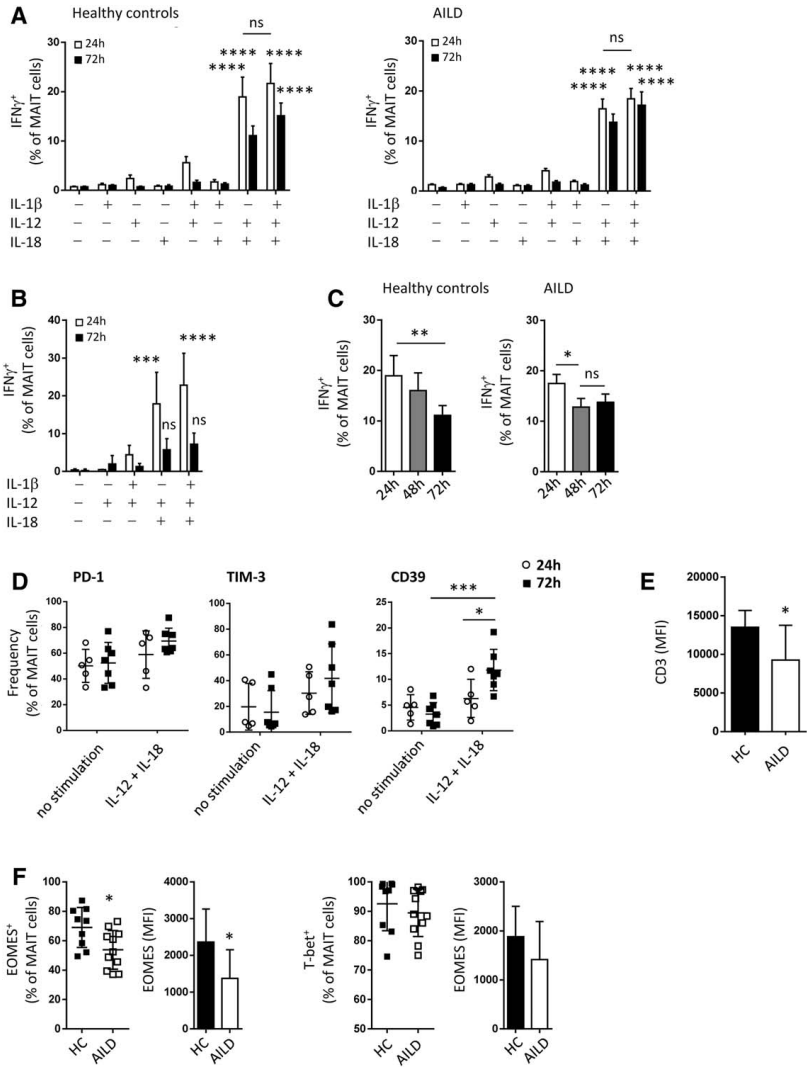

FIG. 4. Long-term exposure to proinflammatory cytokines drives MAIT cell exhaustion. Intracellular IFN-γ expression of (a) MAIT cells in a PMCB pool (n = 12) or (b) purified Vα7.2+ cells (n = 3) stimulated with IL-1β, IL-12, and IL-18 (24-72 hours). (c) Intracellular IFN-γ expression of MAIT cells in a PBMC pool stimulated with IL-12 + IL-18 (72 hours) (n = 12). (d) Surface expression of inhibitory receptors in peripheral blood MAIT cells from healthy controls stimulated with IL-12 + IL-18 (24-72 hours). (e) CD3 expression in hepatic MAIT cells. (f) Eomesodermin (EOMES) and T-bet expression in peripheral blood MAIT cells. Data are presented as the mean ± SEM (a, c), or mean ± SD (b, d-f) and were pooled from at least three independent experiments.$^{*}P < 0.05$, $^{**}P < 0.01$, $^{***}P < 0.001$, $^{****}P < 0.0001$ versus no stimulation, healthy controls (HC), or as indicated. Data were assessed using two-way ANOVA and Sidak's multiple comparisons test (a-d) or a Mann-Whitney test (e-f). ns, not significant.

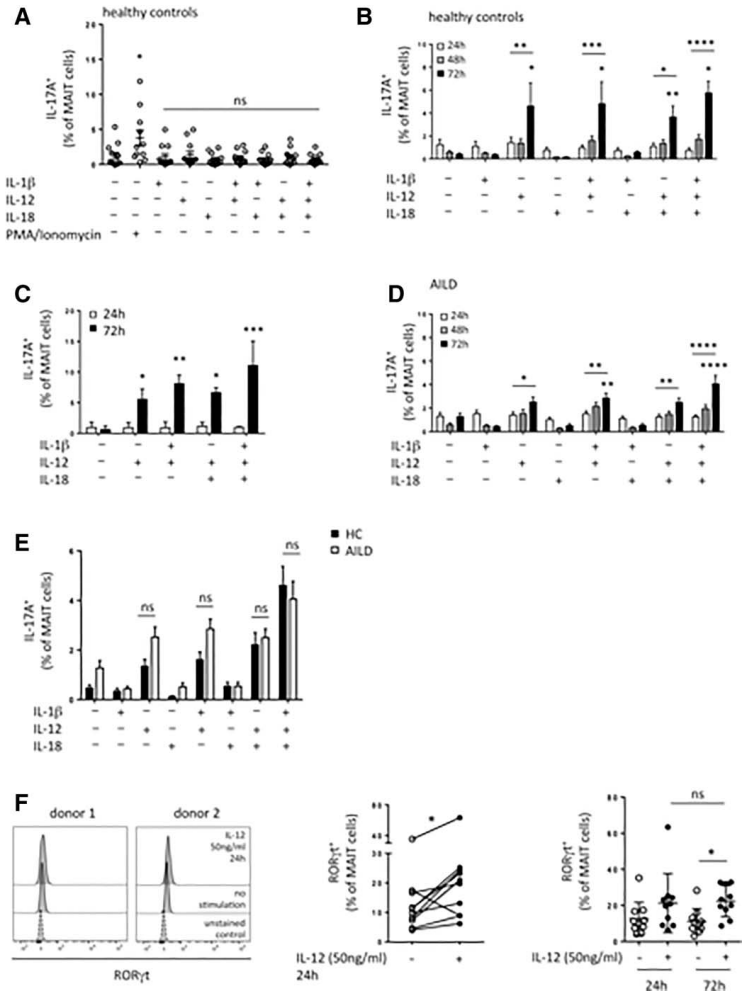

FIG. 5. Repetitive IL-12 stimulation induces IL-17A expression in MAIT cells. Intracellular IL-17A expression in MAIT cells in a PBMC pool from (a, b) healthy controls (HC) (n = 12) and (d) AILD patients (n = 26) stimulated with IL-1*β*, IL-12, and IL-18 for (a) 24 hours or (b, d) 24 -72 hours. (c) Intracellular IL-17A expression of purified Vα7.2$^+$ MAIT cells following cytokine stimulation (24-72 hours) (n = 3). (e) Intracellular IL-17A expression of MAIT cells from HC and AILD patients after cytokine stimulation (72 hours) (HC, n = 9; AILD, n = 26). (f) RORγt expression in MAIT cells after IL-12 stimulation (24-72 hours). Data are presented as the mean ± SEM (a, b; d, e) and were pooled from four independent experiments. (c, f) Data are presented as the mean ± SD and were pooled from at least two independent experiments. *$P < 0.05$, **$P < 0.01$, ***$P < 0.001$, ****$P < 0.0001$ versus no stimulation or as indicated. Data were assessed using two-way ANOVA and Sidak's multiple comparisons test (a-e) or a paired t-test and Kruskal-Wallis test (f).

IL-12 stimulates IL-17A expression in MAIT cells, we analyzed expression of the transcription factor retinoic acid–related orphan receptor γT (RORγt), which is required for the expression of IL-17 in T cells.[28] We detected significantly increased levels of RORγt expression in MAIT cells from healthy controls (Fig. 5f) and AILD patients (Supporting Fig. S5a) following 24-hour IL-12 stimulation, which was sustained in MAIT cells stimulated for 72 hours (Fig. 5f and Supporting Fig. S5a). These data indicate that IL-12 signaling induces robust up-regulation of RORγt expression in MAIT cells, which may mechanistically enable IL-17A expression.

MAIT CELLS STIMULATE PRIMARY HUMAN HSC PROLIFERATION AND INDUCE AN ACTIVATED, PROINFLAMMATORY HSC GENE SIGNATURE IN A CELL–CELL CONTACT AND IL-17–DEPENDENT MANNER

Chronic hepatic inflammation in AILD results in the development of liver fibrosis[12] as a consequence of HSC activation,[29] which can be mediated by IL-17A in murine models.[17,18] As we observed IL-17A expression by MAIT cells upon repetitive stimulation with IL-12, we hypothesized that human MAIT cells are able to activate HSCs in vitro and analyzed hHSC proliferation in the presence of MAIT cells. Coculture of hHSCs with MAIT cells at a ratio of 1:1 resulted in a significant increase in hHSC proliferation (Fig. 6a). We next investigated gene expression in hHSCs cocultured with MAIT cells. MAIT cells induced increased expression of Acta2, coding for the activation marker α smooth muscle actin in hHSCs, as well as a significant increase in expression of the profibrogenic genes collagen 1, lysyl oxidase (LOX), and tissue inhibitor of metalloproteinase 1 (TIMP-1) (Fig. 6b). Similarly, expression of proinflammatory genes (e.g., IL-1β, IL-6, IL-8, and CCL2) was significantly increased in hHSCs following 48-hour coculture with MAIT cells (Fig. 6b). We next investigated whether MAIT cells from AILD patients, although exhausted, were able to increase the expression of genes typical of HSC activation. Similar to MAIT cells from healthy controls, MAIT cells from AILD patients induced gene expression in HSCs regardless of disease type (Fig. 6c) and stimulated hHSC proliferation (Supporting Fig. S6a), indicating that MAIT cells from AILD patients retain their profibrogenic potential. Of note, MAIT cells isolated from patients with different fibrosis stages showed no difference in their ability to induce hHSC proliferation and gene expression. Moreover, similar to AILD MAIT cells, NASH MAIT cells stimulated proinflammatory gene expression in HSCs (Fig. 6d). These data indicate that MAIT cells are able to further promote the features of hHSC activation in vitro, a process that contributes to fibrosis development in the liver *in vivo*.[29] To determine whether IL-17A mediates hHSC activation by MAIT cells, we tested the effect of IL-17RA blockade on hHSC gene expression in our coculture system. Because IL-17 did not induce expression of profibrogenic genes in hHSCs in vitro but was sufficient to induce expression of proinflammatory genes in hHSCs (Supporting Fig. S6b), we tested the effect of IL-17R blockade on proinflammatory gene expression. Indeed, blocking IL-17R resulted in a decrease of IL-1β, IL-8, and CCL2 expression in hHSCs cocultured with MAIT cells (Fig. 6e), indicating that hHSC activation by MAIT cells is partly mediated by IL-17A. We next investigated whether hHSC activation by MAIT cells also requires cell–cell contact. MAIT cells and hHSCs were either cocultured allowing for cell–cell contact or in a transwell system, thereby preventing cellular contact but allowing the exchange of soluble mediators. Separation of MAIT cells and hHSCs in the transwell system partly reversed up-regulation of IL-1β, IL-8, and CCL2 expression and abrogated up-regulation of IL-6, LOX, and TIMP-1 expression in HSCs (Fig. 6f). Taken together, these data suggest that MAIT cells from healthy individuals, as well as from patients with chronic liver disease, can induce hHSC activation in vitro in an IL-17A– and cell–cell contact–dependent manner.

Discussion

The pathogenesis of AILD development is still incompletely understood. However, it has recently become clear that chronic inflammation observed in AILD results from inadequate immune activation and a breakdown of self-tolerance in the liver, culminating in T cell–mediated liver damage and fibrosis development,[12] which is characterized and driven by HSC activation.[29] Here, we demonstrate a potential role of MAIT cells in fibrosis development in AILD. Irrespective of the type of disease, MAIT cells in AILD

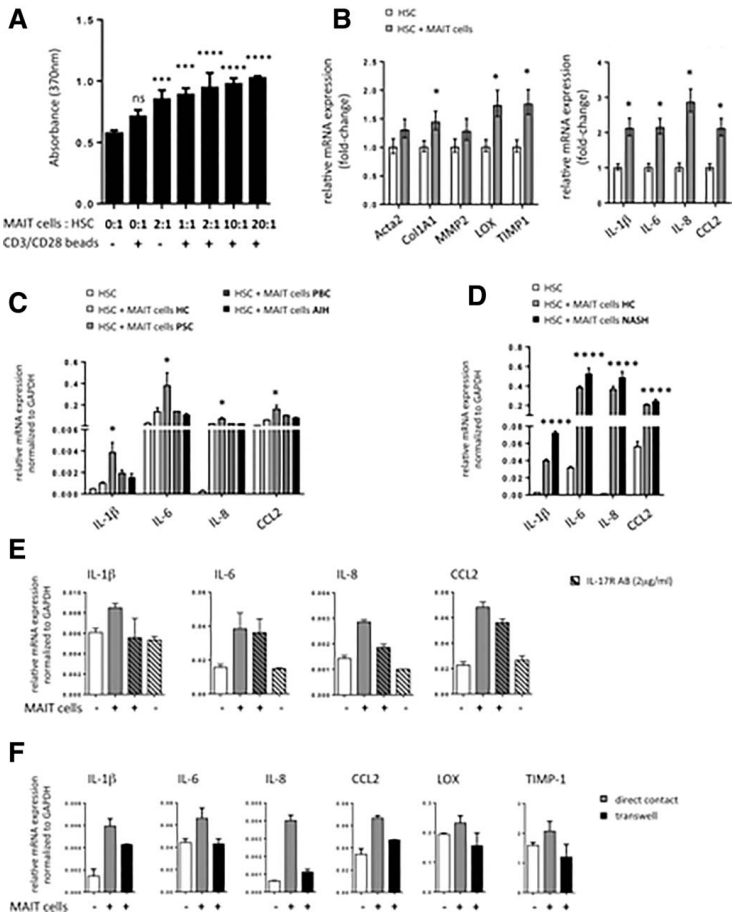

FIG. 6. MAIT cells stimulate HSC activation in a cell–cell contact– and IL-17–dependent manner. (a-d) Bromodeoxyuridine incorporation (n = 4) (a) and gene expression (b-d) of human HSCs after 48-hour coculture with Vα7.2^{+} MAIT cells from (a, b) healthy controls (HC), (c) AILD patients, and (d) NASH patients. (e, f) Gene expression of hHSCs after coculture with Vα7.2^{+} MAIT cells from healthy controls with IL-17R antibody (e) and in transwell system (f). (a, c-f) Data are presented as the mean ± SD. $^{*}P < 0.05$, $^{***}P < 0.001$, $^{****}P < 0.0001$ versus unstimulated control. Data were assessed using one-way ANOVA and Tukey's or Dunn's multiple comparisons test (pooled data from three independent experiments). (b) Data are presented as the mean ± 95% confidence interval. $^{*}P = 0.05$ versus unstimulated control (pooled data from three independent experiments).

patients showed phenotypical and functional features of cellular exhaustion and were severely reduced in number. The severe decline of MAIT cells observed in both peripheral blood and liver tissue of AILD patients probably results from chronic activation and cellular exhaustion, which is commonly characterized by a hierarchical loss of effector function, followed by cell death.[30] T cell exhaustion arises from chronic exposure to various stimuli, e.g. chronic infection with pathogens,[31,32] long-term exposure to viral antigen,[22] antigen-release from tumors,[33] or long-term inflammation and chronic exposure to inflammatory cytokines.[34] Here, we show that exhaustion of human MAIT cells can be driven by long-term stimulation with the proinflammatory, third-signal cytokines IL-12 + IL-18. Because both IL-12 and IL-18 levels are elevated in serum of patients with AILD,[23,24] it seems plausible that MAIT cells are chronically exposed to IL-12 + IL-18 in AILD patients, providing a potential mechanistic explanation for the observed exhaustion of MAIT cell in AILD patients *in vivo*. Moreover, we show that MAIT cells

from AILD patients express significantly lower levels of CD3 as well as of the transcription factor eomesodermin, both of which can be induced by antigen exposure.[25,26] Thus, it is likely that additional mechanisms such as long-term exposure to bacterial-derived antigen contribute to MAIT cell activation and exhaustion *in vivo*. This is of special importance considering that AILD cirrhosis is often characterized by bacterial translocation from the gut to the liver,[35] which might provide a source of bacterial-derived riboflavin derivatives that specifically activate MAIT cells.[36,37]

The proinflammatory cytokine IL-17A is regarded as a key cytokine for the development of tissue-specific autoimmune disorders and has recently been shown to be involved in hepatic fibrosis development in both non–autoimmune-mediated liver disease[18,38,39] and AILD.[13,38-41] PSC, PBC, and AIH patients show elevated serum levels of IL-17,[42-44] along with infiltration of IL-17$^+$ cells into the liver parenchyma.[42,45] Furthermore, the number of liver-infiltrating IL-17$^+$ cells correlates with hepatic inflammation and fibrosis in AIH.[46] Although IL-17 can be secreted by conventional T helper 17 cells at high levels,[47] up to now it is unclear which cells contribute to IL-17 production during human liver inflammation, especially in AILD. Interestingly, MAIT cells represent more than 60% of IL-17$^+$ cells in the liver,[4] suggesting that IL-17 in the liver *in vivo* might be predominantly derived from MAIT cells rather than T helper 17 cells. MAIT cells from AILD patients, despite exhibiting clear features of chronic exhaustion, retain their ability to express the cytokine IL-17A *ex vivo*; therefore, it seems likely that MAIT cells constantly produce IL-17A in the liver of AILD patients. Furthermore, we describe for the first time that chronic stimulation of MAIT cells by the innate, proinflammatory cytokine IL-12 stimulates IL-17A expression in MAIT cells. IL-12 predominantly signals through activation of the transcription factors signal transducer and activator of transcription 1 (STAT1), STAT3, STAT5, and in particular STAT4,[48,49] leading to IFN-γ expression.[50] However, STAT3 signaling can further induce the expression of the transcription factor RORγT, which regulates IL-17 expression[28] and is constitutively expressed in MAIT cells.[3] We show that IL-12 stimulation induces significant up-regulation of RORγt in MAIT cells. Therefore, the observed expression of IL-17 in MAIT cells following prolonged exposure to IL-12 might result from "nonclassical" IL-12 signaling, which is mediated through STAT3-regulated RORγT induction, although further experiments are necessary to fully confirm this hypothesis.

Activation of HSCs is a key event in the development of liver fibrosis, because HSCs transform into hyperproliferative, myofibroblast-like cells producing large amounts of extracellular matrix proteins upon activation, thereby leading to the formation of liver fibrosis and cirrhosis.[29] In murine models of liver fibrosis, it has been demonstrated that fibrosis development depends on IL-17A *in vivo*, and that IL-17A induces HSC activation *in vitro*.[18] However, whether IL-17 contributes to fibrosis development through activation of HSCs in human AILD has not been investigated so far. Our findings show that MAIT cells induce HSC proliferation and an activated, profibrogenic and proinflammatory phenotype in primary human HSCs in vitro. Interestingly, despite an exhausted phenotype, MAIT cells from AILD patients, regardless of the donor's fibrosis stage, retain their ability to secrete IL-17A and are equally able to induce HSC activation. These data suggest that MAIT cells may contribute to fibrosis development in AILD *in vivo* throughout disease progression. Moreover, we show that MAIT cells isolated from NASH patients are highly activated and are able to induce HSC activation *in vitro* as well, suggesting a general profibrogenic role of MAIT cells in chronic liver disease. Mechanistically, the profibrogenic activation of HSCs by MAIT cells depends on IL-17A but also involves direct cell–cell contact between MAIT cells and HSCs, at least *in vitro*.

Taken together, our findings demonstrate a role for IL-17 producing MAIT cells as profibrogenic cellular mediators in AILD, which could serve as a potential therapeutic target for novel antifibrotic approaches.

Acknowledgment: We thank the study participants, as well as Amir Gander and Letizia Gulino for helping with patient recruitment. We also thank Jan Böttcher for critical review of the manuscript.

REFERENCES

1) Porcelli S, Yockey CE, Brenner MB, Balk SP. Analysis of T cell antigen receptor (TCR) expression by human peripheral blood CD4-8- alpha/beta T cells demonstrates preferential use of several V beta genes and an invariant TCR alpha chain. J Exp Med 1993;178:1-16.
2) Tilloy F, Treiner E, Park S-H, Garcia C, Lemonnier F, de la Salle H, et al. An invariant T cell receptor α chain defines a

novel TAP-independent major histocompatibility complex class Ib–restricted α/β T cell subpopulation in mammals. J Exp Med 1999;189:1907-1921.
3) **Dusseaux M**, **Martin E**, Serriari N, Peguillet I, Premel V, Louis D, et al. Human MAIT cells are xenobiotic-resistant, tissue-targeted, CD161hi IL-17-secreting T cells. Blood 2011;117: 1250-1259.
4) **Tang XZ**, **Jo J**, **Tan AT**, **Sandalova E**, Chia A, Tan KC, et al. IL-7 licenses activation of human liver intrasinusoidal mucosal-associated invariant T cells. J Immunol 2013;190:3142-3152.
5) Kjer-Nielsen L, Patel O, Corbett AJ, Le Nours J, Meehan B, Liu L, et al. MR1 presents microbial vitamin B metabolites to MAIT cells. Nature 2012;491:717-723.
6) **Le Bourhis L**, **Dusseaux M**, Bohineust A, Bessoles S, Martin E, Premel V, et al. MAIT cells detect and efficiently lyse bacterially-infected epithelial cells. PLoS Pathog 2013;9: e1003681.
7) Le Bourhis L, Martin E, Péguillet I, Guihot A, Froux N, Coré M, et al. Antimicrobial activity of mucosal-associated invariant T cells. Nat Immunol 2010;11:701-708.
8) **Ussher JE**, **Bilton M**, Attwod E, Shadwell J, Richardson R, de Lara C, et al. CD161 ++CD8 +T cells, including the MAIT cell subset, are specifically activated by IL-12+IL-18 in a TCR-independent manner. Eur J Immunol 2013;44:195-203.
9) **Annibali V**, **Ristori G**, **Angelini DF**, Serafini B, Mechelli R, Cannoni S, et al. CD161highCD8+T cells bear pathogenetic potential in multiple sclerosis. Brain 2011;134:542-554.
10) **Salou M**, **Nicol B**, Garcia A, Baron D, Michel L, Elong-Ngono A, et al. Neuropathologic, phenotypic and functional analyses of mucosal associated invariant T cells in multiple sclerosis. Clin Immunol 2016;166-167:1-11.
11) Serriari N-E, Eoche M, Lamotte L, Fumery M, Marcelo P, Chatelain D, Barre A, et al. Innate mucosal-associated invariant T (MAIT) cells are activated in inflammatory bowel diseases. Clin Exp Immunol 2014;176:266-274.
12) Liaskou E, Hirschfield GM, Gershwin ME. Mechanisms of tissue injury in autoimmune liver diseases. Semin Immunopathol 2014;36:553-568.
13) Hirschfield GM, Siminovitch KA. Toward the molecular dissection of primary biliary cirrhosis. HEPATOLOGY 2009;50: 1347-1350.
14) Yoshida K, Yang G-X, Zhang W, Tsuda M, Tsuneyama K, Moritoki Y, et al. Deletion of IL-12p40 suppresses autoimmune cholangitis in dnTGFβRII mice. HEPATOLOGY 2009;50:1494-1500.
15) **Gil-Farina I**, **Di Scala M**, Salido E, López-Franco E, Rodríguez-García E, Blasi M, et al. Transient expression of transgenic IL-12 in mouse liver triggers unremitting inflammation mimicking human autoimmune hepatitis. J Immunol 2016; 197:2145-2156.
16) Seki E, Schwabe RF. Hepatic inflammation and fibrosis: functional links and key pathways. HEPATOLOGY 2015;61:1066-1079.
17) Meng F, Wang K, Aoyama T, Grivennikov SI, Paik Y, Scholten D, et al. Interleukin-17 signaling in inflammatory, Kupffer cells, and hepatic stellate cells exacerbates liver fibrosis in mice. Gastroenterology 2012;143:765-776.
18) **Tan Z**, **Qian X**, Jiang R, Liu Q, Wang Y, Chen C, et al. IL-17A plays a critical role in the pathogenesis of liver fibrosis through hepatic stellate cell activation. J Immunol 2013;191: 1835-1844.
19) Longato L, Andreola F, Davies SS, Roberts JL, Fusai G, Pinzani M, et al. Reactive gamma-ketoaldehydes as novel activators of hepatic stellate cells in vitro. Free Radic Biol Med 2017; 102:162-173.
20) Castéra L, Vergniol J, Foucher J, Le Bail B, Chanteloup E, Haaser M, et al. Prospective comparison of transient elastography, Fibrotest, APRI, and liver biopsy for the assessment of fibrosis in chronic hepatitis C. Gastroenterology 2005;128:343-350.
21) **Gupta PK**, **Godec J**, **Wolski D**, Adland E, Yates K, Pauken KE, et al. CD39 expression identifies terminally exhausted CD8+ T cells. PLoS Pathog 2015;11:e1005177.
22) Zajac AJ, Blattman JN, Murali-Krishna K, Sourdive DJ, Suresh M, Altman JD, et al. Viral immune evasion due to persistence of activated T cells without effector function. J Exp Med 1998;188: 2205-2213.
23) Landi A, Weismuller TJ, Lankisch TO, Santer DM, Tyrrell DLJ, Manns MP, et al. Differential serum levels of eosinophilic eotaxins in primary sclerosing cholangitis, primary biliary cirrhosis, and autoimmune hepatitis. J Interferon Cytokine Res 2014; 34:204-214.
24) Yamano T, Higashi T, Nouso K, Nakatsukasa H, Kariyama K, Yumoto E, et al. Serum interferon-gamma-inducing factor/IL-18 levels in primary biliary cirrhosis. Clin Exp Immunol 2000;122: 227-231.
25) Valitutti S, Müller S, Salio M, Lanzavecchia A. Degradation of T cell receptor (TCR)–CD3-ζ complexes after antigenic stimulation. J Exp Med 1997;185:1859-1864.
26) Leeansyah E, Svard J, Dias J, Buggert M, Nystrom J, Quigley MF, et al. Arming of MAIT cell cytolytic antimicrobial activity is induced by IL-7 and defective in HIV-1 infection. PLoS Pathog 2015;11:e1005072.
27) **van Wilgenburg B**, **Scherwitzl I**, Hutchinson EC, Leng T, Kurioka A, Kulicke C, et al. MAIT cells are activated during human viral infections. Nat Commun 2016;7:11653.
28) **Ivanov II**, **McKenzie BS**, **Zhou L**, Tadokoro CE, Lepelley A, Lafaille JJ, et al. The orphan nuclear receptor RORγt directs the differentiation program of proinflammatory IL-17+ T helper cells. Cell 2006;126:1121-1133.
29) Pinzani M, Rombouts K. Liver fibrosis: from the bench to clinical targets. Dig Liver Dis 2004;36:231-242.
30) Wherry EJ. T cell exhaustion. Nat Immunol 2011;131:492-499.
31) Day CL, Abrahams DA, Lerumo L, Janse van Rensburg E, Stone L, O'rie T, et al. Functional capacity of Mycobacterium tuberculosis-specific T cell responses in humans is associated with mycobacterial load. J Immunol 2011;187:2222-2232.
32) Bhadra R, Gigley JP, Weiss LM, Khan IA. Control of Toxoplasma reactivation by rescue of dysfunctional CD8+ T-cell response via PD-1–PDL-1 blockade. Proc Natl Acad Sci 2011; 108:9196-9201.
33) Ahmadzadeh M, Johnson LA, Heemskerk B, Wunderlich JR, Dudley ME, White DE, et al. Tumor antigen–specific CD8 T cells infiltrating the tumor express high levels of PD-1 and are functionally impaired. Blood 2009;114:1537-1544.
34) Stelekati E, Shin H, Doering Travis A, Dolfi Douglas V, Ziegler Carly G, Beiting Daniel P, et al. Bystander chronic infection negatively impacts development of CD8+ T cell memory. Immunity 2014;40:801-813.
35) Lin R, Zhou L, Zhang J, Wang B. Abnormal intestinal permeability and microbiota in patients with autoimmune hepatitis. Int J Clin Exp Pathol 2015;8:5153-5160.
36) **Corbett AJ**, **Eckle SBG**, **Birkinshaw RW**, Liu L, Patel O, Mahony J, et al. T-cell activation by transitory neo-antigens derived from distinct microbial pathways. Nature 2014;509: 361-365.
37) **Eckle SB**, **Birkinshaw RW**, Kostenko L, Corbett AJ, McWilliam HE, Reantragoon R, et al. A molecular basis

underpinning the T cell receptor heterogeneity of mucosal-associated invariant T cells. J Exp Med 2014;211:1585-1600.
38) Lafdil F, Miller AM, Ki SH, Gao B. Th17 cells and their associated cytokines in liver diseases. Cell Mol Immunol 2010;7:250-254.
39) Hammerich L, Heymann F, Tacke F. Role of IL-17 and Th17 cells in liver diseases. Clin Dev Immunol 2011;2011:345803.
40) Trivedi PJ, Hirschfield GM. Treatment of autoimmune liver disease: current and future therapeutic options. Ther Adv Chronic Dis 2013;4:119-141.
41) Iwakura Y, Ishigame H. The IL-23/IL-17 axis in inflammation. J Clin Invest 2006;116:1218-1222.
42) Harada K, Shimoda S, Sato Y, Isse K, Ikeda H, Nakanuma Y. Periductal interleukin-17 production in association with biliary innate immunity contributes to the pathogenesis of cholangiopathy in primary biliary cirrhosis. Clin Exp Immunol 2009;157:261-270.
43) Yasumi Y, Takikawa Y, Endo R, Suzuki K. Interleukin-17 as a new marker of severity of acute hepatic injury. Hepatol Res 2007;37:248-254.
44) Zhang H, Bernuzzi F, Lleo A, Ma X, Invernizzi P. Therapeutic potential of IL-17-mediated signaling pathway in autoimmune liver diseases. Mediators Inflamm 2015;2015:436450.
45) Katt J, Schwinge D, Schoknecht T, Quaas A, Sobottka I, Burandt E, et al. Increased T helper type 17 response to pathogen stimulation in patients with primary sclerosing cholangitis. HEPATOLOGY 2013;58:1084-1093.
46) **Zhao L**, **Tang Y**, You Z, Wang Q, Liang S, Han X, et al. Interleukin-17 contributes to the pathogenesis of autoimmune hepatitis through inducing hepatic interleukin-6 expression. PLoS One 2011;6:e18909.
47) Korn T, Bettelli E, Oukka M, Kuchroo VK. IL-17 and Th17 cells. Annu Rev Immunol 2009;27:485-517.
48) Watford WT, Hissong BD, Bream JH, Kanno Y, Muul L, O'Shea JJ. Signaling by IL-12 and IL-23 and the immunoregulatory roles of STAT4. Immunol Rev 2004;202:139-156.
49) Trinchieri G. Interleukin-12 and the regulation of innate resistance and adaptive immunity. Nat Rev Immunol 2003;3:133-146.
50) Lund RJ, Chen Z, Scheinin J, Lahesmaa R. Early Target Genes of IL-12 and STAT4 Signaling in Th Cells. J Immunol 2004;172:6775-6782.

Author names in bold designate shared co-first authorship.

Supporting Information

Additional Supporting Information may be found at onlinelibrary.wiley.com/doi/10.1002/hep.29782/suppinfo.